



The Integral Manifolds of the 4 Body Problem with Equal Masses: Bifurcations at Relative Equilibria

Christopher K. McCord¹

Received: 9 November 2023 / Revised: 16 August 2024 / Accepted: 20 August 2024

© The Author(s), under exclusive licence to Springer Science+Business Media, LLC, part of Springer Nature 2024

Abstract

In the N -body problem, it is classical that there are conserved quantities of center of mass, linear momentum, angular momentum and energy. The level sets $\mathfrak{M}(c, h)$ of these conserved quantities are parameterized by the angular momentum c and the energy h , and are known as the *integral manifolds*. A long-standing goal has been to identify the bifurcation values, especially the bifurcation values of energy for fixed non-zero angular momentum, and to describe the integral manifolds at the regular values. Alain Albouy identified two categories of singular values of energy: those corresponding to bifurcations at relative equilibria; and those corresponding to “bifurcations at infinity”, and demonstrated that these are the only possible bifurcation values. This work completes the identification of bifurcations for the four-body problem with equal masses, confirming that, in this setting, Albouy’s necessary conditions for bifurcation are also sufficient conditions: bifurcations of the integral manifolds occur at all of the singular values of energy. A recent study examined the bifurcations at infinity; this work evaluates the four bifurcations at relative equilibria. To establish that the topology of the integral manifolds changes at each of these values, and to describe the manifolds at the regular values of energy, the homology groups of the integral manifolds are computed for the five energy regions on either side of the singular values. The homology group calculations establish that all four energy levels are indeed bifurcation values, and allows some of the global properties of the integral manifolds to be explored.

Keywords Integral manifold · N -body problem

Mathematics Subject Classification Primary 70F07 · 58F05 · 57R57; Secondary 58F14

Contents

1	Introduction and Results
2	Singular Values and Level Sets of Energy
2.1	Integral Manifolds
2.2	The Reduction Framework
2.3	Singular Values of Energy on the Angular Momentum Manifold
2.4	Global Analysis of the Functions

✉ Christopher K. McCord
mccord@niu.edu

¹ Department of Mathematical Sciences, Northern Illinois University, DeKalb, IL 60115, USA

2.5	The Hills Region
3	The Planar Manifold
3.1	Planar Configuration Spaces
3.2	Planar Integral Manifolds
4	Topological Descriptions
4.1	The Topology of $\mathfrak{B}(d_j)$
4.2	Behavior at \mathfrak{B}_0
4.3	From Planar Configurations to Spatial Configurations
5	Homology of the Integral Manifolds
5.1	The Homology Groups for $\mathfrak{B}(d_j)$ and Pairs $(\mathfrak{B}(d_j), \partial\mathfrak{B}(d_j))$
5.2	The Pairs $(\mathfrak{B}(d_j), \mathfrak{B}_0(d_j))$ and $(\mathfrak{B}(d_j), \partial\mathfrak{B}^+(d_j))$
	References

1 Introduction and Results

This work continues the investigation of the integral manifolds of the spatial N -body problem. The integral manifolds are the level sets of the classical conserved quantities of energy, angular momentum, linear momentum and center of mass. In the spatial problem, they form a family of $(6N - 10)$ -dimensional manifolds. Their structure depends on the values m_1, \dots, m_N of the masses, the angular momentum $\vec{c} \in \mathbb{R}^3$ and energy h . Typically, the dependence on the masses is not displayed explicitly, and the integral manifolds are viewed as a parameterized family $\mathfrak{M}(c, h)$.

The integral manifolds for $c = 0$ have been characterized in [3]. The focus of this work is on $c \neq 0$. Without loss of generality, a global change of coordinates can be made that sets $\vec{c} = \hat{k}$, reducing the problem to studying the level sets of energy on the level sets of angular momentum, linear momentum and center of mass, for a fixed set of masses. Once that orientation is fixed, the problem's SO_3 symmetry reduces to an SO_2 -symmetry of rotations about the z -axis. The equations of motion and the conserved quantities are all preserved by rotation, so there are well-defined dynamics on the *reduced integral manifold* $\mathfrak{M}_R(c, h) = \mathfrak{M}(c, h)/SO_2$.

In this setting, the questions of interest for the global behavior are:

- Identify the bifurcation values of h —the values at which the topology of $\mathfrak{M}(c, h)$ and $\mathfrak{M}_R(c, h)$ change.
- At the regular values of h between those bifurcation values, describe $\mathfrak{M}(c, h)$ and $\mathfrak{M}_R(c, h)$.
- Use that global description to provide insights into the global dynamics of the N -body problem.

The starting point for this program is [1]. There, Albouy produced necessary and sufficient conditions for an energy level h to be a singular value for $\mathfrak{M}(c, h)$, and an algorithm for identifying those values. This is formulated in detail in Sect. 2. At the moment, it suffices to make two observations:

- Singular values arise in two very distinct ways: either at critical points, which we will refer to as *bifurcations at relative equilibria* or more colloquially as *finite bifurcations* or as limiting behavior as configurations diverge to infinity, which we will refer to as *bifurcations at infinity*.
- For a given set of masses m_1, \dots, m_N , the ability to identify the full set of singular values requires knowledge of the full set of planar central configurations [14], both for that set of masses and for all of its subsets.

Table 1 Singular Values of Energy for Four Equal Masses

Parameter label	Configuration	$h_i c^2$	$\delta_i = -2h_i$	Multiplicity
h_0	Zero energy	0	0	
h_1	One binary collinear	$-\frac{1}{4}$	$\frac{1}{2}$	6
h_2	Two binary collinear	-2	4	3
h_3	Equilateral cluster	$-\frac{9}{2}$	9	8
h_4	Triple collinear	$-\frac{25}{4}$	$\frac{25}{2}$	12
h_5	Square	$-18 - 8\sqrt{2}$	58.6274	6
h_6	Isosceles	-34.3017	67.1757	24
h_7	Equilateral	$-18 - 9\sqrt{3}$	67.1769	8
h_8	Collinear	-46.8416	93.6832	12

Of course, singular values are not necessarily bifurcation values. At present, there are no results on sufficient conditions analogous to Albouy’s necessary condition for bifurcation. That is, there is no formula or algorithm that produces a set of energy levels that are guaranteed to be bifurcation values. Instead, a brute force approach has been taken. Given an energy level h_0 that meets Albouy’s necessary condition, we consider $h_- < h_0 < h_+$ such that h_0 is the only candidate value in the interval $[h_-, h_+]$. Then calculate a topological invariant such as the homology groups at h_- and h_+ . If those topological invariants are different, then the integral manifolds underwent bifurcation at h_0 .

While a change in any topological invariant is sufficient to detect bifurcation, computing the homology groups speaks to the next goal as well, by providing a description of sorts of the global structure of the manifolds. Moreover, methods such as Morse theory have a long tradition of deriving insights into global dynamics from homological information. While the non-compactness of $\mathfrak{M}(c, h)$ and $\mathfrak{M}_R(c, h)$ limits the opportunity to apply such techniques, [11] and [12] allow some dynamical information to be obtained.

An important limiting factor in this work is the need to identify all of the planar central configurations. At present, the identification of complete set of central configurations has only been rigorously established for three arbitrary masses, or four, five, six or seven equal masses [2, 13]. The case of three arbitrary masses has been analyzed in [6], with a correction for the case of positive energy provided in [11]. The need for a correction arose from our incomplete understanding of the complexities generated by the behavior at the collinear configurations.

Those complexities motivated the development in [9] of a blow-up construction \mathcal{B} of the configuration space. By adapting the methods of [6] and [17] to this blow-up, the complexities at collinear were controlled, and formulae describing $H_*(\mathfrak{M}(c, h))$ and $H_*(\mathfrak{M}_R(c, h))$ were developed.

The obvious situation to apply the reduction formulae is that of the four-body problem with equal masses. The full set of central configurations is known [2]. Albouy’s algorithm for identifying singular values produces the set of energy levels shown in Table 1. The multiplicity refers to the number of SO_2 -orbits of central configurations that differ by a permutation of the masses.

These eight values, together with $h = 0$, define ten energy regions. These will be denoted

$$\begin{aligned}
 \text{P} &= (0, \infty) & \text{I} &= (h_1, 0) & \text{II} &= (h_2, h_1) & \text{III} &= (h_3, h_2) & \text{IV} &= (h_4, h_3) \\
 \text{V} &= (h_5, h_4) & \text{VI} &= (h_6, h_5) & \text{VII} &= (h_7, h_6) & \text{VIII} &= (h_8, h_7) & \text{IX} &= (-\infty, h_8)
 \end{aligned}$$

The singular values of Table 1 fall naturally into three groups: $h_0 = 0$, the singular values at infinity h_1, \dots, h_4 and the singular values corresponding to relative equilibria h_5, \dots, h_8 . The homology groups of $\mathfrak{M}(c, h)$ and $\mathfrak{M}_R(c, h)$ for $h > 0$ were identified in [4]; those of Region I were identified in [9], which in turn established that $h_0 = 0$ is a bifurcation value.

The goal is to compute the homology groups of $\mathfrak{M}(c, h)$ and $\mathfrak{M}_R(c, h)$ for regions II through IX. This divides itself naturally into two sets of computations: one for the singular values at infinity; another for the singular values at relative equilibria. The first half was addressed in [10]; the second half is addressed here. The results can be tabulated as follows.

Theorem 1.0.1 *For four equal masses, the spatial integral manifolds $\mathfrak{M}(c, h)$ with non-zero angular momentum have the following homology groups in the intervals between the singular values of h :*

k	0	1	2	3	4	5	6	7	8	9	10	11	12
P	\mathbb{Z}^0	\mathbb{Z}^6	0	\mathbb{Z}^{11}	\mathbb{Z}^{18}	0	0	0	0	0	0	0	0
I	\mathbb{Z}^0	\mathbb{Z}^6	0	\mathbb{Z}^{11}	\mathbb{Z}^{18}	0	\mathbb{Z}^{23}	\mathbb{Z}^6	0	\mathbb{Z}^{11}	0	\mathbb{Z}^6	
II	\mathbb{Z}^0	\mathbb{Z}^6	0	\mathbb{Z}^{11}	\mathbb{Z}^{18}	0	0	\mathbb{Z}^{13}	\mathbb{Z}^{30}	\mathbb{Z}^{11}	0	\mathbb{Z}^6	
III	\mathbb{Z}^0	\mathbb{Z}^6	0	\mathbb{Z}^{11}	\mathbb{Z}^{18}	0	0	\mathbb{Z}^7	\mathbb{Z}^{18}	\mathbb{Z}^5	0	\mathbb{Z}^6	
IV	\mathbb{Z}^0	\mathbb{Z}^6	0	\mathbb{Z}^{11}	\mathbb{Z}^{18}	0	0	0	\mathbb{Z}^{20}	\mathbb{Z}^{14}	0	\mathbb{Z}^6	
V	\mathbb{Z}^0	\mathbb{Z}^6	0	\mathbb{Z}^{11}	\mathbb{Z}^{18}	0	0	0	\mathbb{Z}	\mathbb{Z}^6	\mathbb{Z}^{11}	\mathbb{Z}^6	
VI	\mathbb{Z}^0	\mathbb{Z}^6	\mathbb{Z}^6	\mathbb{Z}^{16}	\mathbb{Z}^{17}	0	0	0	0	\mathbb{Z}^{10}	\mathbb{Z}^{16}	\mathbb{Z}^6	
VII	\mathbb{Z}^0	\mathbb{Z}^{25}	\mathbb{Z}^{20}	\mathbb{Z}^{11}	\mathbb{Z}^{17}	0	0	0	0	0	\mathbb{Z}^{20}	\mathbb{Z}^{20}	
$VIII$	\mathbb{Z}^0	\mathbb{Z}^{17}	\mathbb{Z}^{12}	\mathbb{Z}^{11}	\mathbb{Z}^{17}	0	0	0	0	0	\mathbb{Z}^{12}	\mathbb{Z}^{12}	
IX	\mathbb{Z}^0	\mathbb{Z}^{17}	\mathbb{Z}^6	\mathbb{Z}^{11}	\mathbb{Z}^{17}	0	0	0	0	0	0	0	

and the reduced integral manifolds $\mathfrak{M}_R(c, h)$ have homology groups

k	0	1	2	3	4	5	6	7	8	9	10	11	12
P	\mathbb{Z}^0	0	\mathbb{Z}^7	0	\mathbb{Z}^{18}	0	0	0	0	0	0	0	0
I	\mathbb{Z}^0	0	\mathbb{Z}^7	0	\mathbb{Z}^{18}	0	0	\mathbb{Z}^{23}	0	\mathbb{Z}^{17}	0	\mathbb{Z}^6	0
II	\mathbb{Z}^0	0	\mathbb{Z}^7	0	\mathbb{Z}^{18}	0	0	0	\mathbb{Z}^{13}	\mathbb{Z}^{17}	0	\mathbb{Z}^6	0
III	\mathbb{Z}^0	0	\mathbb{Z}^7	0	\mathbb{Z}^{18}	0	0	0	\mathbb{Z}^7	\mathbb{Z}^{11}	0	\mathbb{Z}^6	0
IV	\mathbb{Z}^0	0	\mathbb{Z}^7	0	\mathbb{Z}^{18}	0	0	0	0	\mathbb{Z}^{20}	0	\mathbb{Z}^6	0
V	\mathbb{Z}^0	0	\mathbb{Z}^7	0	\mathbb{Z}^{18}	0	0	0	0	\mathbb{Z}	\mathbb{Z}^5	\mathbb{Z}^6	0
VI	\mathbb{Z}^0	0	\mathbb{Z}^7	\mathbb{Z}^5	\mathbb{Z}^{17}	0	0	0	0	0	\mathbb{Z}^{10}	\mathbb{Z}^6	0
VII	\mathbb{Z}^0	0	\mathbb{Z}^{26}	0	\mathbb{Z}^{17}	0	0	0	0	0	0	\mathbb{Z}^{20}	0
$VIII$	\mathbb{Z}^0	0	\mathbb{Z}^{18}	0	\mathbb{Z}^{17}	0	0	0	0	0	0	\mathbb{Z}^{12}	0
IX	\mathbb{Z}	\mathbb{Z}^6	\mathbb{Z}^{12}	0	\mathbb{Z}^{17}	0	0	0	0	0	0	0	0

Inspection of the table shows that at each singular value, the homology groups change.

Corollary 1.0.1 *For four equal masses and non-zero angular momentum, the bifurcation values of energy are $h_0 - h_8$, with both the integral manifold $\mathfrak{M}(c, h)$ and reduced integral manifold $\mathfrak{M}_R(c, h)$ changing their homotopy type at those values, and at no others.*

That is the first use of the table: to demonstrate changes in the topology. We can go further and use the specific values in the table to draw conclusions about the integral manifolds.

Corollary 1.0.2 *For all h , the following hold:*

- *The reduced integral manifold $\mathfrak{M}_R(c, h)$ does not admit a geodesic flow.*

- The flow on the reduced integral manifold $\mathfrak{M}_R(c, h)$ does not admit a global cross section.
- The full integral manifold $\mathfrak{M}(c, h)$ is an orientable S^1 -bundle over $\mathfrak{M}_R(c, h)$, but does not admit a product structure $\mathfrak{M}_R(c, h) \times S^1$.

Proof The are negative conclusion, asserting that something does not happen. Each conclusion follows from the failure of a necessary homological condition.

In order for a $(2n - 1)$ -manifold \mathcal{P} to admit a geodesic flow structure, it must first admit the topological structure as the unit tangent bundle of an n -manifold. In [12], it was shown that, if the $(2n - 1)$ -manifold \mathcal{P} is non-compact and orientable, with torsion-free homology, then a necessary condition to admit such a topological structure is that $H_{n-1}(\mathcal{P}) \neq 0$. Applying this to the 13-dimensional non-compact orientable manifold $\mathfrak{M}_R(c, h)$, we see that its homology is torsion-free, with $H_6(\mathfrak{M}_R(c, h)) = 0$.

Similarly, it was shown in [11] that, for $\mathfrak{M}_R(c, h)$ to admit a global cross-section and has finitely-generated homology, then the Euler characteristic must satisfy $\chi(\mathfrak{M}_R(c, h)) = 0$. From the table, we see that in each region, $\chi(\mathfrak{M}_R(c, h)) \neq 0$.

Finally, if $\mathfrak{M}(c, h)$ admitted a product structure as $\mathfrak{M}_R(c, h) \times S^1$, then $H_*(\mathfrak{M}(c, h)) \cong H_*(\mathfrak{M}_R(c, h)) \otimes H_*(S^1)$. This clearly fails to hold in any region. \square

Beyond those specific negative conclusions, the table displays patterns that are suggestive of additional structural issues. The most obvious of these is that the changes in the homology groups associated with the bifurcations at infinity (e.g. regions II - V) are quite different than those associated with the finite bifurcations (regions V - IX).

In the former, the changes occur only in dimensions $k \geq 7$. This signals that the changes in the structure of the manifold have more to do with the changes in the structure of momentum fibers over the set of allowable positions, rather than being generated by changes in the set of allowable positions. The most striking of these changes was noted in [9]: for positive energy, the momentum fibers are hyperplanes; as h passes from positive to negative; these fold over to form spheres. This is reflected in the homology, with non-trivial homology appearing in dimensions 7 to 12.

In contrast, in regions VI - IX, the changes in the homology groups confirm that the set of allowable positions (i.e. the Hill's region) undergoes changes at the bifurcations at relative equilibria, which did not occur at the various bifurcations at infinity. At the same time, as the energy level progressed through the finite bifurcations, we see the higher homology groups progressively simplifying, so that once all of the bifurcation values have been passed, all of the homology groups above dimension 5 have become trivial.

There are two other aspects to the distinction between the bifurcations at infinity and the bifurcations at the relative equilibria. Namely, for four equal masses, we can observe that both the Hill's regions and the planar integral manifolds undergo bifurcation at the relative equilibria energy levels h_5, \dots, h_8 but not that the bifurcation at infinity values h_1, \dots, h_4 .

The Hill's region $\mathfrak{H}(c, h)$ is the image of the integral manifold under the projection onto position space. A corollary of the homology reduction formula of [9] is

Corollary 1.0.3 *For any set of N masses, the projection $\Pi : \mathfrak{M}(c, h) \rightarrow \mathfrak{H}(c, h)$ yields an isomorphisms $\Pi_* : H_k(\mathfrak{M}(c, h)) \rightarrow H_k(\mathfrak{H}(c, h))$ and $\pi_* : H_k(\mathfrak{M}_R(c, h)) \rightarrow H_k(\mathfrak{H}_R(c, h))$ for $k \leq 3N - 6$, while $H_k(\mathfrak{H}(c, h)) = H_k(\mathfrak{H}(c, h)) = 0$ for $k > 3N - 6$.*

The planar integral manifolds, denoted $\mathfrak{m}(c, h)$, are the analogous $4N - 6$ dimensional manifolds in which all of the positions and momenta are confined to a common plane orthogonal to the angular momentum vector. It is well-known that the bifurcations of the planar manifolds can occur only at the energy levels corresponding to the relative equilibria [15, 16].

We will see that, not only do the bifurcations of the planar manifolds occur in tandem with the finite bifurcations of the spatial manifolds; for the problem at hand (four equal masses), we will exploit the topological structure of the planar bifurcations to obtain needed information about the spatial finite bifurcations.

This relationship between the planar and spatial manifolds at the finite bifurcations is useful, but may not generalize. The two types of bifurcations make use of different techniques of analysis. The analysis of the bifurcations at infinity proceeded by bootstrapping from region I step-by-step to region V. On the other hand, we will see that the analysis of the finite bifurcations proceeds by anchoring the two ends of the spectrum, regions V and IX, and filling in the intermediate regions by the reduction to the planar manifolds. For both the bifurcations at infinity and the finite bifurcations, the analysis is simplified by the fact that the two types of analysis do not need to be intermingled. That is, for four equal masses, all of the bifurcations at infinity occur at energy levels that are closer to zero than the energy levels of any of the finite bifurcations. It seems clear that either of those processes would be complicated if the two types of bifurcations were interleaved. Unfortunately, that interleaving occurs. As described in [5], for four unequal masses, there are instances where bifurcations at infinity occur at energy levels between those of finite bifurcations. The same occurs for nine or ten equal masses, and is conjectured to persist for equal masses for all $N \geq 9$.

This work takes [1] and [9] as its starting point. The framework established by those works is briefly summarized in Sect. 2. That framework reduces to the study of a real-valued function D on a space \mathcal{B} associated with the 8-dimensional mass ellipsoid, with the homology groups of $\mathfrak{M}(c, h)$ and $\mathfrak{M}_R(c, h)$ computed from those of the super-level sets of D on \mathcal{B} , denoted $\mathfrak{B}(d)$, together with various subspaces of those super-level sets. As mentioned above, the analysis from there will rest on two pillars: establishing the topology of $\mathfrak{B}(d)$ in Regions V and IX, and establishing the relation between the spatial configuration spaces and corresponding planar configuration spaces to fill in the information for the regions in between. We examine the planar configuration spaces and planar integral manifolds in Sect. 3 and take the opportunity in Sect. 3.2 to correct the error in the homology group tables for $H_*(\mathfrak{m}(c, h))$ and $H_*(\mathfrak{m}_R(c, h))$ in [8]. Section 4 completes the preliminaries: the topology and homology of $\mathfrak{B}(d)$ is established in Sect. 4.1 and the relationship between the homology of the planar and spatial configuration spaces is established in Sect. 4.3.

These two steps (Sects. 4.1 and 4.3) represent the most complex elements of the argument. The challenges they present are indicative of the differences between the spatial and planar problems. In the planar case, the analogue of the set $\mathfrak{B}(d_9)$ is simply the super-level set of the potential function approaching infinite energy. This is simply a neighborhood in the planar configuration space around the collision set. As such, a topological description that lends itself to homological calculations is readily obtained for any collection of masses (cf. [8]). For the spatial problem, in contrast, the interplay between the behavior near collinear and the behavior near collision complicates the topological description. Section 4.1 works through these complications to produce the needed homological information: the space is decomposed into manageable elements, then assembled via a series of Mayer–Vietoris arguments. With the homology groups “above” in $\mathfrak{B}(d_9)$ and “below” in $\mathfrak{B}(d_5)$ established, it is natural to look for a Morse-theoretic handlebody approach to constructing the homology groups of the intermediate level sets. This approach works in the planar case, and Sect. 4.3 examines the extent to which those results may be lifted to the spatial case. With all of that established, the calculations of the homology groups required to identify $H_*(\mathfrak{M}(c, h))$ and $H_*(\mathfrak{M}_R(c, h))$ are carried out in Sect. 5.

2 Singular Values and Level Sets of Energy

This section summarizes the results of [1, 9] that provide the framework for the current analysis. As noted, Albouy’s work in [1] identifies the singular values of energy on level set of angular momentum, center of mass and linear momentum. In the intervals between those singular values, [9] provides a reduction formula for computing the homology of the integral manifolds. Section 2.1 introduces the framework, while Sects. 2.2 and 2.3 review the core results from [1] and [9] required for the present work. The essence of this is a reduction from level sets of energy on the $(6N - 9)$ -dimensional angular momentum manifold to level sets of a function defined on a $(3N - 4)$ -dimensional configuration space. Sects. 2.4, 2.5 present new results, the former establishing that the reduction produces a 1 : 1 correspondence between singular values of the functions; the latter identifying the homology of the Hill’s regions.

2.1 Integral Manifolds

The approach to analyzing the integral manifolds follows the decomposition approach deployed in [6, 9, 17]. As that approach is described in detail in those works, we will only sketch it here. As we are examining the 4-body problem with equal masses, the masses are all set to $m_i = 1$. Except for the identification of central configurations (where the assumption of four equal masses is critical), neither the assumption of equal masses nor the restriction to four masses plays a role in the analysis.

Let $\vec{x}_1, \vec{x}_2, \vec{x}_3, \vec{x}_4 \in \mathbb{R}^3$ denote the positions of the four particles, and let $\vec{y}_i = \frac{d\vec{x}_i}{dt} \in \mathbb{R}^3$ be the corresponding velocities. There are four well-known constants of motion: center of mass; linear momentum; angular momentum and energy, as well as a rotational symmetry.

$$\sum_{i=1}^4 \vec{x}_i = \vec{0} \qquad \text{Center of Mass} \qquad (2.1.1a)$$

$$\sum_{i=1}^4 \vec{y}_i = \vec{0} \qquad \text{Linear Momentum} \qquad (2.1.1b)$$

$$\sum_{i=1}^4 \vec{x}_i \times \vec{y}_i = \vec{c} \qquad \text{Angular Momentum} \qquad (2.1.1c)$$

$$\sum_{i=1}^4 |\vec{y}_i|^2 - U(X) = h \qquad \text{Energy} \qquad (2.1.1d)$$

where $U(X)$ is the self potential

$$U = \sum_{i < j} \frac{1}{\|\vec{x}_i - \vec{x}_j\|}. \qquad (2.1.2)$$

The potential function is undefined at collisions (i.e. when $\vec{x}_i = \vec{x}_j$ for some $i \neq j$), so the state space for the spatial four-body problem is $\mathbb{R}^{12} \setminus \Delta \times \mathbb{R}^{12}$, where

$$\Delta = \{(\vec{x}_1, \vec{x}_2, \vec{x}_3, \vec{x}_4) \in \mathbb{R}^{12} \mid \vec{x}_i = \vec{x}_j \exists i \neq j\}$$

is the collision set.

When $\vec{c} = \vec{0}$, there is an SO_3 symmetry. We will focus on the case of non-zero angular momentum, which has \vec{c} as a preferred direction, and admits SO_2 symmetry under rotations

around \vec{c} . There is no loss of generality in assuming that $\vec{c} = c\hat{k}$. The spatial integral manifold is defined formally as

$$\mathfrak{M}(c, h) = \left\{ (\vec{x}, \vec{y}) \in \mathbb{R}^{3N} \setminus \Delta \times \mathbb{R}^{3N} \mid \text{equations 2.1.1 hold} \right\}$$

When $\vec{c} = \vec{0}$, the reduced integral manifold is defined as $\mathfrak{M}_R(c, h) = \mathfrak{M}(c, h)/SO_3$, while for $\vec{c} \neq \vec{0}$, $\mathfrak{M}_R(c, h) = \mathfrak{M}(c, h)/SO_2$. For the spatial problem with non-zero angular momentum, there are ten integrals and the spatial integral manifolds are 14 dimensional spaces, while $\mathfrak{M}_R(c, h)$ is 13-dimensional.

With the angular momentum vector oriented along \hat{k} , the planar N -body problem can be embedded in the spatial problem by setting all $x_{i3} = y_{i3} = 0$. It is a simple calculation to see that this planar submanifold is invariant under the equations of motion. The planar integral manifold is the subset

$$\mathfrak{m}(c, h) = \{(\vec{x}, \vec{y}) \in \mathfrak{M}(c, h) \mid x_{i3} = y_{i3} = 0 \forall i = 1, \dots, N\}.$$

This is invariant under the SO_2 action, so there is a well-defined reduced planar manifold $\mathfrak{m}_R(c, h)$. The planar 4-body manifold has dimension 9, while $\mathfrak{m}_R(c, h)$ is 8-dimensional.

While the integral manifolds present themselves as parameterized by c and h , for non-zero angular momentum, all manifolds with $\nu = hc^2$ constant are diffeomorphic. We will view this as holding c fixed, which allows us to treat the angular momentum manifold as a one-parameter family of energy surfaces parameterized by h . That is, integral manifolds $\mathfrak{M}(c, h)$ are level sets of H on the angular momentum manifold

$$\mathfrak{A}(c) = \left\{ (\vec{x}, \vec{y}) \in \mathbb{R}^{3N} \times \mathbb{R}^{3N} \mid \text{equations 2.1.1a} - \text{2.1.1c hold} \right\}.$$

The analysis of the integral manifolds proceeds through projection onto the *configuration spaces*. The spatial configuration space is

$$\mathcal{S} = \left\{ (\vec{x}_1, \dots, \vec{x}_N) \in \mathbb{R}^{12} \setminus \Delta \mid \sum_i \vec{x}_i = \vec{0}, \sum_i \vec{x}_i^2 = 1 \right\}$$

The spatial configuration space has various subspaces that will be of interest to us. The planar configuration space

$$\mathcal{P} = \left\{ (\vec{x}_1, \vec{x}_2, \vec{x}_3, \vec{x}_4) \in \mathbb{R}^8 \setminus \Delta \mid \sum_i \vec{x}_i = \vec{0}, \sum_i \vec{x}_i^2 = 1 \right\}$$

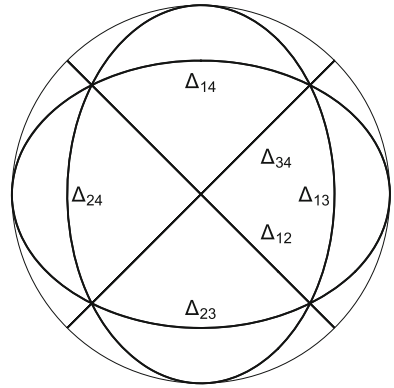
can also be defined by $\mathcal{P} = \{(\vec{x}_1, \vec{x}_2, \vec{x}_3, \vec{x}_4) \in \mathcal{S} \mid x_{i3} = 0 \forall i\}$. The *collinear configuration space*

$$\mathcal{C} = \{(\vec{x}_1, \vec{x}_2, \vec{x}_3, \vec{x}_4) \in \mathcal{S} \mid \exists x_0 \in S^2 \ni x_i = \lambda_i x_0 \forall i\}$$

consists of all configurations with all of the particles lying on a single line. Note that we do not assume collinear configurations to lie in the $x - y$ plane. The set of collinear configurations that lie in the $x - y$ plane, $\mathcal{C}_0 = \mathcal{C} \cap \mathcal{P}$, will be of particular interest to us. For these or any other $X \subset \mathcal{S}$, we will denote $\Delta \cap X$ by Δ_X .

The spatial configuration space \mathcal{S} is a dense open subset of the sphere S^8 , while the planar configuration space is a dense open subset of a 5-sphere. These spaces clearly admit rotational symmetries, and have the obvious corresponding reduced quotient spaces $\mathcal{S}_R = \mathcal{S}/SO_2$ and $\mathcal{P}_R = \mathcal{P}/SO_2$.

Fig. 1 The collision set in \mathcal{C}_L



To remain consistent with the notation in previous works, the sets \mathcal{C} and \mathcal{C}_0 do not contain collisions. However, in the present work, we will want to consider sets that contain both collisions and non-collisional collinear configurations, and to be more explicit about the inclusion or exclusion of collisions. We will therefore make frequent use of the full set of collinear configurations (including collisions) along a single line L :

$$\mathcal{C}_L \cong \{(x_1, x_2, x_3, x_4) \in \mathbb{R}^4 \mid \sum_i x_i = 0, \sum_i x_i^2 = 1\}.$$

This set, which contains collisions, is clearly homeomorphic to S^2 . The collision set $\Delta_L = \Delta \cap \mathcal{C}_L$ consists of six circles Δ_{ijL} , one for each binary intersection $x_i = x_j$. These meet in three pairs of double binary points $\Delta_{ij,klL}$ and four pairs of triple collisions Δ_{ijk} , as shown in Fig. 1. The union of the six circles forms a graph with 14 vertices and 36 edges, so $\chi(\Delta_L) = -22$. The complement $\mathcal{C}_L \setminus \Delta_L$ is homeomorphic to 24 open disks.

The full set of collinear configurations $\mathcal{C} \cup \Delta_{\mathcal{C}}$, including collisions, fibers over $\mathbb{R}P^2$ with fiber \mathcal{C}_L , and similarly, $\mathcal{C}_0 \cup \Delta_{\mathcal{C}_0}$ fibers over $\mathbb{R}P^1$ with fiber \mathcal{C}_L .

Let $\Theta : \mathfrak{M}(c, h) \rightarrow \mathcal{S}$ be the projection $(\vec{x}, \vec{y}) \mapsto \frac{1}{\|\vec{x}\|} \vec{x}$. The projection is equivariant with respect to the SO_2 symmetries, so there is a well-defined projection $\theta : \mathfrak{H}_R \rightarrow \mathcal{S}_R$. The configuration spaces are defined as the images of Θ in \mathcal{S} :

Spatial Configurations	$\mathfrak{R}(c, h) = \{ \vec{x} \in \mathcal{S} \mid (\lambda \vec{x}, \vec{y}) \in \mathfrak{M}(c, h) \exists \lambda > 0, \vec{y} \in \mathbb{R}^{12} \}$
Planar Configurations	$\{ \vec{x} \in \mathcal{P} \mid (\lambda \vec{x}, \vec{y}) \in \mathfrak{m}(c, h) \exists \lambda > 0, \vec{y} \in \mathbb{R}^8 \}$
Collinear Configurations	$\mathfrak{R} \cap \mathcal{C}$.

There is a commutative diagram

$$\begin{array}{ccc}
 \mathfrak{M}(c, h) & \xrightarrow{\Phi_M} & \mathfrak{M}_R(c, h) \\
 \downarrow \Pi & & \downarrow \pi \\
 \mathfrak{H}(c, h) & \xrightarrow{\Phi_H} & \mathfrak{H}_R(c, h) \\
 \downarrow \Omega & & \downarrow \omega \\
 \mathcal{K}(c, h) & \xrightarrow{\Phi_K} & \mathfrak{K}_R(c, h)
 \end{array}$$

and a corresponding planar diagram.

At this point, we introduce a shift in notation, to reflect a shift in perspective. The definitions of the integral manifolds and related spaces were formulated in terms of the positions $\vec{x}_i =$

(x_{i1}, x_{i2}, x_{i3}) and velocities $\vec{y}_i = (y_{i1}, y_{i2}, y_{i3})$ of the individual particles. Moving forward, we will focus instead on the component vectors $q_j = (x_{1j}, x_{2j}, x_{3j}, x_{4j})$ consisting of the projections of \vec{x} onto the x -, y - and z -axis. The notation for configurations in \mathcal{S} will be

$$\mathcal{S} = \{(q_1, q_2, q_3) \in \mathbb{R}^{12} \setminus \Delta \mid (1, 1, 1, 1) \cdot q_i = 0, q_1^2 + q_2^2 + q_3^2 = 0\}$$

with \mathcal{P} consisting of configurations with $q_3 = 0$, and \mathcal{C}_L viewed as configurations with $q_2 = q_3 = 0$. Note that, in this notation, rotations in SO_3 intertwine q_1, q_2 and q_3 .

2.2 The Reduction Framework

As noted, [9] describes a process for reducing the calculation of $H_*(\mathfrak{M})$ to calculations on the configuration space \mathcal{S} . Or, nearly so. The reduction process encounters irregularities at the collinear configurations. These are resolved by deleting some collinear configurations, while introducing a blow-up construction at those that remain.

The projection $\Theta : \mathfrak{M} \rightarrow \mathcal{S}$ naturally invites a description of $\mathfrak{M}(c, h)$ in terms of the image $\mathfrak{K}(c, h)$ and the pre-images $\Theta^{-1}(q)$. Examination of Θ shows that this description can be encoded via the potential function $U(q)$ and a function $Y : \mathcal{S} \rightarrow \mathbb{R}^+$ that measures the square of the distance from the origin to the affine space $J(q)p = c\hat{k}$. For negative energy, we find that $q \in \mathfrak{K}(c, h)$ if and only if $U^2(q) + 2hY(q) \geq 0$. We therefore define $D(q) = \frac{U^2(q)}{Y(q)}$, so that $\mathfrak{K}(c, h) = \{q \in \mathcal{S} \mid D(q) \geq -2h\}$. The pre-image $\Theta^{-1}(q)$ consists of a single point for when $D(q) = -2h$ and is a sphere when $D(q) > -2h$.

While the properties of the potential function have been extensively studied, the function Y does not occupy the same central role, so there has been less occasion to record its properties. For fixed angular momentum $c\hat{k}$ and position vector q , $Y(q)$ is defined by $Y(q) = \min\{p^2 \mid J(q)p = c\hat{k}\}$. There are a variety of ways to express this:

- If $q = (q_1, q_2, q_3)$ is non-collinear, then the moment of inertia tensor

$$I(q) = \begin{bmatrix} q_2^2 + q_3^2 & -q_1 \cdot q_2 & -q_1 \cdot q_3 \\ -q_1 \cdot q_2 & q_1^2 + q_3^2 & -q_2 \cdot q_3 \\ -q_1 \cdot q_3 & -q_2 \cdot q_3 & q_1^2 + q_2^2 \end{bmatrix}$$

is invertible, and $Y(q) = \hat{k}I^{-1}(q)\hat{k}$ is the 3 – 3 entry of $I^{-1}(q)$.

- If q has $q_1 \cdot q_2 = q_1 \cdot q_3 = q_2 \cdot q_3 = 0$ and $q_1^2 \geq q_2^2 \geq q_3^2$, we refer to q as a *standard configuration*. For standard configurations,

$$I(r) = \begin{bmatrix} q_2^2 + q_3^2 & 0 & 0 \\ 0 & q_1^2 + q_3^2 & 0 \\ 0 & 0 & q_1^2 + q_2^2 \end{bmatrix}$$

and $Y(q) = \frac{c^2}{q_1^2 + q_2^2}$.

- An arbitrary position vector q is a rotation of a standard configuration: there is a standard configuration $r = (r_1, r_2, r_3)$ and an $R \in SO_3$ acts component-wise on each (r_{1i}, r_{2i}, r_{3i}) so that $q = Rr$. Then $I(q) = RI(r)R^T$, so $I^{-1}(q) = RI^{-1}(r)R^T$ and $Y(q) = \hat{k}^T RI^{-1}(r)R^T \hat{k}$.
- $I(q)$ is positive semi-definite with non-negative eigenvalues $\alpha_1(q) \leq \alpha_2(q) \leq \alpha_3(q)$ that are invariant under rotation. At a standard configuration, $\alpha_1(q) = r_2^2 + r_3^2, \alpha_2(q) = r_1^2 + r_3^2$ and $\alpha_3(q) = r_1^2 + r_2^2$. If $v = (v_1, v_2, v_3) \in S^3$ has $Rv = \hat{k}$ (or alternatively, $R^T \hat{k} = v$),

then

$$Y(q) = \frac{c^2 v_1}{\alpha_1(q)} + \frac{c^2 v_2}{\alpha_2(q)} + \frac{c^2 v_3}{\alpha_3(q)}$$

This formulation of Y displays the dependence on the shape of the configuration through the eigenvalues $\alpha_1(q), \alpha_2(q), \alpha_3(q)$ and the dependence on the orientation through the components of the vector v_1, v_2, v_3 .

While the characterization of the integral manifolds in terms of the super-level sets of a single function on a sphere has a certain elegance to it, there are some complexities within this formulation. Implicit in the definition of $D(q)$ is that both $U(q)$ and $Y(q)$ must be defined at q . The potential function is undefined at collisions, and the function Y is undefined for collinear configurations that do not lie in the invariant plane. The domain of definition is therefore not the full mass ellipsoid \mathcal{S} , but rather the dense subset

$$\mathcal{S}_0 = \mathcal{S} \setminus (\Delta \cup (\mathcal{C} \setminus \mathcal{C}_0))$$

An added complexity is that Y , and hence D , is discontinuous at \mathcal{C}_0 . Related to that discontinuity, for points q with $D(q) > -2h$, the pre-image $\Theta^{-1}(q)$ in $\mathfrak{M}(c, h)$ is the sphere S^6 for non-collinear configurations, while for collinear configurations, the pre-image is S^7 .

Those complexities are addressed by introducing a blow-up construction. The space \mathcal{B} is formed from \mathcal{S}_0 by replacing each collinear configuration in the invariant plane $q \in \mathcal{C}_0$ with a set of the form $S^4 \setminus S^0$. As \mathcal{S} has dimension 8 and \mathcal{C}_0 has dimension 3, the 4-sphere can be viewed as the sphere of directions normal to \mathcal{C}_0 in \mathcal{S} . The deleted antipodal points correspond to the direction of approach to q from $\mathcal{C} \setminus \mathcal{C}_0$. Removing those directions of approach reflects the fact that collinear configurations outside of the invariant plane are excluded. The punctured sphere attached at $q \in \mathcal{C}_0$ is denoted $\mathcal{B}_0(q)$. The union of those sets is \mathcal{B}_0 and the space resulting from attaching \mathcal{B}_0 to $\mathcal{S}_0 \setminus \mathcal{C}_0$ is \mathcal{B} .

While somewhat awkward, this blow-up set proves to be precisely what is needed to define Y continuously. The intuition is that, if the deleted antipodal points in the 4-sphere attached at $q_0 \in \mathcal{C}_0$ are viewed as the poles and the corresponding S^3 as the equator, then it is the latitude that measures the proximity to the “forbidden” collinear configurations that are not orthogonal to the angular momentum vector. This captures the different limiting values of $Y(q)$ as $q \rightarrow q_0$. This allows Y to be extended continuously to \mathcal{B} . We can clearly extend U to \mathcal{B} by assigning value $U(q)$ at every point in $\mathcal{B}_0(q)$, and so extend D continuously to \mathcal{B} .

Moreover, when the blow-up $\varrho : \mathcal{B} \rightarrow \mathcal{S}$ is pulled back to produce $\mathfrak{N}(c, h) \rightarrow \mathfrak{M}(c, h)$, the discontinuity in the dimension of the fiber is eliminated. The projection $\Theta : \mathfrak{N}(c, h) \rightarrow \mathcal{B}$ then has the properties that $\Theta(\mathfrak{N}(c, h)) = \{q \in \mathcal{B} | D(q) \geq -2h\}$, with $\Theta^{-1}(q) \cong S^{3N-6}$ for all q with $D(q) > -2h$ and $\Theta^{-1}(q)$ collapsing to a single point when $D(q) = -2h$.

The impact on homology groups of the pull-back from $\mathfrak{M}(c, h)$ to $\mathfrak{N}(c, h)$ and projection onto \mathcal{B} can be traced. The pull-back requires us to distinguish behavior at the collinear blow-up set, while the projection distinguishes behavior on $\{D(q) = -2h\}$ vs. $\{D(q) > -2h\}$. In the end, the following subsets of \mathcal{B} are found to play a role in computing the homology groups of $\mathfrak{M}(c, h)$ and $\mathfrak{M}_R(c, h)$:

$$\begin{aligned} \mathfrak{B}(d) &= \{q \in \mathcal{B} | D(q) \geq d\} \\ \partial\mathfrak{B}(d) &= \{q \in \mathcal{B} | D(q) = d\} \\ \mathfrak{B}_0(d) &= \{q \in \mathcal{B}_0 | D(q) \geq d\} \\ \partial\mathfrak{B}^+(d) &= \partial\mathfrak{B}(d) \cup \mathfrak{B}_0(d) \end{aligned}$$

These sets will emerge as our primary objects of study. We will also make frequent use of some related sets

$$\begin{aligned} \mathfrak{B}(d_i, d_j) &= \{q \in \mathcal{B} \mid d_i \leq D(q) \leq d_j\} \\ \mathcal{P}(d) &= \{q \in \mathcal{P} \mid D(q) \geq d\} \\ \partial\mathcal{P}(d) &= \{q \in \mathcal{P} \mid D(q) = d\} \\ \mathcal{P}(d_i, d_j) &= \{q \in \mathcal{P} \mid d_i \leq D(q) \leq d_j\} \end{aligned}$$

Note that, while the sets $\mathcal{P}(d)$, $\partial\mathcal{P}(d)$, $\mathcal{P}(d_i, d_j)$ are clearly related to the corresponding sets $\mathfrak{B}(d)$, $\partial\mathfrak{B}(d)$, $\mathfrak{B}(d_i, d_j)$, the various planar sets are not simply subsets of the corresponding spatial sets, as \mathcal{P} is not a subset of \mathcal{B} . The relationship between the planar and spatial sets will be an important component of the analysis, and will be explored below.

For $N = 4$, it was shown in [9] that the homology groups of $H_*(\mathfrak{M})$ are given by

$$H_k(\mathfrak{M}) \cong \begin{cases} \text{im}(j_* : H_3(\mathfrak{B}) \rightarrow H_3(\mathfrak{B}, \mathfrak{B}_0)) & k = 3 \\ H_k(\mathfrak{B}, \mathfrak{B}_0) \oplus H_{k-6}(\mathfrak{B}, \partial\mathfrak{B}^+) & k = 4, 5, 6, 10, 11, 12 \\ H_k(\mathfrak{B}) \oplus H_{k-6}(\mathfrak{B}, \partial\mathfrak{B}) & k = 0, 1, 2, 7, 8, 9, k > 12 \end{cases}$$

All of these constructions are invariant under the SO_2 rotation around the z -axis (i.e. around \vec{c}). The homology groups of $H_*(\mathfrak{M}_R)$ are given by

$$H_k(\mathfrak{M}_R) \cong \begin{cases} H_k(\mathfrak{B}_R, \mathfrak{B}_{R0}) \oplus H_{k-6}(\mathfrak{B}_R, \partial\mathfrak{B}_R^+) & k = 3, 4, 5, 10, 11 \\ H_k(\mathfrak{B}_R) \oplus H_{k-6}(\mathfrak{B}_R, \partial\mathfrak{B}_R) & \text{otherwise} \end{cases}$$

2.3 Singular Values of Energy on the Angular Momentum Manifold

Albouy [1] provides necessary conditions for an energy level h to be a bifurcation value of $H|_{\mathfrak{A}}$. As a smooth function on a non-compact manifold, bifurcation values of the level sets of H on \mathfrak{A} can occur only at singular values of $H|_{\mathfrak{A}}$, which can arise in one of two ways. The most straightforward is $h = H(q, p)$ for a critical point (q, p) . Critical point occur when $\nabla H(q, p) = \lambda_x \nabla C_x(q, p) + \lambda_y \nabla C_y(q, p) + \lambda_z \nabla C_z(q, p)$ for some $\Lambda = (\lambda_x, \lambda_y, \lambda_z)$, and are well-known to correspond to relative equilibria: planar central configurations uniformly rotating around the center of mass. If \mathfrak{A} were compact, those would be the only singular values. However, \mathfrak{A} has two sources of non-compactness: the collision set has been deleted, and momenta are not bounded. Albouy demonstrated that the former does not generate singular values of H , but the latter can. Namely, singular values also occur when there exists a sequence $\{(q_n, p_n)\} \subset \mathfrak{A}$ and sequence $\Lambda_n = (\lambda_{nx}, \lambda_{ny}, \lambda_{nz})$ such that $\nabla H(q_n, p_n) - \lambda_{nx} \nabla C_x(q_n, p_n) - \lambda_{ny} \nabla C_y(q_n, p_n) - \lambda_{nz} \nabla C_z(q_n, p_n)$ tends to zero and $H(q_n, p_n)$ tends to a finite limit h_s . Albouy refers to such a sequence as a *horizontal critical sequence* and produces necessary and sufficient conditions for a value h_s to be associated with a horizontal critical sequence. These are referred to as *bifurcations at infinity*.

The result of Albouy’s analysis is that, for non-zero angular momentum c , the singular values of $H|_{\mathfrak{A}}$ can be identified by the following algorithm:

- (1) Identify all planar central configurations of the N -body problem with masses m_1, \dots, m_N .
- (2) For each N -body central configuration q , normalized so that $q^2 = 1$, the corresponding singular value is $H = -\frac{1}{2}p^2 = -\frac{U^2(q)}{2c^2}$.
- (3) The set of finite singular values of H is the set of values $-\frac{U^2(q)}{2c^2}$ as q varies over all planar central configurations with $q^2 = 1$.

- (4) Identify all planar central configurations for all subsets of the masses m_{i_1}, \dots, m_{i_k} .
- (5) Take all possible non-trivial partitions of the index set $\{1, \dots, N\}$.
- (6) For any non-trivial partition $\sigma_1, \dots, \sigma_l$, associate with each non-trivial cluster $\sigma_j = \{i_1, \dots, i_k\}$ in the partition a planar central configuration q_{σ_j} of the k -body problem with masses m_{i_1}, \dots, m_{i_k} . Normalize each $q_{\sigma_j} = 1$, and let $U_{\sigma_j}(q_{\sigma_j})$ denote the potential energy of the configuration within the k -body problem.
- (7) If $\sigma_1, \dots, \sigma_l$ are the non-trivial clusters of a partition, and $q_{\sigma_1}, \dots, q_{\sigma_l}$ are the corresponding normalized planar central configurations, then the resulting singular value is

$$H = \frac{-1}{2c^2} \left(\sum_j U_{\sigma_j}^{\frac{2}{3}}(q_{\sigma_j}) \right)^3.$$
- (8) The set of singular values at infinity of H is the set of values $\frac{-1}{2c^2} \left(\sum_j U_{\sigma_j}^{\frac{2}{3}}(q_{\sigma_j}) \right)^3$, ranging over all possible non-trivial partitions of the masses m_1, \dots, m_N and all possible planar central configurations associated with the non-trivial clusters of those partitions.

Applying the algorithm to four equal masses, there are four planar central configurations [2]: the square, isosceles, equilateral and collinear configurations. For sub-clusters with three equal masses, there are two central configurations: the equilateral and collinear configurations. For sub-clusters with two equal masses, there is only the collinear configuration. This produces the following cases, summarized in Table 1:

- Six distinct partitions into a two-body cluster and two trivial clusters. All occur at the same energy level h_1 .
- Three distinct partitions into two two-body clusters, with one collinear configuration for each partition. All occur at the same energy level h_2 . This is the only instance in which two non-trivial clusters occur.
- Eight distinct partitions into a three-body cluster and a trivial cluster, with the three masses forming a Lagrange configuration. All occur at the same energy level h_3 .
- Twelve distinct partitions into a three-body cluster and a trivial cluster, with the three-body cluster forming an Euler configuration. All occur at the same energy level h_4 .
- Six square configurations, corresponding the six cyclical orderings of the masses, which are all distinct relative to the preferred direction of the angular momentum vector, but all occurring at the same energy level h_5 .
- Twenty-four isosceles configurations, corresponding to distinct ordering of the masses. All occur at the same energy level h_6 .
- Eight equilateral triangle configurations, corresponding to the four choices for the center mass and two cyclical orderings of the remaining three masses. All occur at the same energy level h_7 .
- Twelve distinct collinear central configurations (corresponding to the 24 possible orderings of the masses, modulo the rotational symmetry that identifies pairs whose orderings are reversed). All occur at the same energy level h_8 .

Note that, except for the case of h_2 , there is only one non-trivial cluster, with one central configuration q_i . With q_i normalized to $q_i^2 = 1$, then the corresponding singular energy level is $h_i = -\frac{1}{2c^2} U_0^2(q_i)$. At h_2 , where we have two binary clusters, $h_2 = -\frac{1}{2c^2} (2U_0^{\frac{2}{3}}(q_i))^3 = -\frac{4}{c^2} U_0^2(q_i)$. This produces the results displayed in Table 1. Properly speaking, for given non-zero angular momentum c , it is the quotient of the values in the table by c^2 that are the singular values. Also, while it is clearly redundant to list both h_i and $\delta_i = -2h_i$, we list both for the convenience of the reader: on the one hand, it is the values of h_i that are shown to be

the bifurcation values of the integral manifolds; on the other hand, as outlined in Sect. 2.2, all of the calculational effort will be organized around a function D on the configuration space whose singular values are $-2h_i$. We will use d_i to signify a value of d with $\delta_{i-1} < d_i < \delta_i$ (i.e. a value in region i). Finally, note that the energy level for the isosceles configurations is incorrectly stated in [8, 9]. This impacts the ordering of the bifurcation levels, reversing the order of the isosceles and equilateral bifurcation levels.

2.4 Global Analysis of the Functions

The first goal is to show that there is a one-to-one correspondence between bifurcations of D on S_0 and bifurcations of H on the angular momentum manifold $\mathfrak{A}(c)$. This correspondence holds for both finite bifurcations and bifurcations at infinity. More precisely, we show that there is a one-to-one correspondence between singular values of D and singular values of H , and likewise, that there is a one-to-one correspondence between critical sequences of D and critical sequences of H . This validates the reduction approach by establishing that no new singular values are created by the projection onto B .

For H on $\mathcal{A}(c)$, a horizontal critical sequence consists of a sequence of points (q_n, p_n) and a sequence of values $\lambda_{1n}, \lambda_{2n}, \lambda_{3n}$ such that:

- (1) $H(q_n, p_n)$ is bounded and converges to h_s with $-\infty < h_s < 0$.
- (2) $\nabla H(q_n, p_n) - \lambda_{1n} \nabla C_1(q_n, p_n) - \lambda_{2n} \nabla C_2(q_n, p_n) - \lambda_{3n} \nabla C_3(q_n, p_n) \rightarrow 0$ as $n \rightarrow \infty$
- (3) $J(q_n) p_n = c\hat{k}$

The analogue for D on S_0 is a sequence of points q_n such that:

- (1) $D(q_n)$ is bounded and converges to d_s with $0 < d_s < \infty$.
- (2) $\nabla D(q_n) \rightarrow 0$ as $n \rightarrow \infty$.

Both singular values and critical sequences are detected by the vanishing of $\nabla_T D(q)$, the tangent component of ∇D . However, as D is homogeneous of degree 0, $\nabla D(q) = \nabla_T D(q)$. As

$$\nabla D(q) = \frac{2U(q)}{Y(q)} \nabla U(q) - \frac{U^2(q)}{Y^2(q)} \nabla Y(q),$$

$\nabla D(q)$ can only vanish when $\nabla U(q)$ and $\nabla Y(q)$ are parallel.

If $r_{ij} = |\vec{x}_i - \vec{x}_j| = \sqrt{(q_{1i} - q_{1j})^2 + (q_{2i} - q_{2j})^2 + (q_{3i} - q_{3j})^2}$, then

$$\nabla U(q) = \begin{bmatrix} \Xi(q) & 0 & 0 \\ 0 & \Xi(q) & 0 \\ 0 & 0 & \Xi(q) \end{bmatrix} \begin{bmatrix} q_1 \\ q_2 \\ q_3 \end{bmatrix}$$

where

$$\Xi(q) = \begin{bmatrix} -\frac{1}{r_{12}^3} - \frac{1}{r_{13}^3} - \frac{1}{r_{14}^3} & \frac{1}{r_{12}^3} & \frac{1}{r_{13}^3} & \frac{1}{r_{14}^3} \\ \frac{1}{r_{12}^3} & -\frac{1}{r_{12}^3} - \frac{1}{r_{23}^3} - \frac{1}{r_{24}^3} & \frac{1}{r_{23}^3} & \frac{1}{r_{24}^3} \\ \frac{1}{r_{13}^3} & \frac{1}{r_{23}^3} & -\frac{1}{r_{13}^3} - \frac{1}{r_{23}^3} - \frac{1}{r_{34}^3} & \frac{1}{r_{34}^3} \\ \frac{1}{r_{14}^3} & \frac{1}{r_{24}^3} & \frac{1}{r_{34}^3} & -\frac{1}{r_{14}^3} - \frac{1}{r_{24}^3} - \frac{1}{r_{34}^3} \end{bmatrix}$$

To formulate the comparable expression for Y , we introduce the following quantities. For $i \neq j$, let $q_{ij} = q_i \cdot q_j$ denote the inner product, and let

$$\begin{aligned} \kappa_1 &= q_{13}(q_1^2 + q_3^2) + q_{12}q_{23} \\ \kappa_2 &= q_{23}(q_2^2 + q_3^2) + q_{12}q_{13} \\ \kappa_3 &= (q_1^2 + q_3^2)(q_2^2 + q_3^2) - q_{12}^2 \\ \Delta &= \kappa_3(q_1^2 + q_2^2) - q_{13}^2(q_1^2 + q_3^2) - q_{23}^2(q_2^2 + q_3^2) - 2q_{12}q_{13}q_{23} \end{aligned}$$

then $Y(q) = \frac{c^2\kappa_3}{\Delta}$ and

$$\nabla Y(q) = \frac{-2c^2}{\Delta^2} \begin{bmatrix} (\kappa_2^2 + \kappa_3^2)I & -\kappa_1\kappa_2I & -\kappa_1\kappa_3I \\ -\kappa_1\kappa_2I & (\kappa_1^2 + \kappa_3^2)I & -\kappa_2\kappa_3I \\ -\kappa_1\kappa_3I & -\kappa_2\kappa_3I & (\kappa_1^2 + \kappa_2^2)I \end{bmatrix} \begin{bmatrix} q_1 \\ q_2 \\ q_3 \end{bmatrix}. \tag{2.4.1}$$

The eigenvalues are 0 with multiplicity 4 and $\frac{-2c^2(\kappa_1^2 + \kappa_2^2 + \kappa_3^2)}{\Delta^2}$ with multiplicity 8.

We want to identify the points at which ∇Y and ∇U are parallel. The expression above for ∇Y is a bit difficult to work with in general. However, we can significantly restrict the values at which we need to evaluate ∇Y , and the expression simplifies considerably at those values.

To see this, take a standard configuration $r = (r_1, r_2, r_3)$. We will focus on non-collinear configurations. Consider the family Rr for $R \in SO_3$. As U is invariant under rotation, its directional derivative along this family is 0, so $\nabla U(q)$ and $\nabla Y(q)$ can be parallel only if the directional derivative of Y also vanishes. We can sweep out such a family by rotating first about the z -axis, then about the y -axis, then again about the z -axis. As Y is invariant under this last rotation, we restrict attention to the two parameter family swept out by rotations of the form

$$R(\phi, \theta) = \begin{bmatrix} \cos(\phi) \cos(\theta) & -\cos(\phi) \sin(\theta) & -\sin(\phi) \\ \sin(\theta) & \cos(\theta) & 0 \\ \sin(\phi) \cos(\theta) & -\sin(\phi) \sin(\theta) & \cos(\phi) \end{bmatrix}$$

If r has $\alpha_1 = r_2^2 + r_3^2, \alpha_2 = r_1^2 + r_3^2, \alpha_3 = r_1^2 + r_2^2$, then as a function of ϕ and θ ,

$$Y(\phi, \theta) = \frac{c^2 \sin^2(\phi) \cos^2(\theta)}{\alpha_1} + \frac{c^2 \sin^2(\phi) \sin^2(\theta)}{\alpha_2} + \frac{c^2 \cos^2(\phi)}{\alpha_3}.$$

Lemma 2.4.1 *If r is a non-collinear standard configuration, then the critical points of Y on the two-parameter family $R(\phi, \theta)r$ occur at the following values of ϕ, θ and α_i 's:*

- $\alpha_1 = \alpha_2 = \alpha_3$
- $\alpha_1 = \alpha_2$ and $\phi = \frac{n\pi}{2}$
- $\phi = \frac{n\pi}{2}$ and $\theta = \frac{n\pi}{2}$
- $\phi = n\pi$

The first of these situations, when $\alpha_1 = \alpha_2 = \alpha_3$, is easily dealt with:

Lemma 2.4.2 *The unique O_3 -orbit with $\alpha_1 = \alpha_2 = \alpha_3$ is the tetrahedral central configuration.*

Proof If a standard vector r has $\alpha_1(r) = \alpha_2(r) = \alpha_3(r)$, then $I(r) = \frac{2}{3}\text{Id}$, and any rotation $q = Rr$ has $I(q) = RI(r)R^T = \frac{2}{3}\text{Id}$. That is, $q_1 \cdot q_2 = q_1 \cdot q_3 = q_3 \cdot q_3 = 0$ and $q_1^2 = q_2^2 = q_3^2 = \frac{1}{3}$. Solving the system of six equations $q_i \cdot q_j = \frac{1}{3}\delta_{ij}$ in the nine unknowns yields a three-parameter family of solutions in which all of the mutual distances equal $\sqrt{\frac{2}{3}}$. \square

Two valuable results follow from Lemma 2.4.1.

Proposition 2.4.1 *The restriction of Y to S_0 has critical point set consisting of all points in the invariant plane \mathcal{P} .*

Proof As Y is invariant under rotation about the z -axis, the critical point set is invariant. If q is a critical point, then up to rotation about the z -axis, $q = R(\phi, \theta)r$ for some ϕ, θ and r . If q is a critical point of the restriction of Y to S_0 , then it is a critical point of the restriction of Y to the (ϕ, θ) -family. We can therefore restrict to evaluating ∇Y under each of the conditions identified in Lemma 2.4.1.

At the tetrahedral configuration q_0 , $\nabla Y(q_0) = -\frac{3}{2}q_0$, so the tetrahedral configuration is not a critical point of Y .

For all of the other cases ($\alpha_1 = \alpha_2$ and $\phi = \frac{n\pi}{2}$; $\phi = \frac{n\pi}{2}$ and $\theta = \frac{n\pi}{2}$; or $\phi = n\pi$), $\nabla Y(q) = -\frac{2c^2}{(q_1^2+q_2^2)^2}(q_1, q_2, 0)$, which is only equal to its normal component if either $q_3 = 0$ or $q_1 = q_2 = 0$. The latter corresponds to a collinear configuration along the z -axis, which is forbidden, leaving only the case $q_3 = 0$. Conversely, if q is an arbitrary non-collinear configuration in the invariant plane, then $\kappa_1 = \kappa_2 = 0$ and $\Delta = \kappa_3$, in which case $\nabla Y(q) = \frac{-2c}{k_3^2}(q_1, q_2, 0)$, which is its normal component. \square

Proposition 2.4.2 *On S_0 , the set of points where the gradients of U and Y are parallel consists of the invariant plane \mathcal{P} and at the tetrahedral configuration.*

Proof To identify when these vectors are parallel, first note that $\nabla_T U(q) = 0$ is precisely the condition for q to be a central configuration, while $\nabla_T Y(q) = 0$ if and only if $q_3 = 0$. We can therefore focus on the situation when both $\nabla_T U(q)$ and $\nabla_T Y(q)$ are non-zero and $\nabla_T U(q) = \lambda \nabla_T Y(q)$ with $\lambda \neq 0$.

We consider two cases:

- I. The configuration lies in a plane: there is a vector $\vec{v} \in \mathbb{S}^2$ such that each particle position vector \vec{x}_i has $\vec{v} \cdot \vec{x}_i = 0$.
- II. The position vectors span \mathbb{R}^3 .

Case I

In the first case, if all of the position vectors satisfy $\vec{v} \cdot \vec{x}_i = 0$, then $\vec{v} \cdot \nabla_i U(q) = 0$. We show that, in order for $\vec{v} \cdot \nabla_i Y(q) = 0$ for all i , we must have $\vec{v} = \pm \hat{k}$. Since both Y and U are invariant under rotation about \hat{k} , we may assume without loss that $\vec{v} = (-\sin(t), 0, \cos(t))$. Further, for $\vec{v} \neq \pm \hat{k}$, there is no loss in assuming that the position vectors x_i span the orthogonal complement to \vec{v} , as otherwise the configuration would be a collinear configuration that does not lie in the invariant plane.

Observe that $\nabla_i Y(q) = K(q)x_i$ for the symmetric matrix $K(q)$, so the condition $\vec{v} \cdot \nabla_i Y(q) = 0$ for all i is equivalent to $K(q)\vec{v} = 0$. The kernel of $K(q)$ is spanned by $\vec{k} = (\kappa_1, \kappa_2, \kappa_3)$. Under the assumption that $q_1 = \cos(t)q_0, q_3 = \sin(t)q_0$ for some q_0 , the quantities κ_i simplify to

$$\begin{aligned} \kappa_1 &= q_0^2 \cos(t) \sin(t)(1 - q_2^2 \sin^2(\theta)) \\ \kappa_2 &= |q_0||q_2| \sin(t) \cos(\theta) \\ \kappa_3 &= q_0^2(q_2^2(1 - \cos^2(t) \cos^2(\theta)) + q_0^2 \sin^2(t)) \end{aligned}$$

where $q_0 \cdot q_2 = |q_0||q_2| \cos(\theta)$. In order for κ_2 to vanish, we can set aside either $q_0 = 0$ or $q_2 = 0$ (as either corresponds to collinear), while $\sin(t) = 0$ corresponds to $\vec{v} = \pm \hat{k}$. We can

therefore focus on $\cos(\theta) = 0$, in which case

$$\begin{aligned} \kappa_1 &= q_0^2 \cos(t) \sin(t)(1 - q_2^2) \\ \kappa_2 &= 0 \\ \kappa_3 &= q_0^2(q_2^2 + q_0^2) \sin^2(t) \end{aligned}$$

from which we can see $\frac{\kappa_1}{\kappa_3} \neq \tan(t)$.

Case II

Consider once again a standard configuration r with $0 < r_3^2 \leq r_2^2 \leq r_1^2$ and the two parameter family of configurations $R(\phi, \theta)r$. The potential U is invariant under rotation, so $U(R(\phi, \theta))$ is constant on this family, so the directional derivatives of U along this family are zero. But if $\nabla_T U(q)$ is a non-zero scalar multiple of $\nabla_T Y(q)$ at some point q in this family, then the directional derivative of Y along the family must also be zero at q . This limits us once again to the configurations identified in Lemma 2.4.1. Setting aside the tetrahedral configuration, in all other cases,

$$\nabla_T Y(q) = -\frac{2c^2}{(q_1^2 + q_2^2)^2} (q_3^2 q_1, q_3^2 q_2, (q_1^2 + q_2^2) q_3).$$

If $\nabla_T U(q) = \lambda \nabla_T Y(q)$, then

$$\begin{aligned} \Xi(q)q_1 &= \frac{-2\lambda c^2 q_3^2 - U(q)(q_1^2 + q_2^2)^2}{(q_1^2 + q_2^2)^2} q_1 = \lambda_1 q_1 \\ \Xi(q)q_2 &= \frac{-2\lambda c^2 q_3^2 - U(q)(q_1^2 + q_2^2)^2}{(q_1^2 + q_2^2)^2} q_2 = \lambda_1 q_2 \\ \Xi(q)q_3 &= \frac{-2\lambda c^2 (q_1^2 + q_2^2) - U(q)(q_1^2 + q_2^2)^2}{(q_1^2 + q_2^2)^2} q_3 = \lambda_3 q_3 \end{aligned}$$

In particular, each of the component vectors q_i is either zero or an eigenvector of $\Xi(q)$; and if q_1 and q_2 are both non-zero, then they have a common eigenvalue. If $q_1^2 + q_2^2 \neq q_3^2$, then q_3 is either zero or an eigenvector with distinct eigenvalue, and so is orthogonal to q_1 and q_2 .

This implies $q = (q_1, q_2, q_3)$ is a *balanced configuration* [14]. One characterization of balanced configurations is that $X^T X \Xi(q) = \Xi(q) X^T X$, where X is the 3×4 matrix whose rows are q_i . If each q_i has $\Xi_i q_i = \lambda_i q_i$, then

$$\Xi(q)X^T = [\lambda_1 q_1 \quad \lambda_2 q_2 \quad \lambda_3 q_3]$$

and $(\Xi(q)X^T X)_{ij} = \lambda_i q_i \cdot q_j$. On the other side,

$$X \Xi(q) = \begin{bmatrix} \lambda_1 q_1 \\ \lambda_2 q_2 \\ \lambda_3 q_3 \end{bmatrix}$$

and $(X^T X \Xi(q))_{ij} = \lambda_j q_i \cdot q_j$. As $\lambda_1 = \lambda_2, \lambda_1 q_1 \cdot q_2 = \lambda_2 q_1 \cdot q_2$. Similarly, since we either have $\lambda_3 = \lambda_1 = \lambda_2$ or $q_1 \cdot q_3 = q_2 \cdot q_3 = 0$, we have $\lambda_i q_i \cdot q_3 = \lambda_3 q_i \cdot q_3$ for $i = 1, 2$. We can thus conclude that that $X^T X \Xi(q) = \Xi(q) X^T X$ and q is a balanced configuration.

Another characterization of balanced configurations is that $\Xi(q) + \mu \hat{S} q = 0$, where $\hat{S} = \text{diag}(S, S, S, S)$ with $S = -\alpha^2$ and α a 3×3 anti-symmetric matrix. That is, $\text{diag}(\lambda_1, \lambda_1, \lambda_3) + S = 0$, which is only possible if $\lambda_3 = 0$ and $S = \text{diag}(\lambda_1, \lambda_1, 0)$. This implies that the configuration is a planar central configuration. \square

In addition to demonstrating the one-to-one correspondence between singular values of H on $\mathfrak{A}(c)$ and singular values of D on \mathfrak{B} , we will proceed a bit further, and show that both are equivalent to the potentially weaker condition that $\nabla U(q)$ and $\nabla Y(q)$ are parallel (or become parallel in the limit as $q_n \rightarrow q_0 \in \Delta_C$

Proposition 2.4.3 ∇U and ∇Y are parallel at $q \in \mathcal{S}$ if and only if $q \in \mathcal{P}$ is the projection onto \mathcal{S} of a critical point of H on $\mathcal{A}(c)$. A point $q_0 \in \mathcal{S}^8 \setminus \mathcal{S}$ admits a sequence $\{q_n\} \subset \mathcal{S}_0 \setminus \mathcal{C}_0$ that limits to q_0 with $D(q_n) \rightarrow \delta_0$ and $\nabla U(q_n), \nabla Y(q_n)$ limiting to parallel if and only if $\{q_n\}$ is the projection of a horizontal critical sequence of H on $\mathcal{A}(c)$.

Proof For H on $\mathcal{A}(c)$, the quantity of interest is

$$\begin{aligned} \nabla H(Q_n, P_n) - \sum_{i=1}^3 \lambda_{in} \nabla C_i(Q_n, P_n) &= \begin{bmatrix} -\nabla_1 U(Q_n) + c\lambda_{3n} P_{2n} - c\lambda_{2n} P_{3n} \\ -\nabla_2 U(Q_n) + c\lambda_{1n} P_{3n} - c\lambda_{3n} P_{1n} \\ -\nabla_3 U(Q_n) + c\lambda_{2n} P_{1n} - c\lambda_{1n} P_{2n} \\ P_{1n} + c\lambda_{2n} Q_{3n} - c\lambda_{3n} Q_{2n} \\ P_{2n} + c\lambda_{3n} Q_{1n} - c\lambda_{1n} Q_{3n} \\ P_{3n} + c\lambda_{1n} Q_{2n} - c\lambda_{2n} Q_{1n} \end{bmatrix} \\ &= \begin{bmatrix} -\nabla U(Q_n) + cJ^T(P_n)\Lambda_n \\ P_n - J^T(Q_n)\Lambda_n \end{bmatrix} \end{aligned}$$

For D on \mathcal{S}_0 , the homogeneity of D implies that the normal component of ∇D is always zero, so we consider $\nabla D(q_n) = \frac{2U(q_n)}{Y(q_n)} \nabla U(q_n) - \frac{U^2(q_n)}{Y^2(q_n)} \nabla U(q_n)$.

Albouy [1] shows that if there is a horizontal critical sequence associated with energy level h , then there is a *model sequence* (Q_n, P_n) with the following properties:

- When the particles are partitioned so that particles with the same z -value form a partition, the resulting sub-clusters have (x, y) -coordinates that form a central configuration. In particular, the center of mass of the configuration is located on the z -axis, which implies $Q_1 \cdot Q_3 = Q_2 \cdot Q_3 = 0$.
- The z -coordinates diverge to infinity, so that the between-cluster contributions to U diminish to 0 while the within-cluster contributions remain constant.
- The momenta all have $P_z = 0$, while (P_x, P_y) are those of a relative equilibrium. Namely, $P_n = cJ^T(Q_n)\Lambda_n$, where $\Lambda_n = cI^{-1}(Q_n)\hat{k}$. The conditions $Q_i \cdot Q_3 = 0$ imply that $\Lambda_n = (0, 0, \frac{c}{Q_1^2 + Q_2^2})$, and $P_n^2 = c^2 \hat{k} I^{-1}(Q_n) J(Q_n) J^T(Q_n) I^{-1}(Q_n) \hat{k}$, which we recognize as $Y(Q_n)$.

Inserting this into the expressions for $H(Q, P)$ and $\nabla H(Q, P) - \sum_i \lambda_i \nabla C_i$, we see that $H(Q_n, P_n) = \frac{1}{2}Y(Q_n) - U(Q_n) \rightarrow h_s$, with $U(Q_n) = Y(Q_n) = -2h_s$. Further,

$$\begin{aligned} -\nabla U(Q_n) + cJ^T(J^T(Q_n)\Lambda_n)\Lambda_n &\rightarrow 0 \\ P_n - J^T(Q_n)\Lambda_n &= 0 \end{aligned}$$

Applying Eq. 2.4.1, this implies that $2\nabla U(q_n) - \nabla Y(q_n)$ converges to 0.

Now, let $\mu_n = |Q_n|$ and q_n be the projection $q_n = \frac{1}{\mu_n} Q_n$. Note that model critical sequences of H have $\mu_n \rightarrow \infty$. By the homogeneity, $2\nabla U(Q_n) - \nabla Y(Q_n)$ converging to 0 implies that $\frac{2}{\mu_n^2} \nabla U(q_n) - \frac{1}{\mu_n^3} \nabla Y(q_n)$ converges to 0.

$\frac{1}{2}Y(Q_n) - U(Q_n) \rightarrow h_s$. At the same time $\frac{U^2(q_n)}{Y(q_n)} = D(q_n) \rightarrow -2h_s$. Taken together, these imply $U(Q_n)$ and $Y(Q_n)$ converge to a common finite value $-2h_s$ as $n \rightarrow \infty$. That in turn implies $\frac{U(Q_n)}{Y(Q_n)} \rightarrow 1$, so by homogeneity, $\mu_n \frac{U(q_n)}{Y(q_n)} \rightarrow 1$. This allows us to rewrite $\frac{2}{\mu_n^2} \nabla U(Q_n) - \frac{1}{\mu_n^3} \nabla Y(Q_n)$ as $\frac{2U(q_n)}{Y(Q_n)} \nabla U(q_n) - \frac{U(q_n)}{Y^2(q_n)} \nabla Y(q_n)$. This establishes the result in one direction.

To prove the other direction, first suppose that there exist sequences a_n and b_n such that $a_n \nabla U(q_n) - b_n \nabla Y(q_n) \rightarrow 0$. Then $a_n q_n \nabla U(q_n) - b_n q_n \nabla Y(q_n) = (-a_n U(q_n) +$

$2b_n Y(q_n)q_n \rightarrow 0$, so the sequences must have $\frac{a_n}{b_n} \rightarrow \frac{2Y(q_n)}{U(q_n)}$. We may then, without loss, take $a_n = 2Y(q_n)$ and $b_n = U(q_n)$.

Now, take $Q_n = \mu_n q_n$, with $\mu_n = \frac{a_n}{2b_n} = \frac{Y(q_n)}{U(q_n)}$. As q_n (and hence Q_n) are not collinear, $J(Q_n)$ has rank 3 and $I(Q_n) = J(Q_n)J^T(Q_n)$ is invertible. We can then define $\Lambda_n = cI^{-1}(Q_n)\hat{k}$ and $P_n = J^T(Q_n)\Lambda_n = cJ^T(Q_n)I^{-1}(Q_n)\hat{k}$. To show that $\{(Q_n, P_n)\}$ is a horizontal critical sequence for H on the angular momentum manifold $\mathfrak{A}(c)$, we must show that

- $H(Q_n, P_n)$ is bounded.
- $\nabla H(Q_n, P_n) - \sum_i \lambda_i \nabla C_i(Q_n, P_n) \rightarrow 0$.

For the first point, note that P_n was chosen so that $P_n^2 = Y(Q_n)$. The homogeneity of Y and U therefore implies that

$$\begin{aligned} H(Q_n, P_n) &= \frac{1}{2}Y(Q_n) - U(Q_n) \\ &= \frac{1}{2\mu_n^2}Y(q_n) - \frac{1}{\mu_n}U(q_n) \\ &= \frac{U^2(q_n)Y(q_n)}{2Y^2(q_n)} - \frac{U^2(q_n)}{Y(q_n)} \\ &= -\frac{1}{2}D(q_n) \end{aligned}$$

which has finite limit $-\frac{\delta_0}{2}$.

For the second point, direct calculation shows that

$$\begin{aligned} \nabla H(Q_n, P_n) - \sum_{i=1}^3 \lambda_{in} \nabla C_i(Q_n, P_n) &= \begin{bmatrix} -\nabla U(Q_n) + cJ^T(P_n)\Lambda_n \\ P_n - J^T(Q_n)\Lambda_n \end{bmatrix} \\ &= \begin{bmatrix} -\nabla U(Q_n) + cJ^T(J^T(Q_n)\Lambda_n)\Lambda_n \\ 0 \end{bmatrix} \\ &= \begin{bmatrix} -\nabla U(Q_n) + \frac{1}{2}\nabla Y(Q_n) \\ 0 \end{bmatrix} \end{aligned}$$

Focusing on $-\nabla U(Q_n) + \frac{1}{2}\nabla Y(Q_n)$ and once again using the homogeneity, we see

$$\begin{aligned} -\nabla U(Q_n) + \frac{1}{2}\nabla Y(Q_n) &= -\frac{1}{\mu_n^2}\nabla U(q_n) + \frac{1}{2\mu_n^3}\nabla Y(q_n) \\ &= -\frac{U^2(q_n)}{Y^2(q_n)}\nabla U(q_n) + \frac{U^3(q_n)}{2Y^3(q_n)}\nabla Y(q_n) \\ &= -\frac{U^2(q_n)}{2Y^3(q_n)}(2Y(q_n)\nabla U(q_n) - U(q_n)\nabla Y(q_n)) \end{aligned}$$

The scalar multiple $\frac{U^2(q_n)}{2Y^3(q_n)} = \frac{D(q_n)}{Y^2(q_n)}$ is bounded above by $D(q_n)$, which converges to a finite limit, so the sequence converges to 0, as required. □

We may focus henceforth on the behavior of D on \mathcal{B} . To do so, the first observation is that D is a decreasing function of the “vertical” component q_3 . This will allow us to make contact with the bifurcations of U on the planar manifold \mathcal{P} , which is a much better understood problem.

Lemma 2.4.3 *D is a decreasing function of $|q_3|$. That is, for fixed $(q_1, q_2) \in \mathcal{P}$ and q_3 with $q_3^2 = 1$, $D(\sqrt{1-t^2}q_1, \sqrt{1-t^2}q_2, tq_3)$ is a decreasing function of t for $0 < t < 1$.*

Proof For fixed q_1, q_2, q_3 with $q_1^2 + q_2^2 = q_3^2 = 1$, let $q(t) = (\sqrt{1-t^2}q_1, \sqrt{1-t^2}q_2, tq_3)$. Then

$$\frac{d}{dt}D(q(t)) = \left(\frac{-t}{\sqrt{1-t^2}}q_1, \frac{-t}{\sqrt{1-t^2}}q_2, q_3\right) \cdot \nabla D(\sqrt{1-t^2}q_1, \sqrt{1-t^2}q_2, tq_3)$$

As D is homogeneous of degree 0, $\frac{-t}{\sqrt{1-t^2}}(\sqrt{1-t^2}q_1, \sqrt{1-t^2}q_2, tq_3) \cdot \nabla D(q(t)) = 0$, so $\frac{d}{dt}D(q(t)) = \frac{1}{1-t^2}(0, 0, q_3) \cdot \nabla D(q(t))$. That is, it suffices to show $(0, 0, q_3) \cdot \nabla D(q(t)) < 0$ for $0 < t < 1$.

$$(0, 0, q_3) \cdot \nabla D(q) = \frac{2U(q)}{Y(q)}(0, 0, q_3) \cdot \nabla U(q) - \frac{U^2(q)}{Y^2(q)}(0, 0, q_3) \cdot \nabla Y(q)$$

The inner product $(0, 0, q_3) \cdot \nabla U(q)$ has well-known form:

$$(0, 0, q_3) \cdot \nabla U(q) = - \sum_{i \neq j} \frac{(q_{3i} - q_{3j})^2}{r_{ij}^3} < 0.$$

From Eq. 2.4.1, we see

$$(0, 0, q_3) \cdot \nabla Y(q) = \frac{-2c^2}{\Delta^2} ((\kappa_1^2 + \kappa_2^2)q_3^2 - \kappa_1\kappa_3q_1 \cdot q_3 - \kappa_2\kappa_3q_2 \cdot q_3)$$

Evaluating this expression, and writing $c_{ij}q_iq_j$ for $q_i \cdot q_j$, we find

$$(0, 0, q_3) \cdot \nabla U(q) = \frac{2c^2q_1^2q_2^2q_3^2}{\Delta^2} (q_3^4(c_{13}^2 - 2c_{12}c_{13}c_{23} + c_{23}^2) + (1 - c_{12}^2)(c_{13}^2q_1^4 + 2c_{12}c_{13}c_{23}q_1^2q_2^2 + c_{23}^2q_2^4 + 2q_3^2(c_{13}q_1^2 + c_{23}q_2^2)))$$

The quantity $(c_{13}^2 - 2c_{12}c_{13}c_{23} + c_{23}^2)$ is bounded between $(c_{13} - c_{23})^2$ and $(c_{13} + c_{23})^2$, and the quantity $(c_{13}^2q_1^4 + 2c_{12}c_{13}c_{23}q_1^2q_2^2 + c_{23}^2q_2^4)$ is bounded between $(c_{13}q_1^2 - c_{23}q_2^2)^2$ and $(c_{13}q_1^2 + c_{23}q_2^2)^2$, so $(0, 0, q_3) \cdot \nabla Y(q)$ is non-negative for all q . \square

2.5 The Hills Region

We conclude this section with a proof of Corollary 1.0.3. The arguments for $N = 3$ involve somewhat tedious special cases, and were already treated in [6], so we focus on $N \geq 4$ bodies. As the projection $\Omega : \mathfrak{H}(c, h) \rightarrow S_0$ to the configuration space simply collapses intervals to points, $\mathfrak{H}(c, h)$ has the same homotopy type as its image under Ω , $\mathfrak{R}(c, h)$. It suffices then to prove the following:

Lemma 2.5.1 For $N > 4$ masses,

$$H_k(\mathfrak{R}) \cong \begin{cases} H_k(\mathfrak{B}, \mathfrak{B}_0) & k = 2N - 5, 2N - 4, 2N - 3 \\ & 3N - 8, 3N - 7, 3N - 6 \\ H_k(\mathfrak{B}) & \text{otherwise} \end{cases}$$

while for $N = 4$ masses,

$$H_k(\mathfrak{R}) \cong \begin{cases} im(j_* : H_3(\mathfrak{B}) \rightarrow H_3(\mathfrak{B}, \mathfrak{B}_0)) & k = 3 \\ H_k(\mathfrak{B}, \mathfrak{B}_0) & k = 4, 5, 6. \\ H_k(\mathfrak{B}) & \text{otherwise} \end{cases}$$

For all $N \geq 4$,

$$H_k(\mathfrak{R}_R) \cong \begin{cases} H_k(\mathfrak{B}_R, \mathfrak{B}_0) & k = 2N - 5, 2N - 4 \\ & 3N - 8, 3N - 7. \\ H_k(\mathfrak{B}) & \text{otherwise} \end{cases}$$

Proof The sets $\mathfrak{B}(d)$ and $\mathfrak{R}(d)$ differ only at the blow-up of collinear configurations, with $\mathfrak{B}_0(d) \simeq \mathcal{C}(d) \times S^{2N-5}$, and

$$\mathcal{C} \cong \left(\bigsqcup_{\alpha} D^{N-2} \times S^1 \sqcup \bigsqcup_{\beta} S^{N-3} \times [0, 1) \times S^1 \right)$$

Examining the commutative diagram of the map of pairs $\varrho : (\mathfrak{B}(d), \mathfrak{B}_0(d)) \rightarrow (\mathfrak{R}(d), \mathcal{C}_0(d))$

$$\begin{array}{ccccccccc} H_{k+1}(\mathfrak{B}(d), \mathfrak{B}_0(d)) & \longrightarrow & H_k(\mathfrak{B}_0(d)) & \longrightarrow & H_k(\mathfrak{B}(d)) & \longrightarrow & H_k(\mathfrak{B}(d), \mathfrak{B}_0(d)) & \longrightarrow & H_{k-1}(\mathfrak{B}_0(d)) \\ \downarrow \cong & & \downarrow & & \downarrow & & \downarrow \cong & & \downarrow \\ H_{k+1}(\mathfrak{R}(d), \mathcal{C}_0(d)) & \longrightarrow & H_k(\mathcal{C}_0(d)) & \longrightarrow & H_k(\mathfrak{R}(d)) & \longrightarrow & H_k(\mathfrak{R}(d), \mathcal{C}_0(d)) & \longrightarrow & H_{k-1}(\mathcal{C}_0(d)) \end{array}$$

the five lemma implies that $H_k(\mathfrak{B}(d)) \rightarrow H_k(\mathfrak{R}(d))$ is an isomorphism when $H_k(\mathfrak{B}(d)) \rightarrow H_k(\mathfrak{R}(d))$ and $H_{k-1}(\mathfrak{B}(d)) \rightarrow H_{k-1}(\mathfrak{R}(d))$ are, namely, all k outside the range from $2N - 5$ to $2N - 3$ and $3N - 8$ to $3N - 6$. In that range, $H_k(\mathcal{C}_0(d)) = 0$ for all d , so we have isomorphisms $H_k(\mathfrak{R}(d)) \rightarrow H_k(\mathfrak{R}(d), \mathcal{C}_0(d)) \leftarrow H_k(\mathfrak{B}(d), \mathfrak{B}_0(d))$.

The one special case is $k = 3, N = 4$. There, we have

$$\begin{array}{ccccccccc} H_4(\mathfrak{B}(d), \mathfrak{B}_0(d)) & \longrightarrow & H_3(\mathfrak{B}_0(d)) & \longrightarrow & H_3(\mathfrak{B}(d)) & \xrightarrow{j_*} & H_3(\mathfrak{B}(d), \mathfrak{B}_0(d)) & \longrightarrow & H_2(\mathfrak{B}_0(d)) \\ \downarrow \cong & & \downarrow & & \downarrow & & \downarrow \cong & & \downarrow \cong \\ H_4(\mathfrak{R}(d), \mathcal{C}_0(d)) & \longrightarrow & 0 & \longrightarrow & H_3(\mathfrak{R}(d)) & \longrightarrow & H_3(\mathfrak{R}(d), \mathcal{C}_0(d)) & \longrightarrow & H_2(\mathcal{C}_0(d)) \end{array}$$

A simple diagram chase yields the result.

The arguments for $H_k(\mathfrak{R}(d))$ are similar. □

Comparison with the formulae in [9, Theorem 7.1, Theorem 7.2] provides the last step needed to prove Corollary 1.0.3.

3 The Planar Manifold

While the results of [1, 6, 10] show that the bifurcations of the spatial manifolds involve more than just the structure of the planar manifold, it is still the case that the planar manifold and its bifurcations play a critical role in understanding the behavior of the spatial manifolds. In this section, we focus on the planar configuration space \mathcal{P} and the behavior of D on it. We record the results here for two purposes: to establish the baseline of planar results that will be needed for our subsequent analysis of the spatial configurations; and to correct the erroneous values in [8] for the homology of the planar integral manifolds.

3.1 Planar Configuration Spaces

The behavior of D on the planar manifold is simplified by the observation that $Y(q) = 1$ for planar configurations, so the level sets and super-level sets of D are the same as those of U , and the bifurcation points are the critical points of U , i.e. the central configurations. The local structure is well-known: on the reduced manifold \mathcal{P} , the central configurations are all non-degenerate, with potential levels, multiplicities and Morse indices in \mathcal{P} as shown in Table 2.

Table 2 Planar Central Configurations

Configuration	$\delta_i = U^2$	Multiplicity	Morse Index
Square	58.6274	6	0
Isosceles	67.1757	24	1
Equilateral	67.1769	8	2
Collinear	93.6832	12	2

Given regular values $d_i < d_j$, it will be useful to identify the homology groups of pairs of the form $(\mathcal{P}(d_i, d_j), \partial\mathcal{P}(d_i))$ and $(\mathcal{P}(d_i, d_j), \partial\mathcal{P}(d_j))$. To do so, we use a Morse-theoretic approach:

- Given $d_5 < \delta_5 < \delta_8 < d_9$, there is a maximal set \mathcal{I} that is invariant under ΔU and contained in $\mathcal{P}_R(d_5, d_9)$, which has the homotopy type of $\mathcal{P}_R \setminus \Delta_{RP}$.
- The critical points of U form a Morse decomposition of \mathcal{I} . That is, \mathcal{I} consists of the critical points and connecting orbits between them.
- For every $i < j$ in $\{5, 6, 7, 8\}$, let $C_{ij}^+ = \bigoplus_{k=i}^{j-1} H_*(\mathcal{P}_R(d_k, d_{k+1}), \partial\mathcal{P}_R(d_{k+1}))$ and $C_{ij}^- = \bigoplus_{k=i}^{j-1} H_*(\mathcal{P}_R(d_k, d_{k+1}), \partial\mathcal{P}_R(d_k))$. There exist degree -1 maps $\chi^+ : C_{58}^+ \rightarrow C_{58}^+$ and $\chi^- : C_{58}^- \rightarrow C_{58}^-$ with $(\chi^\pm)^2 = 0$ such that if χ^\pm is restricted to C_{ij}^\pm , then the resulting homology $H_*(\chi_{ij}^+) \cong H_*(\mathcal{P}_R(d_i, d_j), \partial\mathcal{P}_R(d_j))$ and $H_*(\chi_{ij}^-) \cong H_*(\mathcal{P}_R(d_i, d_j), \partial\mathcal{P}_R(d_i))$.

To compute these *connection matrices* χ^\pm , we observe that the values for C_{58}^\pm are determined by the multiplicity and Morse indices of the critical points. Further, $(\mathcal{P}(d_5, d_9), \partial\mathcal{P}(d_5)) \simeq (\mathcal{P} \setminus \Delta_P)$ and $H_*(\mathcal{P}(d_5, d_9), \partial\mathcal{P}(d_9)) \cong H_*(\mathcal{P}, \Delta_P)$ by excision. These are well-known values:

k	0	1	2	3	4	k	0	1	2	3	4
C_{56}^-	\mathbb{Z}^6	0	0	0	0	C_{56}^+	0	0	0	0	\mathbb{Z}^6
C_{67}^-	0	\mathbb{Z}^{24}	0	0	0	C_{67}^+	0	0	0	\mathbb{Z}^{24}	0
C_{78}^-	0	0	\mathbb{Z}^8	0	0	C_{78}^+	0	0	\mathbb{Z}^8	0	0
C_{89}^-	0	0	\mathbb{Z}^{12}	0	0	C_{89}^+	0	0	\mathbb{Z}^{12}	0	0
C_{59}^-	\mathbb{Z}	\mathbb{Z}^5	\mathbb{Z}^6	0	0	C_{59}^+	0	0	\mathbb{Z}^6	\mathbb{Z}^5	\mathbb{Z}

That is, there are chain complexes $\mathbb{Z}^{20} \xrightarrow{\chi^-} \mathbb{Z}^{24} \xrightarrow{\chi^-} \mathbb{Z}^6$ and $\mathbb{Z}^6 \xrightarrow{\chi^+} \mathbb{Z}^{24} \xrightarrow{\chi^+} \mathbb{Z}^{20} \xrightarrow{\chi^-} 0 \xrightarrow{\chi^-} 0$ whose homology groups are $(\mathbb{Z}, \mathbb{Z}^5, \mathbb{Z}^6, 0, \dots)$ and $(0, 0, \mathbb{Z}^6, \mathbb{Z}^5, \mathbb{Z}, 0, \dots)$ respectively. These requirements constrain $\chi^- : \mathbb{Z}^{20} \rightarrow \mathbb{Z}^{24}$ to have rank 14 and $\chi^- : \mathbb{Z}^{24} \rightarrow \mathbb{Z}^6$ to have rank 5, with χ^+ dual.

This leaves undetermined the rank of χ_{67}^- . To determine that, we observe that the collinear manifold C_0 is repelling in \mathcal{P} , so we can consider $C_0 \cup \Delta_{\mathcal{P}}$ to be a repeller in S^5 . The dual attractor has the homology of $\mathcal{P} \setminus C_0 = S^5 \setminus (\Delta_{\mathcal{P}} \cup C_0)$. The homology groups of $(\mathcal{P} \setminus C_0) / SO_2$ have been calculated in [8] as $(\mathbb{Z}, \mathbb{Z}^{11}, 0, \dots)$. If we view the non-collinear central configurations

as a Morse decomposition of the attractor, we have a chain complex $\mathbb{Z}^8 \xrightarrow{\chi_{67}^-} \mathbb{Z}^{24} \xrightarrow{\chi_{56}^-} \mathbb{Z}^6$ whose homology groups generate $H_*(\mathcal{P}_R \setminus C_{0R})$. This implies $\mathbb{Z}^8 \xrightarrow{\chi_{67}^-} \mathbb{Z}^{24}$ is injective.

From this, we can compute all of the values of the pairs $H_*(\mathcal{P}(d_i, d_j), \partial\mathcal{P}(d_i))$ and $H_*(\mathcal{P}(d_i, d_j), \partial\mathcal{P}(d_j))$

Lemma 3.1.1 For regular values $d_i < d_j$, we have the following homology groups

k	$\mathcal{P}(d)$				$\mathcal{P}_R(d)$		
	0	1	2	3	0	1	2
$(\mathcal{P}(d_5, d_6), \partial\mathcal{P}(d_5))$	\mathbb{Z}^6	\mathbb{Z}^6	0	0	\mathbb{Z}^6	0	0
$(\mathcal{P}(d_6, d_7), \partial\mathcal{P}(d_6))$	0	\mathbb{Z}^{24}	\mathbb{Z}^{24}	0	0	\mathbb{Z}^{24}	0
$(\mathcal{P}(d_7, d_8), \partial\mathcal{P}(d_7))$	0	0	\mathbb{Z}^8	\mathbb{Z}^8	0	0	\mathbb{Z}^8
$(\mathcal{P}(d_8, d_9), \partial\mathcal{P}(d_8))$	0	0	\mathbb{Z}^{12}	\mathbb{Z}^{12}	0	0	\mathbb{Z}^{12}
$(\mathcal{P}(d_5, d_7), \partial\mathcal{P}(d_5))$	\mathbb{Z}	\mathbb{Z}^{20}	\mathbb{Z}^{19}	0	\mathbb{Z}	\mathbb{Z}^{19}	0
$(\mathcal{P}(d_6, d_8), \partial\mathcal{P}(d_6))$	0	\mathbb{Z}^{16}	\mathbb{Z}^{16}	0	0	\mathbb{Z}^{16}	0
$(\mathcal{P}(d_7, d_9), \partial\mathcal{P}(d_7))$	0	0	\mathbb{Z}^{20}	\mathbb{Z}^{20}	0	0	\mathbb{Z}^{20}
$(\mathcal{P}(d_5, d_8), \partial\mathcal{P}(d_5))$	\mathbb{Z}	\mathbb{Z}^{12}	\mathbb{Z}^{11}	0	\mathbb{Z}	\mathbb{Z}^{11}	0
$(\mathcal{P}(d_6, d_9), \partial\mathcal{P}(d_6))$	0	\mathbb{Z}^{10}	\mathbb{Z}^{16}	\mathbb{Z}^6	0	\mathbb{Z}^{10}	\mathbb{Z}^6
$(\mathcal{P}(d_5, d_9), \partial\mathcal{P}(d_5))$	\mathbb{Z}	\mathbb{Z}^6	\mathbb{Z}^{11}	\mathbb{Z}^6	\mathbb{Z}	\mathbb{Z}^5	\mathbb{Z}^6

and

k	\mathcal{P}						\mathcal{P}_R				
	0	1	2	3	4	5	0	1	2	3	4
$(\mathcal{P}(d_5, d_6), \partial\mathcal{P}(d_6))$	0	0	0	0	\mathbb{Z}^6	\mathbb{Z}^6	0	0	0	0	\mathbb{Z}^6
$(\mathcal{P}(d_6, d_7), \partial\mathcal{P}(d_7))$	0	0	0	\mathbb{Z}^{24}	\mathbb{Z}^{24}	0	0	0	0	\mathbb{Z}^{24}	0
$(\mathcal{P}(d_7, d_8), \partial\mathcal{P}(d_8))$	0	0	\mathbb{Z}^8	\mathbb{Z}^8	0	0	0	0	\mathbb{Z}^8	0	0
$(\mathcal{P}(d_8, d_9), \partial\mathcal{P}(d_9))$	0	0	\mathbb{Z}^{12}	\mathbb{Z}^{12}	0	0	0	0	\mathbb{Z}^{12}	0	0
$(\mathcal{P}(d_5, d_7), \partial\mathcal{P}(d_7))$	0	0	0	\mathbb{Z}^{19}	\mathbb{Z}^{20}	\mathbb{Z}	0	0	0	\mathbb{Z}^{19}	\mathbb{Z}
$(\mathcal{P}(d_6, d_8), \partial\mathcal{P}(d_8))$	0	0	0	\mathbb{Z}^{16}	\mathbb{Z}^{16}	0	0	0	0	\mathbb{Z}^{16}	0
$(\mathcal{P}(d_7, d_9), \partial\mathcal{P}(d_9))$	0	0	\mathbb{Z}^{20}	\mathbb{Z}^{20}	0	0	0	0	\mathbb{Z}^{20}	0	0
$(\mathcal{P}(d_5, d_8), \partial\mathcal{P}(d_8))$	0	0	0	\mathbb{Z}^{11}	\mathbb{Z}^{12}	\mathbb{Z}	0	0	0	\mathbb{Z}^{11}	\mathbb{Z}
$(\mathcal{P}(d_6, d_9), \partial\mathcal{P}(d_9))$	0	0	\mathbb{Z}^6	\mathbb{Z}^{16}	\mathbb{Z}^{10}	0	0	0	\mathbb{Z}^6	\mathbb{Z}^{10}	0
$(\mathcal{P}(d_5, d_9), \partial\mathcal{P}(d_9))$	0	0	\mathbb{Z}^6	\mathbb{Z}^{11}	\mathbb{Z}^6	\mathbb{Z}	0	0	\mathbb{Z}^6	\mathbb{Z}^5	\mathbb{Z}

Proof The values for the reduced spaces follow immediately from χ^\pm . The values for the total spaces follow from the Gysin sequences, except for $(\mathcal{P}(d_5, d_9), \partial\mathcal{P}(d_5))$ and $(\mathcal{P}(d_5, d_9), \partial\mathcal{P}(d_9))$. There, $(\mathcal{P}(d_5, d_9), \partial\mathcal{P}(d_5)) \simeq (\mathcal{P} \setminus \Delta_P, \emptyset)$ and $(\mathcal{P}(d_5, d_9), \partial\mathcal{P}(d_9)) \simeq (\mathcal{P}, \Delta_P)$, whose values are known. \square

3.2 Planar Integral Manifolds

As noted in Sect. 2, the energy levels and Morse indices of the isosceles configurations are incorrectly stated in [7]. The homology calculations that follow are therefore incorrect as well. Before considering the bifurcations of the spatial manifolds, we correct the calculation of the planar manifolds. To do so, we make use of the formulae from [8], restated in the notation of the current work:

$$\begin{aligned}
 H_*(\mathfrak{m}(d)) &= H_*(\mathfrak{m}_R(d)) \otimes H_*(S^1) \\
 H_k(\mathfrak{m}_R(d)) &= H_k(\mathcal{P}_R(d)) \oplus H_{k-5}(\mathcal{P}_R(d), \partial\mathcal{P}_R(d))
 \end{aligned}$$

Inserting the values from Lemma 3.1.1, we obtain immediately the homology of the planar integral manifolds:

Theorem 3.2.1 *planar integral manifold homology* For four equal masses, the planar integral manifolds $\mathfrak{m}(h, c)$ and reduced manifolds $\mathfrak{m}_R(h, c)$ undergo bifurcation at values h_i for $i = 0, 5, 6, 7, 8$, corresponding to zero energy and energy levels of the planar relative equilibria. At regular values, the homology of the planar integral manifolds is

Region	0	1	2	3	4	5	6	7	8
0	\mathbb{Z}	\mathbb{Z}^6	\mathbb{Z}^{11}	\mathbb{Z}^6	0	0	0	0	0
I – V	\mathbb{Z}	\mathbb{Z}^6	\mathbb{Z}^{11}	\mathbb{Z}^6	0	\mathbb{Z}	\mathbb{Z}^6	\mathbb{Z}^{11}	\mathbb{Z}^6
VI	\mathbb{Z}	\mathbb{Z}^6	\mathbb{Z}^{11}	\mathbb{Z}^{12}	\mathbb{Z}^6	0	\mathbb{Z}^{10}	\mathbb{Z}^{16}	\mathbb{Z}^6
VII	\mathbb{Z}	\mathbb{Z}^6	\mathbb{Z}^{30}	\mathbb{Z}^{26}	\mathbb{Z}	0	0	\mathbb{Z}^{20}	\mathbb{Z}^{20}
VIII	\mathbb{Z}	\mathbb{Z}^6	\mathbb{Z}^{22}	\mathbb{Z}^{18}	\mathbb{Z}	0	0	\mathbb{Z}^{12}	\mathbb{Z}^{12}
IX	\mathbb{Z}	\mathbb{Z}^{12}	\mathbb{Z}^{22}	\mathbb{Z}^{12}	\mathbb{Z}	0	0	0	0

while the homology of the reduced planar manifolds is

Region	0	1	2	3	4	5	6	7
0	\mathbb{Z}	\mathbb{Z}^5	\mathbb{Z}^6	0	0	0	0	0
I – V	\mathbb{Z}	\mathbb{Z}^5	\mathbb{Z}^6	0	0	\mathbb{Z}	\mathbb{Z}^5	\mathbb{Z}^6
VI	\mathbb{Z}	\mathbb{Z}^5	\mathbb{Z}^6	\mathbb{Z}^6	0	0	\mathbb{Z}^{10}	\mathbb{Z}^6
VII	\mathbb{Z}	\mathbb{Z}^5	\mathbb{Z}^{25}	\mathbb{Z}	0	0	0	\mathbb{Z}^{20}
VIII	\mathbb{Z}	\mathbb{Z}^5	\mathbb{Z}^{17}	\mathbb{Z}	0	0	0	\mathbb{Z}^{12}
IX	\mathbb{Z}	\mathbb{Z}^{11}	\mathbb{Z}^{11}	\mathbb{Z}	0	0	0	0

Proof The values for $H_{k-5}(\mathcal{P}_R(d), \partial\mathcal{P}_R(d))$ are read off directly from Lemma 3.1.1. To obtain the values for $H_k(\mathcal{P}_R(d_i))$, we consider the exact sequences of pairs $(\mathcal{P}_R(d_i), \mathcal{P}_R(d_9))$. The homology groups of $\mathcal{P}_R(d_9)$ are known to be $(\mathbb{Z}, \mathbb{Z}^{11}, \mathbb{Z}^{11}, \mathbb{Z}, 0, \dots)$ (see [8, Sect. 3]), and by excision, $H_*(\mathcal{P}_R(d_i), \mathcal{P}_R(d_9)) \cong H_*(\mathcal{P}_R(d_i, d_9), \partial\mathcal{P}_R(d_9))$. It suffices to determine the boundary operator $H_{k+1}(\mathcal{P}_R(d_i), \mathcal{P}_R(d_9)) \rightarrow H_k(\mathcal{P}_R(d_9))$. To do so, we first consider the exact sequence of the pair $(\mathcal{P}(d_5, d_9), \partial\mathcal{P}(d_9))$. Inserting the known values for $H_*(\mathcal{P}(d_9))$, $H_*(\mathcal{P}(d_5))$ and $H_*(\mathcal{P}(d_9), \mathcal{P}(d_5))$, we see that the boundary operator $H_{k+1}(\mathcal{P}(d_9), \mathcal{P}(d_5)) \rightarrow H_k(\mathcal{P}(d_5))$ is injective.

In the exact sequence of the pair $(\mathcal{P}_R(d_i), \mathcal{P}_R(d_9))$, the boundary operator $\partial_{i9} : H_k(\mathcal{P}_R(d_i), \mathcal{P}_R(d_9)) \rightarrow H_{k-1}(\mathcal{P}_R(d_9))$ factors as $H_k(\mathcal{P}_R(d_i), \mathcal{P}_R(d_9)) \xrightarrow{\iota_{i5}^*} H_k(\mathcal{P}(d_5), \mathcal{P}_R(d_9)) \xrightarrow{\partial_{59}} H_{k-1}(\mathcal{P}_R(d_9))$. As ∂_{59} is injective, the rank of ∂_{i9} is that of ι_{i5}^* . This can be computed from the exact sequence of the triple $(\mathcal{P}(d_5, d_9), \mathcal{P}(d_i, d_9), \partial\mathcal{P}(d_9))$. Inserting the known values into the exact sequences yields the following information

k	0	1	2	3	4
ι_{69}	0	0	6	5	0
ι_{79}	0	0	6	0	0
ι_{89}	0	0	6	0	0
$rk(\iota_{i5}^*)$					

The values for $H_*(\mathcal{P}(d_i))$ for $i = 6, 7, 8$ follow from this. □

4 Topological Descriptions

In this section, we work through some of the topological preliminaries needed to set the stage for the homological calculations. A key step in identifying the changes in topology at

the relative equilibria will be to ground the computations of $H_*(\mathfrak{B}(d))$ by first identifying the homology groups at the two ends $d_5 < \delta_5$ and $\delta_8 < d_9$. At the lower end, $H_*(\mathfrak{B}(d_5))$ has been established (see [10, Sect. 4.5]). At the upper end, $\delta_8 < d_9 < \infty$, we produce a topological description of $\mathfrak{B}(d_9)$, then translate it into a homological description. The identification of $H_*(\mathfrak{B}(d_9))$ and $H_*(\mathfrak{B}_R(d_9))$ is the most intricate calculation in this work. This is in contrast with the planar case, where the corresponding set is a tubular neighborhood of the planar collision set, and as such is relatively simple to understand. In the spatial case, the interplay of $U^2(q)$ and $Y(q)$ near collinear collision adds a layer of complexity. We know from Sect. 2.4 that there are no bifurcations of $\partial\mathfrak{B}(d)$ for $d > \delta_8$, which will facilitate approximating $\mathfrak{B}(d_9) \simeq \partial\mathfrak{B}(d_9)$ and computing its homology. This analysis will pave the way for the results that follow. In addition, in Sect. 4.2, the changes in the structure of D on the boundary \mathcal{B}_0 are recorded. Completing the topological preliminaries, the relations between the topology of the planar configuration sets $\mathcal{P}(d)$ and corresponding spatial configuration sets $\mathfrak{B}(d)$ are established in Sect. 4.3.1.

4.1 The Topology of $\mathfrak{B}(d_9)$

In this section, we develop the topological description of $\mathfrak{B}(d_9)$. We do so by separately characterizing the behavior near collinear and away from collinear. To do so, note that since $D(q) = U^2(q)Y^{-1}(q) \leq U^2(q)$, we have $\mathfrak{B}(d_9) \subset U^{-1}(\sqrt{d_9})$. In particular, for $d_9 \gg \delta_8$, the set $\mathfrak{B}(d_9)$ lies in an ϵ -collar of Δ .

For the four-body problem, the binary collision sets Δ_{ij} intersect only in Δ_C . That is, $\Delta \setminus \Delta_C = \bigsqcup_{i \neq j} \Delta_{ij} \setminus \Delta_{ijC}$. While the collision sets Δ_{ij} are disjoint in $S^8 \setminus \mathcal{C}$, the ϵ -collars around them intersect near \mathcal{C} . Sandwiched between the two, we manage the description of $\mathfrak{B}(d_9)$ by first taking a set of disjoint collars G_{ij} around the sets $\Delta_{ij} \setminus \Delta_{ijC}$. Let $G = \bigsqcup_{i \neq j} G_{ij}$. We next identify a set F near collinear that contains $\mathfrak{B}(d_9) \setminus G$, so that if $J = F \cap G$, then we have a decomposition $\mathfrak{B}(d_9) = F \cup_J G$.

We make use of a construction deployed in [9, 10]. For $q_0 \in \mathcal{C}_L$, define

$$\mathcal{T}^0(q_0, \tau) = \varrho^{-1} \left(\left\{ (\sqrt{1-t^2}q_0, tq_2, tq_3) \mid q_2 \cdot q_0 = q_3 \cdot q_0 = 0, q_2^2 + q_3^2 = 1, t \leq \tau \right\} \right),$$

$\mathcal{X}^0(q_0) = \{(q_0, q_2, q_3, t = 0) \in \mathcal{T}^0(q_0)\}$ and for rotation $R(\phi)$ by ϕ around the y -axis, define

$$\mathcal{T}(q_0, \tau) = \left\{ R(\phi)q(t) \mid -\frac{\pi}{2} \leq \phi \leq \frac{\pi}{2}, q(t) \in \mathcal{T}^0(q_0, \tau) \right\}.$$

and

$$\mathcal{T}^1(q_0, \tau) = \left\{ R\left(\frac{\pi}{2}\right)q(t) \mid q(t) \in \mathcal{T}^0(q_0, \tau) \right\}.$$

For any $A \subseteq \mathcal{C}_L$, let $\mathcal{T}(A, \tau)$ and $\mathcal{T}^i(A, \tau)$ denote the obvious unions over $q_0 \in A$ of the appropriate sets. Then rotation around the z -axis of $\mathcal{T}(\mathcal{C}_L, \tau)$ forms neighborhood of a blow-up at \mathcal{C} . Two useful observations about the behavior of D in this framework are

- $D(R(\phi)q)$ is a decreasing function of $|\phi|$.
- For $q(t) = (tq_1, tq_2, \sqrt{1-t^2}q_3) \in \mathcal{T}^1(\mathcal{C}, \tau)$, $D(q(t)) = \left(\frac{t}{c}U(q(t))\right)^2$

So, if we define $\mathcal{I}_\tau = \mathcal{T}^1(\mathcal{C}_L, (0, \tau]) \cap D^{-1}([d_9, \infty))$, then

$$\mathcal{I}_\tau = \{q = (tq_1, tq_2, \sqrt{1-t^2}q_3) \mid q_1 \cdot q_3 = q_2 \cdot q_3 = 0, q_1^2 + q_2^2 = 1, \\ U(q) \geq \frac{\sqrt{d_9}}{t}, 0 < t \leq \tau\}$$

Given $\epsilon > 0$, there is a sufficiently large d_9 such that $\{U(\frac{q}{t}) \geq \sqrt{d_9}\} \subset \bigcup_{i \neq j} \{r_{ij} < \epsilon\}$, or $\{U(\frac{q}{t}) \geq \sqrt{d_9}\} \subset \bigcup_{i \neq j} \{|\frac{q_i - q_j}{t}| < \epsilon\}$, or

$$\mathcal{I}_\tau \subset \bigcup_{i \neq j} \{q = (tq_1, tq_2, \sqrt{1-t^2}q_3) \mid q_1 \cdot q_3 = q_2 \cdot q_3 = 0, q_1^2 + q_2^2 = 1, \\ r_{ij} < \epsilon t, 0 < t \leq \tau\}$$

The point is, these sets are mutually disjoint, with each contained in a collar of Δ_{ij} .

Next, for τ_0 sufficiently small, there is a ϕ_0 such that for all $|\phi| > |\phi_0|$, the sets $R(\phi - \frac{\pi}{2})\mathcal{I}_{ij}$ remain disjoint. Further, for $|\phi_2| < |\phi_1| \leq |\phi_0|$, there is containment

$$R(\phi_2 - \phi_1) (\mathfrak{B}(d_9) \cap R(\phi_1)T^0(\mathcal{C}_L, \tau_0)) \subset \mathfrak{B}(d_9) \cap R(\phi_2)T^0(\mathcal{C}_L, \tau_0)$$

so $\mathfrak{B}(d_9) \cap \mathcal{T}(\mathcal{C}_L, \tau_0)$ admits a retraction onto $\mathfrak{B}(d_9) \cap T^0(\mathcal{C}_L, \tau_0)$.

It suffices then to identify a neighborhood of $\mathfrak{B}(d_9) \cap T^0(\mathcal{C}_L, \tau_0)$. We do so as follows:

- Let K be the intersection of $\mathcal{X}^0(\Delta_C)$ with $cl(\Delta \setminus \Delta_C)$
- Let J be a neighborhood around K in $\mathcal{X}^0(\mathcal{C}_0)$ (i.e. the rotation of $\mathcal{X}^0(\mathcal{C}_L)$ around the z -axis).
- Let N be a neighborhood of $\mathcal{X}^0(\Delta_C)$ in $\mathcal{X}^0(\mathcal{C}_0)$ that contains $cl(J)$ in its interior. This is initially described as the rotation of $\Delta_C \cup U^{-1}([\sqrt{d_9}, \infty))$
- Let F be the complement of K in N .
- Let G be the closure in \mathcal{B} of a collar in \mathcal{S}_0 around $\Delta \setminus \Delta_C$, chosen so that $G \cap \mathcal{S}_0$ is the disjoint union of collars around the sets $\Delta_{ij} \setminus \Delta_{ijC}$.

Properly speaking, to form a collar around $\mathfrak{B}_0(d_9)$, we should consider $(L \setminus K) \times [0, \epsilon]$. However, the $[0, \epsilon]$ factor does not change the homotopy type, and so can be eliminated.

Lemma 4.1.1 *For $d_9 > \delta_8$, $\mathfrak{B}(d_9) \simeq \partial\mathfrak{B}(d_9)$. There is a $\tau_0 > 0$ such that $\mathfrak{B}(d_9)$ is homotopic to $(F \times [0, \tau_0]) \cup J \cup G$, with*

$$\begin{aligned} G &\cong \bigsqcup_6 SO_3 \times \bar{D}^2 \times (D^3 \setminus \{0\}) \\ J &\cong \bigsqcup_6 T^3 \times (D^3 \setminus \{0\}) \\ K &\cong (\bigsqcup_6 S^1 \times S^1 \times S^1) / \mathbb{Z}_2 \cong \bigsqcup_6 T^3 \\ N &\cong (\Delta_L \times S^1 \times S^3) / \mathbb{Z}_2 \cong (\bigvee_{12} S^1) \times S^1 \times S^3 \end{aligned}$$

Proof By the discussion above, we may approximate $\mathfrak{B}(d_9)$ by a collar around the components of $\Delta \setminus \Delta_C$ together with a neighborhood in \mathcal{B} of $\mathfrak{B}_0(d_9)$. Further, as $D(q)$ is a decreasing function of $q_3 \cdot q_0$ on the boundary \mathcal{B}_0 , we may further simplify by focusing on the behavior near $\mathcal{X}^0(\mathcal{C}_L)$ in $T^0(\mathcal{C}_L)$.

We have noted that the non-collinear binary collision sets $\Delta_{ij} \setminus \Delta_{ijC}$ are disjoint and each homeomorphic to $D^2 \times SO_3$. While in the configuration space S^8 , their closures intersect, the analysis in [9, 10] showed that the closure of each $\Delta_{ij} \setminus \Delta_{ijC}$ in $\mathcal{X}^0(\Delta_C)$ formed a 2-torus over the circle Δ_{C_L} , and that these tori do not intersect each other. When rotated around the z -axis, these sweep out six disjoint 3-tori.

Turning next to the behavior near collinear, the behavior of D on $\mathcal{X}^0(\mathcal{C}_L)$ is well-known: D is undefined on $\Delta_L \times S^3$ and $D(q) \geq d_9$ on $U^{-1}(\sqrt{d_9}) \times S^3$, with $U^{-1}(\sqrt{d_9})$ a disjoint set of

twenty-four annuli surrounding Δ_L . Let N_L denote $\Delta_L \times S^3$ together with the neighborhood surrounding it. Note that the annuli all retract onto Δ_L , so $N_L \simeq \Delta_L \times S^3$.

Moreover, as there are no critical values of U above $\sqrt{\delta_8}$ on \mathcal{B}_0 , level sets of $D = U^2$ are transverse to \mathcal{B}_0 . So, for τ_0 sufficiently small, on $T^0(\mathcal{C}_L, \tau_0) \setminus \mathcal{X}^0(\mathcal{C}_L)$, $D^{-1}([d_9, \infty]) \cong N \times (0, \tau_0]$, with $D^{-1}(\infty) \cong \bigsqcup_6 T^3$.

These sets provide a description of the intersection with $T^0(\mathcal{C}_L)$, that is, near collinear oriented along the x -axis. The set N is formed by rotation of N_L around the z -axis. Taking into account the antipodal symmetry, we see $N = (N \times S^1)/\mathbb{Z}_2$ and $N_R = N_L/\mathbb{Z}_2$. \square

Lemma 4.1.2 *For $\delta_8 < d_9$, we have homology groups*

	\mathfrak{B}						\mathfrak{B}_R						
	0	1	2	3	4	5	6	0	1	2	3	4	5
$\mathfrak{B}(d_9)$	\mathbb{Z}	\mathbb{Z}^6	\mathbb{Z}^{17}	$\mathbb{Z}^7 \oplus \mathbb{Z}_2^5$	\mathbb{Z}^{13}	\mathbb{Z}^{18}	0	\mathbb{Z}	\mathbb{Z}^6	\mathbb{Z}^{12}	\mathbb{Z}^1	\mathbb{Z}^{18}	0
$(\mathfrak{B}(d_9), \partial\mathfrak{B}(d_9))$	0	0	0	0	0	0	0	0	0	0	0	0	0

The maps $\zeta_{9*} : H_*(\mathfrak{B}_0(d_9)) \rightarrow H_*(\mathfrak{B}(d_9))$ and $\iota_{R0*} : H_*(\mathfrak{B}_{R0}(d_9)) \rightarrow H_*(\mathfrak{B}_R(d_9))$ behave as follows:

dim	$\ker(\zeta_{9*})$	$\text{coker}(\zeta_{9*})$	$\ker(\zeta_{R9*})$	$\text{coker}(\zeta_{R9*})$
5	0	\mathbb{Z}^6	0	0
4	\mathbb{Z}^{11}	0	0	\mathbb{Z}^6
3	\mathbb{Z}^{11}	\mathbb{Z}^6	\mathbb{Z}^{11}	0
2	\mathbb{Z}^6	\mathbb{Z}^{11}	0	\mathbb{Z}^{12}
1	\mathbb{Z}^{18}	0	\mathbb{Z}^6	0
0	\mathbb{Z}^{11}	0	\mathbb{Z}^{11}	0

Proof This description of $\mathfrak{B}(d_9) \simeq F \cup_J G$ lends itself naturally to computing the homology groups of $\mathfrak{B}(d_9)$ via a Mayer–Vietoris decomposition. As the homology groups of G and J are immediate from the topological descriptions, our task is to identify $H_*(F)$ and the inclusion maps $\iota_{JF} : H_*(J) \rightarrow H_*(F)$ and $\iota_G : H_*(J) \rightarrow H_*(G)$. The set $F = N \setminus K$ is presented as a complement, which is not a construction that lends itself to homological calculation. We therefore employ yet another Mayer–Vietoris decomposition of F . In order to also compute the inclusion map ι_F , the decomposition of F is intersected with J , and the maps ι_{JFi} on the various components are identified and collated. Once $\mathfrak{B}(d_9)$ is recovered, the last step will be to identify the map $\iota_{0*} : H_*(\mathfrak{B}_0(d_9)) \rightarrow H_*(\mathfrak{B}(d_9))$ by factoring it through $H_*(F)$.

Beginning with the most straightforward steps, we have:

	\mathfrak{B}						\mathfrak{B}_R						
	0	1	2	3	4	5	6	0	1	2	3	4	5
J	\mathbb{Z}^6	\mathbb{Z}^{18}	\mathbb{Z}^{24}	\mathbb{Z}^{24}	\mathbb{Z}^{18}	\mathbb{Z}^6	0	\mathbb{Z}^6	\mathbb{Z}^{12}	\mathbb{Z}^{12}	\mathbb{Z}^{12}	\mathbb{Z}^6	0
$\iota_{G*} \downarrow$	$\downarrow \cong$	\downarrow	\downarrow	\downarrow		0		$\downarrow \cong$		$\downarrow rk\ 6$		$\downarrow 0$	
G	\mathbb{Z}^6	\mathbb{Z}_2^6	\mathbb{Z}^6	$\mathbb{Z}^6 \oplus \mathbb{Z}_2^5$	0	\mathbb{Z}^6	0	\mathbb{Z}^6	0	\mathbb{Z}^{12}	0	\mathbb{Z}^6	0

The values for $H_*(G)$ and $H_*(G_R)$, $H_*(J)$ and $H_*(J_R)$ are immediate from the topological descriptions. For each of the six components, the product structures for $J_R \rightarrow G_R$ are $S^1 \times S^1 \times S^2 \rightarrow S^2 \times D^2 \times S^2$, which implies $H_2(J_R) \rightarrow H_2(G_R)$ has rank 6 and $H_4(J_R) \rightarrow H_4(G_R)$ is trivial. To identify $H_*(J) \rightarrow H_*(G)$, note that there are two commutative diagram of Gysin sequences: one with fiber S^2 , the other with fiber S^1 . Comparing values between

the two sequences shows that $H_k(J) \rightarrow H_k(G)$ is surjective for $k \leq 2$, maps onto the torsion component of $H_3(J)$ and is trivial for $k > 3$.

We next consider the groups $H_*(F)$ and $H_*(F_R)$ and maps $\iota_{F*} : H_*(J) \rightarrow H_*(F)$ and $\iota_{FR*} : H_*(J_R) \rightarrow H_*(F_R)$. As a starting point, we know that $F = N \setminus K$ is the rotation around the z -axis of $(N_L \setminus K_L) \times [0, \tau_0]$, where

$$\begin{aligned} K_L &= K \cap \mathcal{X}^0(\mathcal{C}_L) \cap \mathfrak{B}_0(d_9) \cong \bigsqcup_6 T^2 \\ N_L &= N \cap \mathcal{X}^0(\mathcal{C}_L) \cap \mathfrak{B}_0(d_9) \cong \Delta_L(d_9) \times S^3 \end{aligned}$$

are double-covers of D_R and N_R respectively.

For the purposes of computing the homology groups, without loss we suppress the $[0, \tau_0]$ factor and view N, K, J and F as subsets of \mathcal{B}_0 .

The set N is an S^3 bundle over Δ_C . More precisely, $N \simeq (\Delta_L \times S^1 \times S^3)/\mathbb{Z}_2$, where Z_2 acts antipodally on all three factors. Similar to the situation above for $J \rightarrow G$, the inclusion $K \rightarrow N$ may be factored either as an S^1 -bundle or as an S^3 bundle. The set $\tilde{\Delta}_L = \Delta_L/\mathbb{Z}_2$ was described in [9], and shown to be a wedge of twelve circles. The spaces and corresponding reduced spaces have the following structures:

$$\begin{aligned} K &\cong (\bigsqcup_6 S^1 \times S^1 \times S^1)/\mathbb{Z}_2 \cong \bigsqcup_6 T^3 \\ K_R &\cong (\bigsqcup_6 S^1 \times S^1)/\mathbb{Z}_2 \cong \bigsqcup_6 T^2 \\ N &\cong (\Delta_L \times S^1 \times S^3)/\mathbb{Z}_2 \cong (\bigvee_{12} S^1) \times S^1 \times S^3 \\ N_R &\cong (\Delta_L \times S^3)/\mathbb{Z}_2 \cong (\bigvee_{12} S^1) \times S^3 \end{aligned}$$

Next, consider the commutative diagram of pairs $(J \cup K, K) \rightarrow (N, F)$. By excision, $H_*(N, F) \cong H_*(J \cup K, J) \cong \bigoplus_6 H_*(T^3) \otimes H_*(D^3, S^2)$, while $H_*(J \cup K) \cong H_*(K) \cong \bigoplus_6 H_*(T^3)$.

$$\begin{array}{ccccccc} \dots & \longrightarrow & H_k(J) & \longrightarrow & H_k(J \cup D) & \longrightarrow & H_k(J \cup K, J) & \longrightarrow & \dots \\ & & \downarrow & & \downarrow & & \downarrow \cong & & \\ \dots & \longrightarrow & H_k(F) & \longrightarrow & H_k(N) & \longrightarrow & H_k(N, F) & \longrightarrow & \dots \end{array} \tag{4.1.1}$$

Note that $H_*(J) \rightarrow H_*(J \cup K)$ is surjective, so $H_*(J \cup K) \rightarrow H_*(J \cup K, J)$ is trivial, which means that the composition $H_*(J \cup K) \rightarrow H_*(N) \rightarrow H_*(N, F)$ is trivial. That is, the image of $H_*(J \cup K) \rightarrow H_*(N)$ is contained in the image of $H_*(F) \rightarrow H_*(N)$.

Viewing the map $K \rightarrow N$ as an inclusion of products $\bigsqcup_{12} S^1 \times S^1 \times S^1 \rightarrow \tilde{\Delta}_L \times S^1 \times S^3$, the map on the first factor is injective, on the middle factor, it is an isomorphism, on the last factor it is trivial. We therefore have the following maps:

	k	0	1	2	3	4	5
$H_k(K)$	$H_k(S^1) \otimes H_k(S^1) \otimes H_k(S^1)$	\mathbb{Z}^6	$\mathbb{Z}^6 \oplus \mathbb{Z}^6 \oplus \mathbb{Z}^6$	$\mathbb{Z}^6 \oplus \mathbb{Z}^6 \oplus \mathbb{Z}^6$	\mathbb{Z}^6	0	0
\downarrow	\downarrow	\downarrow	$\downarrow \oplus \downarrow \oplus 0$	$\downarrow \oplus 0 \oplus 0$	0		
$H_k(N)$	$H_k(\tilde{\Delta}_L) \otimes H_k(S^1) \otimes H_k(S^3)$	\mathbb{Z}	$\mathbb{Z}^{12} \oplus \mathbb{Z} \oplus 0$	$\mathbb{Z}^{12} \oplus 0 \oplus 0$	\mathbb{Z}	\mathbb{Z}^{13}	\mathbb{Z}^{12}

While N and K have relatively simply topological descriptions, the complement F is not as readily described. We rely upon a further Mayer–Vietoris decomposition to compute $H_*(F_R)$, which can then be leveraged to compute $H_*(F)$. If we view Δ_{CR} as a graph with 18 edges and 7 vertices (4 with valence 6 corresponding to triple collision; 3 with valence 4 corresponding to double binary collision), then we can take F_{R1} to be the preimage in F_R of the open edges, and F_{R2} to be the preimage in F_R of a neighborhood around the vertices.

The description of F_{R1} is fairly straightforward. Over each of the eighteen intervals of Δ_{ijC}^o , we have a neighborhood $\mathbb{I} \times \mathbb{I} \times S^3$ in $\mathcal{X}^0(C_L)$, with the limit set

$$cl(\Delta_{ij} \setminus \Delta_{ijC}) \cong \mathbb{I} \times \{\vec{0}\} \times S^1$$

deleted. Over neighborhoods of the intersections $\Delta_{ij,kl}$ and Δ_{ijk} , we again have neighborhoods $D^2 \times S^3$, this time with either two (in the case of $\Delta_{ij,kl}$) or three (in the case of Δ_{ijk}) non-intersecting limit sets of the form $\mathbb{I} \times \{\vec{0}\} \times S^1$ deleted. That is,

$$\begin{aligned} F_{R1} &\cong \bigsqcup_{18} (D^2 \times S^3) \setminus (\mathbb{I} \times \{0\} \times S^1) \\ F_{R2} &\cong (\bigsqcup_3 D^2 \times S^3 \setminus ((\mathbb{I}_{ij} \sqcup \mathbb{I}_{jk} \sqcup \mathbb{I}_{ik}) \times S^1)) \sqcup (\bigsqcup_4 D^2 \times S^3 \setminus ((\mathbb{I}_{ij} \sqcup \mathbb{I}_{kl}) \times S^1)) \\ F_{R0} &\cong \bigsqcup_{18} (\partial \mathbb{I} \times \mathbb{I} \times S^3) \setminus (\partial \mathbb{I} \times \{0\} \times S^1) \end{aligned}$$

where the lines \mathbb{I}_{ij} etc. represent the directions along the collision sets.

Each component of F_{R1} has the homotopy type of $S^3 \times [-1, 1]$ with $S^1 \times \{\vec{0}\}$ deleted, which is in turn homotopic to $S^3 \cup_{S^1} S^3$, which has the homology of $S^3 \vee S^2 \vee S^3$. Components of F_{R0} have the same structure. Components of F_2 corresponding to binary double (resp. triple) collision are homeomorphic to $S^3 \times D^2$ with two (resp. three) non-intersecting copies of $S^1 \times [-1, 1]$ deleted. These yield three components with homology groups $(\mathbb{Z}, 0, \mathbb{Z}^2, \mathbb{Z}^3, 0)$ and four components with homology groups $(\mathbb{Z}, 0, \mathbb{Z}^3, \mathbb{Z}^4, 0)$

The inclusion-induced maps $\iota_{R1*} : H_k(F_{R0}) \rightarrow H_k(F_{R1})$ and $\iota_{R2*} : H_k(F_{R0}) \rightarrow \oplus H_k(F_{R2})$ devolve to careful tracking of which component of F_{R1} and F_{R2} each sphere generating $H_k(F_{R0})$ maps to. The resulting matrices of 0's and 1's has the kernels and cokernels indicated,

k	$\ker(\iota_{R1*} \oplus \iota_{R2*})$	$H_k(F_{R0})$	$H_k(F_{R1}) \oplus H_k(F_{R2})$	$\text{coker}(\iota_{R1*} \oplus \iota_{R2*})$
3	\mathbb{Z}^{12}	\mathbb{Z}^{72}	$\mathbb{Z}^{36} \oplus \mathbb{Z}^{25}$	$\mathbb{Z} \oplus \mathbb{Z}_2^5$
2	\mathbb{Z}^6	\mathbb{Z}^{36}	$\mathbb{Z}^{18} \oplus \mathbb{Z}^{18}$	\mathbb{Z}^6
1	0	0	0	0
0	\mathbb{Z}^{12}	\mathbb{Z}^{36}	$\mathbb{Z}^{18} \oplus \mathbb{Z}^7$	\mathbb{Z}

From this, we see that $H_*(F_R) \cong (\mathbb{Z}, \mathbb{Z}^{12}, \mathbb{Z}^6, \mathbb{Z}^7 \oplus \mathbb{Z}_2^5, \mathbb{Z}^{12}, 0, \dots)$. To complete the computation of $H_*(\mathfrak{B}_R(d_9))$, we next identify the map $H_*(J_R) \rightarrow H_*(F_R)$. The diagram 4.1.1 supplies almost all of the information needed to do so. The one ambiguity is the intersection of the image of $i_{JFR} : H_3(J_R) \rightarrow H_3(F_R)$ with the torsion subgroup \mathbb{Z}_2^5 of $H_3(F_R)$.

To understand that intersection, intersect J_R with the Mayer–Vietoris decomposition of F_R :

$$\begin{aligned} J_{R1} &\cong \bigsqcup_{18} \mathbb{I} \times S^1 \times S^2 && \cong \bigsqcup_{18} S^1 \times S^2 \\ J_{R2} &\cong \bigsqcup_4 (D^2 \times (\mathbb{I}_{ij} \sqcup \mathbb{I}_{kl}) \times S^1) \sqcup \bigsqcup_3 (D^2 \times (\mathbb{I}_{ij} \sqcup \mathbb{I}_{jk} \sqcup \mathbb{I}_{ik}) \times S^1) && \cong \bigsqcup_{18} S^1 \times S^2 \\ J_{R0} &\cong \bigsqcup_{18} S^0 \times S^1 \times S^2 && \cong \bigsqcup_{36} S^1 \times S^2 \end{aligned}$$

There is commutative diagram

$$\begin{array}{ccccc} H_3(J_{R0}) & \xrightarrow{i_J} & H_3(J_{R1}) \oplus H_3(J_{R2}) & \xrightarrow{j_J} & H_3(J_R) \\ \downarrow \iota_{J0} & & \downarrow \iota_{JF1} \oplus \iota_{JF2} & & \downarrow \iota_{JF} \\ H_3(F_{R0}) & \xrightarrow{i_F} & H_3(F_{R1}) \oplus H_3(F_{R2}) & \xrightarrow{j_F} & H_3(F_R) \end{array}$$

with $H_3(F_{R1}) \oplus H_3(F_{R2}) \rightarrow H_3(F_R)$ mapping onto the torsion subgroup of $H_3(F_R)$. The maps $H_3(J_{Ri}) \rightarrow H_3(F_{Ri})$ are determined by the exact sequences of the pairs (F_{Ri}, J_{Ri}) . The homology groups of the pairs are obtained by use of excision to fill in the deleted tubes around K , yielding the following:

$$\begin{aligned} H_*(F_{R1}, J_{R1}) &\cong \bigoplus_{18} H_*(S^3 \times D^2, S^1 \times D^4) \\ H_*(F_{R2}, J_{R12}) &\cong \left(\bigoplus_4 H_*(S^3 \times D^2, S^1 \times D^2 \times (\mathbb{I}_{ij} \sqcup \mathbb{I}_{kl})) \right) \\ &\quad \oplus \left(\bigoplus_3 H_*(S^3 \times D^2, S^1 \times D^2 \times (\mathbb{I}_{ij} \sqcup \mathbb{I}_{jk} \sqcup \mathbb{I}_{ik})) \right) \\ H_*(F_{R0}, J_{R0}) &\cong \bigoplus_{36} H_*(S^3 \times \mathbb{I}, S^1 \times D^3) \end{aligned}$$

This shows that, for $i = 0, 1, 2$, $H_k(J_{Ri}) \rightarrow H_k(F_{Ri})$ is injective with torsion-free cokernel for $k = 3$, an isomorphism for $k = 2$ and surjective for $k = 0$. Inserting the known values yields

$$\begin{array}{ccccc} \mathbb{Z}^{36} & \longrightarrow & \mathbb{Z}^{18} \oplus \mathbb{Z}^{18} & \twoheadrightarrow & \mathbb{Z}^6 \\ \downarrow & & \downarrow & & \downarrow \\ \mathbb{Z}^{72} & \longrightarrow & \mathbb{Z}^{36} \oplus \mathbb{Z}^{25} & \twoheadrightarrow & \mathbb{Z} \oplus \mathbb{Z}_2^5 \end{array}$$

Since

$$\begin{aligned} \text{im}(\iota_{JF} \circ j_J) &= \text{im}(j_F \circ (\iota_{JF1} \oplus \iota_{JF2})) = j_F(\text{im}(\iota_{JF1} \oplus \iota_{JF2})) \\ &\cong \text{im}(\iota_{JF1} \oplus \iota_{JF2}) / (\text{im}(\iota_{JF1} \oplus \iota_{JF2}) \cap \text{im}(i_F)) \\ &\cong (\text{im}(\iota_{JF1} \oplus \iota_{JF2}), \text{im}(i_F)) / \text{im}(i_F) \end{aligned}$$

It suffices to compute the difference between $\text{im}(\iota_{JF1} \oplus \iota_{JF2})$, $\text{im}(i_F)$ and $\text{im}(i_F)$. Direct computation of shows that $(\text{im}(\iota_{JF1} \oplus \iota_{JF2}), \text{im}(i_F)) / \text{im}(i_F) \cong \mathbb{Z}_2^5$. Combining that with the information derived from diagram 4.1.1’s corresponding reduced-space diagram, we obtain the following for $\iota_{JF} : H_k(J_R) \rightarrow H_k(F_R)$:

k	0	1	2	3	4	5
$H_k(J_R)$	\mathbb{Z}^6	\mathbb{Z}^{12}	\mathbb{Z}^{12}	\mathbb{Z}^{12}	\mathbb{Z}^6	0
ι_{F*}	\downarrow	\downarrow rk 6	\downarrow rk 6	\downarrow ι_{F3*}	\downarrow	0
$H_k(F_R)$	\mathbb{Z}	\mathbb{Z}^{12}	\mathbb{Z}^6	$\mathbb{Z}^7 \oplus \mathbb{Z}_2^5$	\mathbb{Z}^{12}	0

with $\text{coker}(\iota_{F3*}) \cong \mathbb{Z}$.

Note that the only dimension in which both $\iota_{F*} : H_k(J_R) \rightarrow H_k(F_R)$ and $\iota_{G*} : H_k(J_R) \rightarrow H_k(G_R)$ are non-trivial is $k = 2$. The map ι_G is non-trivial only on the factor $H_2(S^2)$, while inspection of the commutative diagram 4.1.1 shows that $H_2(J) \rightarrow H_2(F)$ is trivial on that factor. Thus $\text{rk}(\iota_{F*}, \iota_{G*}) = \text{rk}(\iota_{F*}) + \text{rk}(\iota_{G*})$. The data for the Mayer–Vietoris diagram of $\mathfrak{B}_R(d_9) \simeq F_R \cup_{J_R} G_R$ is therefore

	$\text{ker}(\iota_{FR*}, \iota_{GR*})$	$H_k(J_R)$	$\text{rk}(i_{FR*}, i_{GR*})$	$H_*(F_R) \oplus H_*(G_R)$	$\text{coker}(\iota_{FR*}, \iota_{GR*})$
6	0	0	0	0	0
5	0	0	0	0	0
4	0	\mathbb{Z}^6	6	\mathbb{Z}^{18}	\mathbb{Z}^{12}
3	\mathbb{Z}^6	\mathbb{Z}^{12}	6	$\mathbb{Z}^7 \oplus \mathbb{Z}_2^5$	\mathbb{Z}
2	0	\mathbb{Z}^{12}	12	\mathbb{Z}^{18}	\mathbb{Z}^6
1	\mathbb{Z}^6	\mathbb{Z}^{12}	6	\mathbb{Z}^{12}	\mathbb{Z}^6
0	0	\mathbb{Z}^6	6	\mathbb{Z}^7	\mathbb{Z}

This yields the values for $H_*(\mathfrak{B}_R(d_9))$.

To compute $H_*(\mathfrak{B}(d_9))$, we follow a similar path, computing $H_*(F)$ and the map $H_*(J) \rightarrow H_*(F)$. For the first of these, we exploit the observation that F can be fibered either as $S^1 \rightarrow F \rightarrow F_R$ or as $F_C \rightarrow F \rightarrow \mathbb{R}P^1$, with F_C a double-cover of F_R . Both of these are restrictions of the corresponding fibrations of N . In particular, as the fibration $S^1 \rightarrow N \rightarrow N_R$ is orientable, the pullback (i.e. restriction) $S^1 \rightarrow F \rightarrow F_R$ is as well. There is a Gysin braid diagram for the exact sequence of the pair (N, F) (see [10] for discussion of braid diagrams).

$$\begin{array}{ccccccc}
 \dots & \longrightarrow & H_{k-1}(F_R) & \longrightarrow & H_{k-1}(N_R) & \longrightarrow & H_{k-1}(N_R, F_R) \longrightarrow \dots \\
 & & \downarrow & & \downarrow & & \downarrow \\
 \dots & \longrightarrow & H_k(F) & \longrightarrow & H_k(N) & \longrightarrow & H_k(N, F) \longrightarrow \dots \\
 & & \downarrow & & \downarrow & & \downarrow \\
 \dots & \longrightarrow & H_k(F_R) & \longrightarrow & H_k(N_R) & \longrightarrow & H_k(N_R, F_R) \longrightarrow \dots
 \end{array}$$

Inserting the known values into the diagram shows that the Gysin sequence for F has trivial boundary operators, so there are short exact sequences $0 \rightarrow H_{k-1}(F_R) \rightarrow H_k(F) \rightarrow H_k(F_R) \rightarrow 0$. Further, in order for the spectral sequence of the fibration $F_C \rightarrow F \rightarrow \mathbb{R}P^1$ to converge to the same values for $H_*(F)$, that spectral sequence has E^2 terms that yield $0 \rightarrow H_k(F_R) \rightarrow H_k(F) \rightarrow H_{k-1}(F_R) \rightarrow 0$. That is, the short exact sequences are split exact, and

$$H_*(F) \cong H_*(F_R) \otimes H_*(S^1).$$

As the same is true for $H_*(J)$, inserting the known values into the commutative diagram for $(J \cup D, J) \rightarrow (N, F)$, the values for the maps $H_k(J) \rightarrow H_k(F)$ follow immediately. The values are

k	0	1	2	3	4	5	6
$H_k(J)$	\mathbb{Z}^6	\mathbb{Z}^{18}	\mathbb{Z}^{24}	\mathbb{Z}^{24}	\mathbb{Z}^{18}	\mathbb{Z}^6	0
i_{F*}	\downarrow	\downarrow rk 7	\downarrow rk 12	\downarrow ι_{F3}	\downarrow ι_{F4}	\downarrow rk 6	0
$H_k(F)$	\mathbb{Z}	\mathbb{Z}^{13}	\mathbb{Z}^{18}	$\mathbb{Z}^{13} \oplus \mathbb{Z}_2^5$	$\mathbb{Z}^{19} \oplus \mathbb{Z}_2^5$	\mathbb{Z}^{12}	0

where $\iota_{F3} : H_3(J) \rightarrow H_3(F)$ has cokernel \mathbb{Z} and $\iota_{F4} : H_4(J) \rightarrow H_4(F)$ has cokernel \mathbb{Z}^7 .

To compute $H_*(\mathfrak{B}(d_9))$ from the Gysin braid of the Mayer–Vietoris sequence, first note that the diagram immediately determines $H_0(\mathfrak{B}(d_9))$ and $H_5(\mathfrak{B}(d_9))$. To determine the other dimensions, we examine on the sub-diagrams

$$\begin{array}{ccccc}
 H_{k-1}(J_R) & \hookrightarrow & H_k(J) & \twoheadrightarrow & H_k(J_R) \\
 \downarrow & & \downarrow \iota_{F \oplus \iota_G} & & \downarrow \\
 H_{k-1}(F_R) \oplus H_2(G_R) & \longrightarrow & H_k(F) \oplus H_k(G) & \longrightarrow & H_k(F_R) \oplus H_k(G_R)
 \end{array}$$

Inserting known values into this diagram shows that, for $k = 4$, $\iota_F \oplus \iota_G$ has kernel \mathbb{Z}^6 and cokernel \mathbb{Z}^7 , while for $k = 2$, the kernel and cokernel are both \mathbb{Z}^6 , while for $k = 1$, $\iota_F \oplus \iota_G$ has \mathbb{Z}^{11} and cokernel \mathbb{Z}^6 .

The determination of $\iota_F \oplus \iota_G$ for $k = 3$ is more subtle. For that, we turn to the following diagram.

$$\begin{array}{ccccccc}
 H_4(J_R) & \hookrightarrow & H_4(F_R) \oplus H_4(G_R) & \longrightarrow & H_4(\mathfrak{B}_R(d_9)) & \xrightarrow{rk\ 6} & H_3(J_R) \\
 \downarrow \partial_J & & \downarrow \partial_F \oplus \partial_G & & \downarrow \partial_B & & \downarrow 0 \\
 H_2(J_R) & \xrightarrow{6\oplus 6} & H_2(F_R) \oplus H_2(G_R) & \longrightarrow & H_2(\mathfrak{B}_R(d_9)) & \longrightarrow & H_1(J_R) \\
 \downarrow & & \downarrow & & \downarrow & & \downarrow \\
 H_3(J) & \longrightarrow & H_3(F) \oplus H_3(G) & \longrightarrow & H_3(\mathfrak{B}(d_9)) & \longrightarrow & H_2(J) \\
 \downarrow & & \downarrow & & \downarrow & & \downarrow \\
 H_3(J_R) & \longrightarrow & H_3(F_R) \oplus H_3(G_R) & \longrightarrow & H_3(\mathfrak{B}_R(d_9)) & \longrightarrow & H_2(J_R)
 \end{array}$$

Inserting the known values yields

$$\begin{array}{ccccccc}
 \mathbb{Z}^6 & \hookrightarrow & \mathbb{Z}^{12} \oplus \mathbb{Z}^6 & \xrightarrow{6\oplus 6} & \mathbb{Z}^{18} & \xrightarrow{rk\ 6} & \mathbb{Z}^{12} \\
 \downarrow 0 & & \downarrow 0 \oplus \partial_G & & \downarrow \partial_B & & \downarrow 0 \\
 \mathbb{Z}^{12} & \xrightarrow{6\oplus 6} & \mathbb{Z}^6 \oplus \mathbb{Z}^{12} & \xrightarrow{rk\ 6} & \mathbb{Z}^{12} & \xrightarrow{rk\ 6} & \mathbb{Z}^{12} \\
 \downarrow & & \downarrow & & \downarrow & & \downarrow \\
 \mathbb{Z}^{24} & \longrightarrow & \mathbb{Z}^{13} \oplus \mathbb{Z}_2^5 \oplus \mathbb{Z}^6 \oplus \mathbb{Z}_2^6 & \longrightarrow & H_3(\mathfrak{B}(d_9)) & \xrightarrow{rk\ 6} & \mathbb{Z}^{24} \\
 \downarrow & & \downarrow & & \downarrow & & \downarrow \\
 \mathbb{Z}^{12} & \xrightarrow{\iota_{FR} \oplus 0} & \mathbb{Z}^7 \oplus \mathbb{Z}^5 \oplus 0 & \longrightarrow & \mathbb{Z} & \xrightarrow{0} & \mathbb{Z}^{12}
 \end{array}$$

Since ∂_G has cokernel $\mathbb{Z}^6 \oplus \mathbb{Z}_2^6$, the image of ∂_G is $2\mathbb{Z}^6$. The diagram then implies that ∂_B likewise has image $2\mathbb{Z}^6$, from which we conclude $H_3(\mathfrak{B}(d_9)) \cong \mathbb{Z}^7 \oplus \mathbb{Z}_2^6$. This in turn implies that that cokernel of $\iota_F \oplus \iota_G$ is $\mathbb{Z} \oplus \mathbb{Z}_2^6$ and that the kernel is \mathbb{Z}^6 .

Collating all of the information, the Mayer–Vietoris data for $H_*(\mathfrak{B}(d_9))$ is

	$\ker(\iota_{F*}, \iota_{G*})$	$H_k(J)$	$\text{rk}(\iota_{F*}, \iota_{G*})$	$H_*(F) \oplus H_*(G)$	$\text{coker}(\iota_{F*}, \iota_{G*})$
6	0	0	0	0	0
5	0	\mathbb{Z}^6	6	\mathbb{Z}^{18}	\mathbb{Z}^{12}
4	\mathbb{Z}^6	\mathbb{Z}^{18}	12	$\mathbb{Z}^{19} \oplus \mathbb{Z}_2^5$	\mathbb{Z}^7
3	\mathbb{Z}^6	\mathbb{Z}^{24}	18	$\mathbb{Z}^{19} \oplus \mathbb{Z}_2^{11}$	$\mathbb{Z} \oplus \mathbb{Z}_2^6$
2	\mathbb{Z}^6	\mathbb{Z}^{24}	18	\mathbb{Z}^{24}	\mathbb{Z}^6
1	\mathbb{Z}^{11}	\mathbb{Z}^{18}	7	$\mathbb{Z}^{13} \oplus \mathbb{Z}_2^6$	\mathbb{Z}^6
0	0	\mathbb{Z}^6	6	\mathbb{Z}^7	\mathbb{Z}

This yields the values for $H_*(\mathfrak{B}(d_9))$.

To complete the proof of Lemma 4.1.2, observe that $\mathfrak{B}_{R0}(d_9) \subset F_R$, so we can factor $\iota_{0*} : H_*(\mathfrak{B}_{R0}(d_9)) \rightarrow H_*(F_R) \rightarrow H_*(\mathfrak{B}_R(d_9))$ as

$$H_*(\mathfrak{B}_0(d_9)) \rightarrow H_*(F) \rightarrow H_*(\mathfrak{B}(d_9))$$

We can obtain the maps $H_*(F) \rightarrow H_*(\mathfrak{B}(d_9))$ from the exact sequence of the pair $(\mathfrak{B}(d_9), F)$, making use of the excisive isomorphism $H_*(G, J) \rightarrow H_*(\mathfrak{B}(d_9), F)$. This

yields

	\mathfrak{B}							\mathfrak{B}_R					
	0	1	2	3	4	5	6	0	1	2	3	4	5
F	\mathbb{Z}	\mathbb{Z}^{13}	\mathbb{Z}^{18}	\mathbb{Z}^{13}	$\mathbb{Z}^{19} \oplus \mathbb{Z}_2^5$	\mathbb{Z}^{12}	0	\mathbb{Z}	\mathbb{Z}^{12}	\mathbb{Z}^6	$\mathbb{Z}^7 \oplus \mathbb{Z}^5$	\mathbb{Z}^{12}	0
$\iota_{F*} \downarrow$	$\downarrow \cong$	\downarrow	$\downarrow \text{rk } 6$	$\downarrow \text{rk } 1$	$\downarrow \text{rk } 7$	$\downarrow \text{rk } 6$		$\downarrow \cong$	\downarrow	$\downarrow 0$	$\downarrow \text{rk } 1$	$\downarrow \text{rk } 6$	
$\mathfrak{B}(d_9)$	\mathbb{Z}	\mathbb{Z}^6	\mathbb{Z}^{17}	\mathbb{Z}^7	\mathbb{Z}^{13}	\mathbb{Z}^{18}	0	\mathbb{Z}	\mathbb{Z}^6	\mathbb{Z}^{12}	\mathbb{Z}	\mathbb{Z}^{18}	0

It remains to identify $H_*(\mathfrak{B}_0(d_9)) \rightarrow H_*(F)$. We follow the same approach as for $H_*(J) \rightarrow H_*(F)$, applying the Mayer–Vietoris decomposition of F_R to $\mathfrak{B}_0(d_9)$, then lifting from the reduced spaces to the total spaces. Let $K_{Ri} = \mathfrak{B}_{R0}(d_9) \cap F_{Ri}$. Then

$$\begin{aligned}
 K_{R1} &\cong \bigsqcup_{18} \mathbb{I} \times (\mathbb{I} \setminus \{0\}) \times S^3 && \simeq \bigsqcup_{36} S^3 \\
 K_{R2} &\cong (\bigsqcup_3 (D^2 \setminus \{\ell_1 \cup \ell_2\}) \times S^3) && \simeq \bigsqcup_{36} S^3 \\
 &\quad \sqcup (\bigsqcup_4 (D^2 \setminus \{\ell_1 \cup \ell_2 \cup \ell_3\}) \times S^3) \\
 K_{R0} &\cong \bigsqcup_{18} S^0 \times (\mathbb{I} \setminus \{0\}) \times S^3 && \simeq \bigsqcup_{72} S^3
 \end{aligned}$$

Consider the commutative diagram

$$\begin{array}{ccccccc}
 H_{k+1}(\mathfrak{B}_{R0}(d_9)) & \xrightarrow{\quad} & H_k(K_{R0}) & \xrightarrow{i_{K*}} & H_k(K_{R1}) \oplus H_k(K_{R2}) & \xrightarrow{j_{K*}} & H_k(K_R) \\
 \downarrow \iota_{K*} & & \downarrow \iota_{K0*} & & \downarrow \iota_{K1*} \oplus \iota_{K2*} & & \downarrow \iota_{K*} \\
 H_{k+1}(F_R) & \xrightarrow{\quad} & H_k(F_{R0}) & \xrightarrow{i_{F*}} & H_k(F_{R1}) \oplus H_k(F_{R2}) & \xrightarrow{j_{F*}} & H_k(F_R)
 \end{array}$$

For both $k = 0$ and $k = 3$, the inclusion maps ι_{K0*} and $\iota_{K1*} \oplus \iota_{K2*}$ is surjective, with ι_{K0*} an isomorphism for $k = 3$. Since $\iota_{K1*} \oplus \iota_{K2*}$ is surjective, it follows that ι_{K*} maps onto the the image of $H_3(F_R)$, namely $\mathbb{Z} \oplus \mathbb{Z}_2^5$. On the other hand, the restriction of ι_{K0*} to $\ker(i_{K*})$ is an isomorphism onto $\ker(i_{F*})$. The same arguments apply at $k = 0$.

As ι_{K*} is surjective for $k = 0, 1, 4$, it is immediate that $H_k(\mathfrak{B}_{R0}(d_9)) \rightarrow H_k(\mathfrak{B}_R(d_9))$ has the same image as $H_k(F_R) \rightarrow H_k(\mathfrak{B}_R(d_9))$. For $k = 3$, $\text{im}(i_{K*}) = \text{im}(i_{J*})$ maps onto $H_3(\mathfrak{B}_R(d_9))$, so $H_3(\mathfrak{B}_{R0}(d_9)) \rightarrow H_3(\mathfrak{B}_R(d_9))$ is surjective.

The values for $\iota_{0*} : H_*(\mathfrak{B}_0(d_9)) \rightarrow H_*(\mathfrak{B}(d_9))$ follow in turn from the commutative diagram of Gysin sequences. While most of the calculations are straightforward, the identification of $\iota_{0*} : H_3(\mathfrak{B}_0(d_9)) \rightarrow H_3(\mathfrak{B}(d_9))$ merits comment. The relevant portion of the commutative Gysin sequence diagram is

$$\begin{array}{ccccccc}
 \dots & \longrightarrow & H_2(\mathfrak{B}_{R0}(d_9)) & \longrightarrow & H_3(\mathfrak{B}_0(d_9)) & \longrightarrow & H_3(\mathfrak{B}_{R0}(d_9)) & \longrightarrow & \dots \\
 & & \downarrow \alpha_{R*} & & \downarrow \alpha_* & & \downarrow \alpha_{R*} & & \\
 \dots & \longrightarrow & H_2(F_R) & \longrightarrow & H_3(F) & \longrightarrow & H_3(F_R) & \longrightarrow & \dots \\
 & & \downarrow j_{R*} & & \downarrow j_* & & \downarrow j_{R*} & & \\
 \dots & \longrightarrow & H_2(\mathfrak{B}_R(d_9)) & \longrightarrow & H_3(\mathfrak{B}(d_9)) & \longrightarrow & H_3(\mathfrak{B}_R(d_9)) & \longrightarrow & \dots
 \end{array}$$

Inserting the known values, this becomes

$$\begin{array}{ccccc}
 0 & \longrightarrow & \mathbb{Z}^{12} & \xrightarrow{\cong} & \mathbb{Z}^{12} \\
 \downarrow & & \downarrow & & \downarrow \\
 \mathbb{Z}^6 & \twoheadrightarrow & \mathbb{Z}^{13} \oplus \mathbb{Z}_2^5 & \twoheadrightarrow & \mathbb{Z}^7 \oplus \mathbb{Z}_2^5 \\
 \downarrow & & \downarrow \text{rk1} & & \downarrow \\
 \mathbb{Z}^{12} & \xrightarrow{\text{rk6}} & \mathbb{Z}^7 \oplus \mathbb{Z}_2^5 & \twoheadrightarrow & \mathbb{Z}
 \end{array}$$

The right hand column shows that ι_* has rank at least one, while the fact that it factors through j_* which has rank 1 shows that ι_* has rank one. □

4.2 Behavior at \mathcal{B}_0

We briefly review the structure of the collinear blow-up \mathcal{B} and the behavior of D at collinear. On \mathcal{B}_0 itself, we need only consider two levels: above and below δ_8 , the level of the collinear central configurations. The sets $\mathfrak{B}_0(d)$, $\partial\mathfrak{B}_0(d)$ above and below δ_8 are

$$\begin{array}{ccc}
 & \mathfrak{B}_0(d) & \partial\mathfrak{B}_0(d) \\
 d < \delta_8 & S^3 \times S^1 \times D^2 \times (-1, 1) & S^3 \times S^1 \times D^2 \times S^0 \\
 d_9 > \delta_8 & S^3 \times S^1 \times S^1 \times [0, 1) \times (-1, 1) & S^3 \times S^1 \times S^1 \times \{0\} \times (-1, 1)
 \end{array}$$

The SO_2 symmetry is reflected in each of these as an S^1 factor, so the reduced spaces simply remove that factor.

$$\begin{array}{ccc}
 & \mathfrak{B}_{R0}(d) & \partial\mathfrak{B}_{R0}(d) \\
 d < \delta_8 & S^3 \times D^2 \times (-1, 1) & S^3 \times D^2 \times S^0 \\
 d_9 > \delta_8 & S^3 \times S^1 \times [0, 1) \times (-1, 1) & S^3 \times S^1 \times \{0\} \times (-1, 1)
 \end{array}$$

In the 7-manifold \mathcal{S}_R , each point in the 2-manifold \mathcal{C}_{R0} has been blown up to $S^3 \times (-1, 1)$. The normal to a point in \mathcal{B}_0 is then a ray. Bifurcations occur at the equator $S^3 \times \{0\}$ for collinear central configurations q_c . At those points, the normal lies in the invariant plane, where $Y = 1$ and $D = U^2$. Further, we know that, at collinear central configurations, U is decreasing in the normal direction [14].

So, if we extend from $\mathfrak{B}_{R0}(d_9) \setminus \mathfrak{B}_{R0}(d_8)$ to a neighborhood of $\mathcal{B}_{R0}(q_c)$ in \mathcal{S}_{R0} , that neighborhood has the form $S^3 \times D^2 \times (-1, 1) \times [0, 1)$, which we will rewrite as $S^3 \times D^2 \times H^2$, with half-disk $H^2 \cong \{(x, y) | x^2 + y^2 < 1, x \geq 0\}$. The function D is constant on S^3 , increasing radially on D^2 , decreasing radially on H^2 . The intersection of the boundary of this set with $\mathfrak{A}(d_8)$ is therefore $S^3 \times D^2 \times \{(x, y) \in H^2 | x^2 + y^2 \geq \frac{1}{2}\}$. That is,

$$H_*(\mathfrak{B}_R(d_8, d_9), \partial\mathfrak{B}_R(d_8)) \cong \bigoplus_{12} H_*(S^3 \times D^2 \times H^2, S^3 \times d^2 \times \partial H^+) = 0.$$

4.3 From Planar Configurations to Spatial Configurations

The key to linking the topology of the spatial super-level sets $\mathfrak{B}(d)$ and the planar super-level sets $\mathcal{P}(d)$ is Lemma 2.4.3. The planar configurations are attracting in the gradient flow of ∇D , repelling in the reverse flow $-\nabla D$, from which we obtain the following relationships:

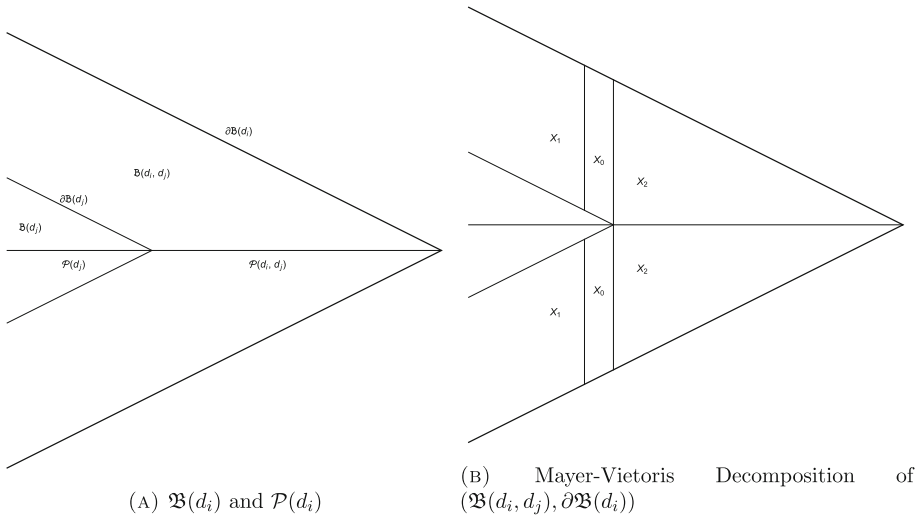


Fig. 2 Mayer–Vietoris Decomposition of $(\mathfrak{B}(d_i, d_j), \partial\mathfrak{B}(d_i))$

Corollary 4.3.1 For $5 \leq i \leq j \leq 8$, there are isomorphisms

$$\begin{aligned}
 H_k(\mathfrak{B}(d_i, d_j), \partial\mathfrak{B}(d_i)) &\cong H_{k-3}(\mathcal{P}(d_i, d_j), \partial\mathcal{P}(d_i)) \\
 H_k(\mathfrak{B}_R(d_i, d_j), \partial\mathfrak{B}_R(d_i)) &\cong H_{k-3}(\mathcal{P}_R(d_i, d_j), \partial\mathcal{P}_R(d_i)) \\
 H_k(\mathfrak{B}(d_i, d_j), \partial\mathfrak{B}(d_j)) &\cong H_k(\mathcal{P}(d_i, d_j), \partial\mathcal{P}(d_j)) \\
 H_k(\mathfrak{B}_R(d_i, d_j), \partial\mathfrak{B}_R(d_j)) &\cong H_k(\mathcal{P}_R(d_i, d_j), \partial\mathcal{P}_R(d_j))
 \end{aligned}$$

Proof To show $H_{k+3}(\mathfrak{B}(d_i, d_j), \mathfrak{B}(d_5, d_i)) \cong H_k(\mathcal{P}(d_i, d_j), \partial\mathcal{P}(d_i))$, first note that, since d_j is a regular value of D , $\mathfrak{B}(d_i, d_j)$ is homotopic to the half-open set $\mathfrak{B}^o(d_i, d_j) = \mathfrak{B}(d_i, d_j) \setminus \partial\mathfrak{B}(d_j)$. Similarly, as d_j is a regular value for D restricted to \mathcal{P} , there is an $\epsilon > 0$ such that $\mathcal{P}(d_j, d_j + \epsilon)$ has strong deformation retraction onto $\partial\mathcal{P}(d_j)$.

We construct a Mayer–Vietoris decomposition of the pair $(\mathfrak{B}^o(d_i, d_j), \partial\mathfrak{B}(d_i))$ with

$$\begin{aligned}
 X_1 &= \{(q_1, q_2, q_3) \in \mathcal{B}^o(d_i, d_j) \mid D(q_1, q_2, 0) < d_j + \epsilon\} \\
 X_2 &= \{(q_1, q_2, q_3) \in \mathcal{B}^o(d_i, d_j) \mid D(q_1, q_2, 0) > d_j\}
 \end{aligned}$$

and $X_0 = X_1 \cap X_2$ (See Fig. 2). The pairs $(X_i, X_i \cap \partial\mathfrak{B}(d_i))$ have homology groups $H_*(X_0, X_0 \cap \partial\mathfrak{B}(d_i)) \cong H_*(X_2, X_2 \cap \partial\mathfrak{B}(d_i)) = 0$ and

$$\begin{aligned}
 H_*(X_1, X_1 \cap \partial\mathfrak{B}(d_i)) &\cong H_*(\mathcal{P}^o(d_i, d_j) \times D^3, \partial\mathcal{P}(d_i) \times D^3 \cup \mathcal{P}^o(d_i, d_j) \times S^2) \\
 &\cong H_*(\mathcal{P}^o(d_i, d_j), \partial\mathcal{P}(d_i)) \otimes H_*(D^3, S^2)
 \end{aligned}$$

To show $H_k(\mathfrak{B}(d_i, d_j), \partial\mathfrak{B}(d_j)) \cong H_k(\mathcal{P}(d_i, d_j), \partial\mathcal{P}(d_j))$ for $5 \leq i \leq j \leq 8$, it suffices to produce a strong deformation retraction of $\mathfrak{B}(d_i, d_j)$ onto $\mathcal{P}(d_i, d_j) \cup \partial\mathfrak{B}(d_j)$. Define $R : \mathfrak{B}(d_i, d_j) \times [0, 1] \rightarrow \mathfrak{B}(d_i, d_j)$ as follows. If $q = (q_1, q_2, q_3) \in \mathfrak{B}(d_i, d_j)$, define $\tau(q) \in [0, 1]$ so that if $D(q_1, q_2, 0) > d_j$, then $D(\sqrt{\frac{1-\tau^2(q)q_3^2}{1-q_3^2}}q_1, \sqrt{\frac{1-\tau^2(q)q_3^2}{1-q_3^2}}q_2, \tau(q)q_3) = d_j$, and $\tau(q) = 0$ otherwise. Then define

$$R(q_1, q_2, q_3, t) = \left(\sqrt{\frac{1 - (1 - t + t\tau(q))^2 q_3^2}{1 - q_3^2}} q_2, \sqrt{\frac{1 - (1 - t + t\tau(q))^2 q_3^2}{1 - q_3^2}} q_2, (1 - t + t\tau(q)) q_3 \right)$$

□

From this analysis, we can now read off an array of homology groups of pairs in $\mathfrak{B}(d_5)$ and $\mathfrak{B}_R(d_5)$. We focus on the homology of pairs as this allows us to temporarily set aside the complicated internal structure of $\mathfrak{B}(d_9)$ and focus on the ways in which the progression from $\mathcal{P}(d_5)$ to (d_9) mediate the corresponding changes from $\mathfrak{B}(d_5)$ to $\mathfrak{B}(d_9)$.

Lemma 4.3.1 *For all values $\delta_4 < d_5 < \dots < \delta_8 < d_9$, we have the following homology group values:*

	$H_k(\mathfrak{B}(d_i, d_j), \partial\mathfrak{B}(d_i))$						$H_k(\mathfrak{B}_R(d_i, d_j), \partial\mathfrak{B}(d_i))$						
	0	1	2	3	4	5	6	0	1	2	3	4	5
$(\mathfrak{B}(d_5, d_6), \partial\mathfrak{B}(d_5))$	0	0	0	\mathbb{Z}^6	\mathbb{Z}^6	0	0	0	0	0	\mathbb{Z}^6	0	0
$(\mathfrak{B}(d_6, d_7), \partial\mathfrak{B}(d_6))$	0	0	0	0	\mathbb{Z}^{24}	\mathbb{Z}^{24}	0	0	0	0	0	\mathbb{Z}^{24}	0
$(\mathfrak{B}(d_7, d_8), \partial\mathfrak{B}(d_7))$	0	0	0	0	0	\mathbb{Z}^8	\mathbb{Z}^8	0	0	0	0	0	\mathbb{Z}^8
$(\mathfrak{B}(d_8, d_9), \partial\mathfrak{B}(d_8))$	0	0	0	0	0	0	0	0	0	0	0	0	0
$(\mathfrak{B}(d_5, d_7), \partial\mathfrak{B}(d_5))$	0	0	0	\mathbb{Z}	\mathbb{Z}^{20}	\mathbb{Z}^{19}	0	0	0	0	\mathbb{Z}	\mathbb{Z}^{19}	0
$(\mathfrak{B}(d_6, d_8), \partial\mathfrak{B}(d_6))$	0	0	0	0	\mathbb{Z}^{16}	\mathbb{Z}^{16}	0	0	0	0	0	\mathbb{Z}^{16}	0
$(\mathfrak{B}(d_7, d_9), \partial\mathfrak{B}(d_7))$	0	0	0	0	0	\mathbb{Z}^8	\mathbb{Z}^8	0	0	0	0	0	\mathbb{Z}^8
$(\mathfrak{B}(d_5, d_8), \partial\mathfrak{B}(d_5))$	0	0	0	\mathbb{Z}	\mathbb{Z}^{12}	\mathbb{Z}^{11}	0	0	0	0	\mathbb{Z}	\mathbb{Z}^{11}	0
$(\mathfrak{B}(d_6, d_9), \partial\mathfrak{B}(d_6))$	0	0	0	0	\mathbb{Z}^{16}	\mathbb{Z}^{16}	0	0	0	0	0	\mathbb{Z}^{16}	0
$(\mathfrak{B}(d_5, d_9), \partial\mathfrak{B}(d_5))$	0	0	0	\mathbb{Z}	\mathbb{Z}^{12}	\mathbb{Z}^{11}	0	0	0	0	\mathbb{Z}	\mathbb{Z}^{11}	0

and

	$H_k(\mathfrak{B}(d_i, d_j), \partial\mathfrak{B}(d_j))$						$H_k(\mathfrak{B}_R(d_i, d_j), \partial\mathfrak{B}(d_j))$						
	0	1	2	3	4	5	6	0	1	2	3	4	5
$(\mathfrak{B}(d_5, d_6), \partial\mathfrak{B}(d_6))$	0	0	0	0	0	\mathbb{Z}^6	\mathbb{Z}^6	0	0	0	0	0	\mathbb{Z}^6
$(\mathfrak{B}(d_6, d_7), \partial\mathfrak{B}(d_7))$	0	0	0	0	\mathbb{Z}^{24}	\mathbb{Z}^{24}	0	0	0	0	\mathbb{Z}^{24}	0	0
$(\mathfrak{B}(d_7, d_8), \partial\mathfrak{B}(d_8))$	0	0	\mathbb{Z}^8	\mathbb{Z}^8	0	0	0	0	0	\mathbb{Z}^8	0	0	0
$(\mathfrak{B}(d_8, d_9), \partial\mathfrak{B}(d_9))$	0	0	\mathbb{Z}^{12}	\mathbb{Z}^{12}	0	\mathbb{Z}^{12}	\mathbb{Z}^{12}	0	0	\mathbb{Z}^{12}	0	0	\mathbb{Z}^{12}
$(\mathfrak{B}(d_5, d_7), \partial\mathfrak{B}(d_7))$	0	0	0	\mathbb{Z}^{19}	\mathbb{Z}^{20}	\mathbb{Z}	0	0	0	0	\mathbb{Z}^{19}	\mathbb{Z}	0
$(\mathfrak{B}(d_6, d_8), \partial\mathfrak{B}(d_8))$	0	0	0	\mathbb{Z}^{16}	\mathbb{Z}^{16}	0	0	0	0	0	\mathbb{Z}^{16}	0	0
$(\mathfrak{B}(d_7, d_9), \partial\mathfrak{B}(d_9))$	0	0	\mathbb{Z}^{20}	\mathbb{Z}^{20}	0	\mathbb{Z}^{12}	\mathbb{Z}^{12}	0	0	\mathbb{Z}^{20}	0	0	\mathbb{Z}^{12}
$(\mathfrak{B}(d_5, d_8), \partial\mathfrak{B}(d_8))$	0	0	0	\mathbb{Z}^{11}	\mathbb{Z}^{12}	\mathbb{Z}	0	0	0	0	\mathbb{Z}^{11}	\mathbb{Z}	0
$(\mathfrak{B}(d_6, d_9), \partial\mathfrak{B}(d_9))$	0	0	\mathbb{Z}^6	\mathbb{Z}^{16}	\mathbb{Z}^{10}	\mathbb{Z}^{12}	\mathbb{Z}^{12}	0	0	\mathbb{Z}^6	\mathbb{Z}^{10}	0	\mathbb{Z}^{12}
$(\mathfrak{B}(d_5, d_9), \partial\mathfrak{B}(d_9))$	0	0	\mathbb{Z}^6	\mathbb{Z}^{11}	\mathbb{Z}^6	\mathbb{Z}^{13}	\mathbb{Z}^{12}	0	0	\mathbb{Z}^6	\mathbb{Z}^5	\mathbb{Z}^1	\mathbb{Z}^{12}

Proof The values for $H_*(\mathfrak{B}(d_i, d_j), \partial\mathfrak{B}(d_i))$ and $H_*(\mathfrak{B}(d_i, d_j), \partial\mathfrak{B}(d_j))$ with $i < j < 9$ follow immediately from Lemma 3.1.1 and Corollary 4.3.1.

Next, to compute $H_*(\mathfrak{B}(d_i, d_9), \partial\mathfrak{B}(d_i))$, observe that $H_*(\mathfrak{B}(d_5, d_9), \partial\mathfrak{B}(d_5)) \cong H_*(\mathfrak{B}(d_5), \partial\mathfrak{B}(d_5))$ was computed in [10]. For $i = 6, 7, 8$, the exact sequence of the triple $(\mathfrak{B}(d_5, d_9), \mathfrak{B}(d_5, d_i), \partial\mathfrak{B}(d_5))$ may be used to compute $H_*(\mathfrak{B}(d_5, d_9), \mathfrak{B}(d_5, d_i)) \cong$

$H_*(\mathfrak{B}(d_i, d_9), \partial\mathfrak{B}(d_i))$. This requires determining the map $H_k(\mathfrak{B}(d_5, d_i), \partial\mathfrak{B}(d_5)) \rightarrow H_k(\mathfrak{B}(d_5, d_9), \partial\mathfrak{B}(d_5))$. We factor this as

$$H_k(\mathfrak{B}(d_5, d_i), \partial\mathfrak{B}(d_5)) \rightarrow H_k(\mathfrak{B}(d_5, d_8), \partial\mathfrak{B}(d_5)) \rightarrow H_k(\mathfrak{B}(d_5, d_9), \partial\mathfrak{B}(d_5)).$$

Sect. 4.2 demonstrated that $H_k(\mathfrak{B}(d_5, d_8), \partial\mathfrak{B}(d_5)) \rightarrow H_k(\mathfrak{B}(d_5, d_9), \partial\mathfrak{B}(d_5))$ is an isomorphism, while the map $H_k(\mathfrak{B}(d_5, d_i), \partial\mathfrak{B}(d_5)) \rightarrow H_k(\mathfrak{B}(d_5, d_8), \partial\mathfrak{B}(d_5))$ is determined by the exact sequence of the triple $(\mathfrak{B}(d_5, d_8), \mathfrak{B}(d_5, d_i), \partial\mathfrak{B}(d_5))$.

Finally, for the pairs $(\mathfrak{B}_R(d_i, d_9), \partial\mathfrak{B}_R(d_9))$, note that the values for $i = 8$ also follow from Sect. 4.2. For $i = 5, 6, 7$, consider the exact sequences of triples $(\mathfrak{B}_R(d_i, d_9), \mathfrak{B}_R(d_8, 5d_9), \partial\mathfrak{B}_R(d_9))$. For $i = 7$, the sequence immediately yields the result. For $i = 5, 6$, it is necessary to compute the boundary map

$$\partial : H_3(\mathfrak{B}_R(d_i, d_9), \mathfrak{B}_R(d_8, d_9)) \rightarrow H_2(\mathfrak{B}_R(d_8, d_9), \partial\mathfrak{B}_R(d_9))$$

To do so, we make use of the projection $\rho(q_1, q_2, q_3) = \frac{1}{1-q_3^2}(q_1, q_2)$ and the following construction:

- For each of the sets X in the triple $(\mathfrak{B}_R(d_i, d_9), \mathfrak{B}_R(d_8, d_9), \partial\mathfrak{B}_R(d_9))$, let $X' = X \setminus \mathcal{B}_{R0}$. Note that the inclusion $X' = X \setminus \mathcal{B}_{R0} \rightarrow X$ is a homotopy equivalence. That is, we can replace the triple with $(\mathfrak{B}'_R(d_i, d_9), \mathfrak{B}'_R(d_8, d_9), \partial\mathfrak{B}'_R(d_9))$.
- Similarly, for subsets Y of \mathcal{P}_R , let $Y' = Y \setminus \mathcal{C}_{R0}$.

This allows us to bridge the gap between the subsets of \mathcal{P} , which retain the collinear configurations, and the corresponding subsets of \mathfrak{B} , where the collinear configurations have been replaced by the blow-up construction. We then have inclusions $(\mathcal{P}'_R(d_i, d_9), \mathcal{P}'_R(d_8, d_9), \partial\mathcal{P}'_R(d_9)) \xrightarrow{\iota} (\mathfrak{B}'_R(d_i, d_9), \mathfrak{B}'_R(d_8, d_9), \partial\mathfrak{B}'_R(d_9))$ and projections $(\mathfrak{B}'_R(d_i, d_9), \mathfrak{B}'_R(d_8, d_9), \partial\mathfrak{B}'_R(d_9)) \xrightarrow{\rho} (\mathcal{P}_R(d_i), \mathcal{P}_R(d_8), \mathcal{P}_R(d_9))$ such that the composition $\rho \circ \iota$ is simply the inclusion $(\mathcal{P}'_R(d_i, d_9), \mathcal{P}'_R(d_8, d_9), \partial\mathcal{P}'_R(d_9)) \xrightarrow{\iota} (\mathcal{P}_R(d_i), \mathcal{P}_R(d_8), \mathcal{P}_R(d_9))$. There is a commutative diagram

$$\begin{CD} H_3(\mathcal{P}'_R(d_i, d_9), \mathcal{P}'_R(d_8, d_9)) @>\partial>> H_2(\mathcal{P}'_R(d_8, d_9), \partial\mathcal{P}'_R(d_9)) \\ @VV\iota_*V @VV\rho_*V \\ H_3(\mathfrak{B}'_R(d_i, d_9), \mathfrak{B}'_R(d_8, d_9)) @>\partial>> H_2(\mathfrak{B}'_R(d_8, d_9), \partial\mathfrak{B}'_R(d_9)) \\ @VV\rho_*V @VV\rho_*V \\ H_3(\mathcal{P}_R(d_i), \mathcal{P}_R(d_8)) @>\partial>> H_2(\mathcal{P}_R(d_8), \mathcal{P}_R(d_9)) \end{CD}$$

By excision, the inclusions $H_3(\mathcal{P}'_R(d_i, d_9), \mathcal{P}'_R(d_8, d_9)) \rightarrow H_3(\mathcal{P}_R(d_i), \mathcal{P}_R(d_8))$ and $H_2(\mathcal{P}'_R(d_8, d_9), \partial\mathcal{P}'_R(d_9)) \rightarrow H_2(\mathcal{P}_R(d_8), \mathcal{P}_R(d_9))$ can be replaced by $H_3(\mathcal{P}'_R(d_i, d_9), \mathcal{P}'_R(d_8, d_9)) \rightarrow H_3(\mathcal{P}_R(d_i, d_9), \mathcal{P}_R(d_8, d_9))$ and $H_2(\mathcal{P}'_R(d_8, d_9), \partial\mathcal{P}'_R(d_9)) \rightarrow H_2(\mathcal{P}_R(d_8, d_9), \partial\mathcal{P}_R(d_9))$. Each of these is in turn part of a long exact sequence of triples $(\mathcal{P}_R(d_i, d_9), \mathcal{P}_R(d_8, d_9) \cup \mathcal{P}'_R(d_i, d_9), \mathcal{P}_R(d_8, d_9))$ and $(\mathcal{P}_R(d_8, d_9), \partial\mathcal{P}_R(d_9) \cup \mathcal{P}'_R(d_8, d_9), \partial\mathcal{P}_R(d_9))$.

Focusing for a moment on $H_3(\mathcal{P}'_R(d_i, d_9), \mathcal{P}'_R(d_8, d_9)) \rightarrow H_3(\mathcal{P}_R(d_i, d_9), \mathcal{P}_R(d_8, d_9))$, this inclusion is flanked in the exact sequence of the triple by $H_k(\mathcal{P}_R(d_i, d_9), \mathcal{P}_R(d_8, d_9)) \cup \mathcal{P}'_R(d_i, d_9)$ for $k = 3, 4$. The sets $\mathcal{P}_R(d_i, d_9)$ and $\mathcal{P}_R(d_8, d_9) \cup \mathcal{P}'_R(d_i, d_9)$ differ from each other by $\mathcal{C}_{R0} \cap \mathcal{P}_R(d_i, d_9)$, that is, by twelve 2-disks. By duality, then, $H_3(\mathcal{P}_R(d_i, d_9), \mathcal{P}_R(d_8, d_9) \cup \mathcal{P}'_R(d_i, d_9)) = 0$ and the map $H_3(\mathcal{P}'_R(d_i, d_9), \mathcal{P}'_R(d_8, d_9)) \rightarrow H_3(\mathcal{P}_R(d_i, d_9), \mathcal{P}_R(d_8, d_9))$ is surjective. A similar argument shows that $H_2(\mathcal{P}'_R(d_8, d_9), \partial\mathcal{P}'_R(d_9)) \rightarrow H_2(\mathcal{P}_R(d_8, d_9), \partial\mathcal{P}_R(d_9))$ is an isomorphism.

With the values for $H_*(\mathfrak{B}_R(d_i, d_9), \partial\mathfrak{B}_R(d_j))$ established, the values for $H_*(\mathfrak{B}(d_i, d_9), \partial\mathfrak{B}(d_j))$ follow from the Gysin braid of the triple $(\mathfrak{B}(d_i, d_9), \mathfrak{B}(d_8, d_9), \partial\mathfrak{B}(d_9))$. \square

5 Homology of the Integral Manifolds

In this section, we complete the study by translating the topological information of the previous section into homological calculations required to compute $H_*(\mathfrak{M})$ and $H_*(\mathfrak{M}_R)$. For $N = 4$, the homology formulae of [9] yields

$$H_k(\mathfrak{M}) \cong \begin{cases} \text{im}(j_* : H_3(\mathfrak{B}) \rightarrow H_3(\mathfrak{B}, \mathfrak{B}_0)) & k = 3 \\ H_k(\mathfrak{B}, \mathfrak{B}_0) \oplus H_{k-6}(\mathfrak{B}, \partial\mathfrak{B}^+) & k = 4, 5, 6, 10, 11, 12 \\ H_k(\mathfrak{B}) \oplus H_{k-6}(\mathfrak{B}, \partial\mathfrak{B}) & k = 0, 1, 2, 7, 8, 9, k > 12 \end{cases}$$

Note that for $d < d_8$, $H_2(\mathfrak{B}_0(d)) = 0$, so $H_3(\mathfrak{M}) \cong H_3(\mathfrak{B}, \mathfrak{B}_0)$.

For $N = 4$, the homology groups of $H_*(\mathfrak{M}_R(c, h))$ are given by

$$H_k(\mathfrak{M}_R(c, h)) \cong \begin{cases} H_k(\mathfrak{B}_R(d), \mathfrak{B}_{R0}(d)) \oplus H_{k-6}(\mathfrak{B}_R(d), \partial\mathfrak{B}_R^+(d)) & k = 3, 4, 5, 10, 11 \\ H_k(\mathfrak{B}_R(d)) \oplus H_{k-6}(\mathfrak{B}_R(d), \partial\mathfrak{B}_R(d)) & \text{otherwise} \end{cases}$$

Starting with the baseline of the homology of the relevant spaces for regions V and IX, we will use the information from the planar manifold to obtain the homology information for regions VI, VII and VIII. The identification of $H_*(\mathfrak{B}(d_i), \partial\mathfrak{B}(d_i))$ follows immediately from the work above. The identification of $H_*(\mathfrak{B}(d_i))$ will come next, and from those, the computations of $H_*(\mathfrak{B}(d_i), \partial\mathfrak{B}^+(d_i))$ and $H_*(\mathfrak{B}(d_i), \partial\mathfrak{B}_0(d_i))$.

5.1 The Homology Groups for $\mathfrak{B}(d_i)$ and Pairs $(\mathfrak{B}(d_i), \partial\mathfrak{B}(d_i))$

With the homology group values for regions V and region IX (i.e. just below the relative equilibria and just above) in hand, we can now use the information from Sect. 4.3 to compute the values for the regions in between. For completeness we include the values for regions V and IX.

Lemma 5.1.1 *For $\delta_{i-1} < d_i < \delta_i, i = 5, \dots, 9$, we have the following homology groups:*

	\mathfrak{B}						\mathfrak{B}_R						
	0	1	2	3	4	5	6	0	1	2	3	4	5
$\mathfrak{B}(d_5)$	\mathbb{Z}	0	\mathbb{Z}^6	$\mathbb{Z} \oplus \mathbb{Z}_2^5$	0	\mathbb{Z}^6	0	\mathbb{Z}	0	\mathbb{Z}^7	0	\mathbb{Z}^6	0
$(\mathfrak{B}(d_5), \partial\mathfrak{B}(d_5))$	0	0	0	\mathbb{Z}	\mathbb{Z}^{12}	\mathbb{Z}^{11}	0	0	0	0	\mathbb{Z}	\mathbb{Z}^{11}	0
$\mathfrak{B}(d_6)$	\mathbb{Z}	0	\mathbb{Z}^6	$\mathbb{Z}^7 \oplus \mathbb{Z}_2^5$	\mathbb{Z}^6	\mathbb{Z}^6	0	\mathbb{Z}	0	\mathbb{Z}^7	\mathbb{Z}^6	\mathbb{Z}^6	0
$(\mathfrak{B}(d_6), \partial\mathfrak{B}(d_6))$	0	0	0	0	\mathbb{Z}^{16}	\mathbb{Z}^{16}	0	0	0	0	0	\mathbb{Z}^{16}	0
$\mathfrak{B}(d_7)$	\mathbb{Z}	0	\mathbb{Z}^{25}	$\mathbb{Z}^{21} \oplus \mathbb{Z}_2^5$	\mathbb{Z}	\mathbb{Z}^6	0	\mathbb{Z}	0	\mathbb{Z}^{26}	\mathbb{Z}	\mathbb{Z}^6	0
$(\mathfrak{B}(d_7), \partial\mathfrak{B}(d_7))$	0	0	0	0	0	\mathbb{Z}^8	\mathbb{Z}^8	0	0	0	0	0	\mathbb{Z}^8
$\mathfrak{B}(d_8)$	\mathbb{Z}	0	\mathbb{Z}^{17}	$\mathbb{Z}^{13} \oplus \mathbb{Z}_2^5$	\mathbb{Z}	\mathbb{Z}^6	0	\mathbb{Z}	0	\mathbb{Z}^{18}	\mathbb{Z}	\mathbb{Z}^6	0
$(\mathfrak{B}(d_8), \partial\mathfrak{B}(d_8))$	0	0	0	0	0	0	0	0	0	0	0	0	0
$\mathfrak{B}(d_9)$	\mathbb{Z}	\mathbb{Z}^6	\mathbb{Z}^{17}	$\mathbb{Z}^7 \oplus \mathbb{Z}_2^5$	\mathbb{Z}^{13}	\mathbb{Z}^{18}	0	\mathbb{Z}	\mathbb{Z}^6	\mathbb{Z}^{12}	\mathbb{Z}	\mathbb{Z}^{18}	0
$(\mathfrak{B}(d_9), \partial\mathfrak{B}(d_9))$	0	0	0	0	0	0	0	0	0	0	0	0	0

Proof The homology groups of $H_*(\mathfrak{B}(d_i), \partial\mathfrak{B}(d_i))$ and $H_*(\mathfrak{B}_R(d_i), \partial\mathfrak{B}_R(d_i))$ are provided directly from Lemma 4.3.1.

Working off of the two known values $H_*(\mathfrak{B}_R(d_5))$ and $H_*(\mathfrak{B}_R(d_9))$, the remaining values for $H_*(\mathfrak{B}_R(d_i))$ are computed from the exact sequences of the pairs $(\mathfrak{B}_R(d_5), \mathfrak{B}_R(d_i))$ and $(\mathfrak{B}_R(d_i), \mathfrak{B}_R(d_9))$. The Gysin braids of the pairs $(\mathfrak{B}(d_5), \mathfrak{B}(d_i))$ compute $H_*(\mathfrak{B}(d_i))$, leaving undetermined the torsion subgroup T_i of $H_3(\mathfrak{B}(d_i))$. To determine T_i , we begin with the observation $T_5 \cong \mathbb{Z}_2^5$ and make use of the fact that all of the groups $H_*(\mathfrak{B}(d_{i-1}), \mathfrak{B}(d_i))$ are torsion-free to conclude that $T_i \cong \mathbb{Z}_2^5$ for all i .

To illustrate, the computation of $H_*(\mathfrak{B}_R(d_6))$ and $H_*(\mathfrak{B}(d_6))$ is typical. First, inserting the known values into the exact sequences of the pair $(\mathfrak{B}_R(d_5), \mathfrak{B}_R(d_6))$, we see

$$H_4(\mathfrak{B}_R(d_6)) \rightarrow \mathbb{Z}^6 \rightarrow \mathbb{Z}^6 \rightarrow H_3(\mathfrak{B}_R(d_6)) \rightarrow 0 \rightarrow 0 \rightarrow H_2(\mathfrak{B}_R(d_6)) \rightarrow \mathbb{Z}^7 \rightarrow 0 \rightarrow H_1(\mathbb{B}_R(d_6))$$

On the other hand, from the exact sequence of the pair $(\mathfrak{B}_R(d_6), \mathfrak{B}_R(d_9))$ we have

$$0 \rightarrow \mathbb{Z}^{12} \rightarrow \mathbb{Z}^{18} \rightarrow H_4(\mathfrak{B}_R(d_6)) \rightarrow 0$$

These together determine $H_*(\mathfrak{B}_R(d_6))$. Inserting this into the Gysin braid of the pair $(\mathfrak{B}(d_5), \mathfrak{B}(d_6))$, we first see from the exact sequence of $(\mathfrak{B}(d_5), \mathfrak{B}(d_6))$ that $H_6(\mathfrak{B}(d_6)) = H_1(\mathfrak{B}(d_6)) = 0$. Next, the Gysin sequence of $\mathfrak{B}(d_6)$ shows that $H_5(\mathfrak{B}(d_6)) = H_2(\mathfrak{B}(d_6)) \cong \mathbb{Z}^6$. Inserting this value for $H_5(\mathfrak{B}(d_6))$ back into the exact sequence of the pair next yields

$$0 \rightarrow H_5(\mathfrak{B}(d_6)) \rightarrow \mathbb{Z}^6 \rightarrow \mathbb{Z}^6 \rightarrow H_4(\mathfrak{B}(d_6)) \rightarrow 0$$

which implies $H_4(\mathfrak{B}(d_6)) \cong \mathbb{Z}^6$, while the sequence

$$0 \rightarrow \mathbb{Z}^6 \rightarrow H_3(\mathfrak{B}(d_6)) \rightarrow \mathbb{Z} \oplus \mathbb{Z}_2^5 \rightarrow 0$$

determines the torsion-free component of $H_3(\mathfrak{B}(d_6))$.

To determine the torsion component, the braid diagram contains the commutative diagram of exact sequences:

$$\begin{array}{ccccccc}
 H_4(\mathfrak{B}_R(d_5), \mathfrak{B}_R(d_6)) & \longrightarrow & H_3(\mathfrak{B}_R(d_6)) & \longrightarrow & H_3(\mathfrak{B}_R(d_5)) & \longrightarrow & H_3(\mathfrak{B}_R(d_5), \mathfrak{B}_R(d_6)) \\
 \downarrow & & \downarrow & & \downarrow & & \downarrow \\
 H_5(\mathfrak{B}(d_5), \mathfrak{B}(d_6)) & \longrightarrow & H_4(\mathfrak{B}(d_6)) & \longrightarrow & H_4(\mathfrak{B}(d_5)) & \longrightarrow & H_4(\mathfrak{B}(d_5), \mathfrak{B}(d_6)) \\
 \downarrow & & \downarrow & & \downarrow & & \downarrow \\
 H_5(\mathfrak{B}_R(d_5), \mathfrak{B}_R(d_5)) & \longrightarrow & H_4(\mathfrak{B}_R(d_6)) & \longrightarrow & H_4(\mathfrak{B}_R(d_5)) & \longrightarrow & H_4(\mathfrak{B}_R(d_5), \mathfrak{B}_R(d_5)) \\
 \downarrow & & \downarrow \partial_6 & & \downarrow \partial_5 & & \downarrow \\
 H_3(\mathfrak{B}_R(d_5), \mathfrak{B}_R(d_6)) & \longrightarrow & H_2(\mathfrak{B}_R(d_6)) & \longrightarrow & H_2(\mathfrak{B}_R(d_5)) & \longrightarrow & H_2(\mathfrak{B}_R(d_5), \mathfrak{B}_R(d_6)) \\
 \downarrow & & \downarrow & & \downarrow & & \downarrow \\
 H_4(\mathfrak{B}(d_5), \mathfrak{B}(d_6)) & \longrightarrow & H_3(\mathfrak{B}(d_6)) & \longrightarrow & H_3(\mathfrak{B}(d_5)) & \longrightarrow & H_3(\mathfrak{B}(d_5), \mathfrak{B}(d_6)) \\
 \downarrow & & \downarrow & & \downarrow & & \downarrow \\
 H_4(\mathfrak{B}_R(d_5), \mathfrak{B}_R(d_5)) & \longrightarrow & H_3(\mathfrak{B}_R(d_6)) & \longrightarrow & H_3(\mathfrak{B}_R(d_5)) & \longrightarrow & H_3(\mathfrak{B}_R(d_5), \mathfrak{B}_R(d_5))
 \end{array}$$

Inserting the known values, this yields commutative diagram

$$\begin{array}{ccccc}
 \mathbb{Z}^6 & \xrightarrow{\cong} & \mathbb{Z}^6 & & \\
 \downarrow \partial_6 & & \downarrow \partial_5 & & \\
 \mathbb{Z}^7 & \xrightarrow{\cong} & \mathbb{Z}^7 & & \\
 \downarrow & & \downarrow & & \\
 \mathbb{Z}^6 \hookrightarrow H_3(\mathfrak{B}(d_6)) & \twoheadrightarrow & \mathbb{Z} \oplus \mathbb{Z}^5 & & \\
 \downarrow & & \downarrow & & \\
 \mathbb{Z}^6 & \longrightarrow & 0 & &
 \end{array}$$

Since ∂_5 has cokernel $\mathbb{Z} \oplus \mathbb{Z}^5_2$, so does ∂_6 , which implies $H_3(\mathfrak{B}(d_6)) \cong \mathbb{Z}^6 \oplus \mathbb{Z}^5_2$.

The arguments for $H_3(\mathfrak{B}(d_i))$ for $i = 7, 8, 9$ are similar. □

With the values of $H_*(\mathfrak{B}(d_5))$, $H_*(\mathfrak{B}(d_9))$ and $H_*(\mathfrak{B}_R(d_5))$, $\mathfrak{B}_R(d_9)$ established, inspection of the exact sequence of the pair shows that

Corollary 5.1.1 *The inclusion-induced maps $\iota : H_*(\mathfrak{B}(d_9)) \rightarrow H_*(\mathfrak{B}(d_5))$ and $\iota_R : H_*(\mathfrak{B}_R(d_9)) \rightarrow H_*(\mathfrak{B}_R(d_5))$ are surjective.*

5.2 The Pairs $(\mathfrak{B}(d_i), \mathfrak{B}_0(d_i))$ and $(\mathfrak{B}(d_i), \partial\mathfrak{B}^+(d_i))$

We complete the homology calculations by identifying $H_*(\mathfrak{B}(d_i), \mathfrak{B}_0(d_i))$ and $H_*(\mathfrak{B}(d_i), \partial\mathfrak{B}^+(d_i))$, along with the corresponding reduced spaces.

Lemma 5.2.1 *The homology groups of the pairs $(\mathfrak{B}(d_i), \partial\mathfrak{B}^+(d_i))$ and $(\mathfrak{B}_R(d_i), \partial\mathfrak{B}^+_R(d_i))$ are as follows:*

	$H_*(\mathfrak{B}(d_i), \partial\mathfrak{B}^+(d_i))$						$(\mathfrak{B}_R(d_i), \partial\mathfrak{B}^+_R(d_i))$							
	0	1	2	3	4	5	6	0	1	2	3	4	5	6
d_5	0	0	\mathbb{Z}^{12}	\mathbb{Z}^{13}	\mathbb{Z}^6	\mathbb{Z}^{11}	\mathbb{Z}^6	0	0	\mathbb{Z}^{12}	\mathbb{Z}	\mathbb{Z}^5	\mathbb{Z}^6	0
d_6	0	0	\mathbb{Z}^{12}	\mathbb{Z}^{12}	\mathbb{Z}^{10}	\mathbb{Z}^{16}	\mathbb{Z}^6	0	0	\mathbb{Z}^{12}	0	\mathbb{Z}^{10}	\mathbb{Z}^6	0
d_7	0	0	\mathbb{Z}^{12}	\mathbb{Z}^{12}	0	\mathbb{Z}^{20}	\mathbb{Z}^{20}	0	0	\mathbb{Z}^{12}	0	0	\mathbb{Z}^{20}	0
d_8	0	0	\mathbb{Z}^{12}	\mathbb{Z}^{12}	0	\mathbb{Z}^{12}	\mathbb{Z}^{12}	0	0	\mathbb{Z}^{12}	0	0	\mathbb{Z}^{12}	0
d_9	0	0	0	0	0	0	0	0	0	0	0	0	0	0

Proof To compute $H_*(\mathfrak{B}(d_i), \partial\mathfrak{B}^+(d_i))$, there is the exact sequence

$$H_k(\mathfrak{B}_{R0}(d_i), \partial\mathfrak{B}_{R0}(d_i)) \rightarrow H_k(\mathfrak{B}_R(d_i), \partial\mathfrak{B}_R(d_i)) \rightarrow H_k(\mathfrak{B}(d_i), \partial\mathfrak{B}^+(d_i))$$

For any two values of $d_i < d_j < \delta_8$, there is no change in structure at \mathcal{B}_0 , so we have $H_k(\mathfrak{B}_{R0}(d_i), \partial\mathfrak{B}_{R0}(d_i)) \xrightarrow{\cong} H_k(\mathfrak{B}_{R0}(d_j), \partial\mathfrak{B}_{R0}(d_j))$ and braid diagram

$$\begin{array}{ccccc}
 0 & \longrightarrow & H_k(\mathfrak{B}(d_i, d_j), \partial\mathfrak{B}(d_i)) & \xrightarrow{\cong} & H_k(\mathfrak{B}(d_i, d_j) \cup \mathfrak{B}_0(d_i), \partial\mathfrak{B}(d_i)) \cup \mathfrak{B}_0(d_i) \\
 \downarrow & & \downarrow & & \downarrow \\
 H_k(\mathfrak{B}_0(d_i), \partial\mathfrak{B}_0(d_i)) & \longrightarrow & H_k(\mathfrak{B}(d_i), \partial\mathfrak{B}(d_i)) & \longrightarrow & H_k(\mathfrak{B}(d_i), \partial\mathfrak{B}^+(d_i)) \\
 \downarrow \cong & & \downarrow & & \downarrow \\
 H_k(\mathfrak{B}_0(d_j), \partial\mathfrak{B}_0(d_j)) & \longrightarrow & H_k(\mathfrak{B}(d_j), \partial\mathfrak{B}(d_j)) & \longrightarrow & H_k(\mathfrak{B}(d_j), \partial\mathfrak{B}^+(d_j))
 \end{array}$$

with corresponding reduced braid diagrams.

Using these braid diagrams, we can compute $H_*(\mathfrak{B}(d_6), \partial\mathfrak{B}^+(d_6))$ and $H_*(\mathfrak{B}_R(d_6), \partial\mathfrak{B}_R^+(d_6))$ in two stages. The reduced braid diagram for d_5 and d_6 suffices to compute the reduced homology; then the Gysin braid of the triple $(\mathfrak{B}(d_6), \partial\mathfrak{B}^+(d_6), \partial\mathfrak{B}(d_6))$ computes the unreduced homology. Proceeding to Region VII, the Gysin braid of the triple $(\mathfrak{B}_R(d_7), \partial\mathfrak{B}_R^+(d_7), \partial\mathfrak{B}_R(d_7))$ computes both the reduced and unreduced homology groups. For Region VIII, as $H_*(\mathfrak{B}(d_8), \partial\mathfrak{B}(d_8)) = 0$, the values for $H_*(\mathfrak{B}(d_8), \partial\mathfrak{B}^+(d_8))$ follow trivially. Finally, for Region IX, both $H_*(\mathfrak{B}(d_9), \partial\mathfrak{B}(d_9))$ and $H_*(\mathfrak{B}_0(d_9), \partial\mathfrak{B}_0(d_9))$ are trivial, so $H_*(\mathfrak{B}(d_9), \partial\mathfrak{B}^+(d_9))$ is as well. □

To complete the results, the last step is to identify $H_*(\mathfrak{B}(d_i), \mathfrak{B}_0(d_i))$. This will proceed in two steps, based on the observations that $\mathfrak{B}_0(d)$ bifurcates only at δ_8 , and that when $H_k(\mathfrak{B}(d_i)) \neq 0$, the inclusion-induced map $\gamma_{i9} : H_k(\mathfrak{B}_0(d_9)) \rightarrow H_k(\mathfrak{B}_0(d_i))$ is an isomorphism. The map ζ_9 was identified in Lemma 4.1.2. Then for all other i , the non-zero values of $H_k(\mathbb{B}_0(d_i))$ admit factorization

$$\begin{array}{ccc} H_k(\mathbb{B}_0(d_9)) & \xrightarrow{\zeta_9} & H_k(\mathbb{B}(d_9)) \\ \cong \downarrow \gamma_{i9} & & \downarrow \iota_{i9} \\ H_k(\mathbb{B}_0(d_i)) & \xrightarrow{\zeta_i} & H_k(\mathbb{B}(d_i)) \end{array}$$

so the remaining ζ_i follow from the compositions $\iota_{i9} \circ \zeta_9$.

Lemma 5.2.2 *The homology groups of the pairs $(\mathfrak{B}(d_i), \mathfrak{B}_0(d_i))$ and $(\mathfrak{B}_R(d_i), \mathfrak{B}_{R0}(d_i))$ are as follows:*

	$H_*(\mathfrak{B}(d_i), \mathfrak{B}_0(d_i))$						$H_*(\mathfrak{B}_R(d_i), \mathfrak{B}_{R0}(d_i))$							
	0	1	2	3	4	5	6	0	1	2	3	4	5	6
d_5	0	\mathbb{Z}^{11}	\mathbb{Z}^{18}	0	\mathbb{Z}^{11}	\mathbb{Z}^{18}	0	0	\mathbb{Z}^{11}	\mathbb{Z}^7	0	\mathbb{Z}^{18}	0	0
d_6	0	\mathbb{Z}^{11}	\mathbb{Z}^{18}	\mathbb{Z}^6	\mathbb{Z}^{16}	\mathbb{Z}^{17}	0	0	\mathbb{Z}^{11}	\mathbb{Z}^7	\mathbb{Z}^5	\mathbb{Z}^{17}	0	0
d_7	0	\mathbb{Z}^{11}	\mathbb{Z}^{37}	\mathbb{Z}^{20}	\mathbb{Z}^{11}	\mathbb{Z}^{17}	0	0	\mathbb{Z}^{11}	\mathbb{Z}^{26}	0	\mathbb{Z}^{17}	0	0
d_8	0	\mathbb{Z}^{11}	\mathbb{Z}^{29}	\mathbb{Z}^{12}	\mathbb{Z}^{11}	\mathbb{Z}^{17}	0	0	\mathbb{Z}^{11}	\mathbb{Z}^{18}	0	\mathbb{Z}^{17}	0	0
d_9	0	\mathbb{Z}^{11}	\mathbb{Z}^{29}	\mathbb{Z}^{12}	\mathbb{Z}^{11}	\mathbb{Z}^{17}	0	0	\mathbb{Z}^{11}	\mathbb{Z}^{18}	0	\mathbb{Z}^{17}	0	0

The image $im(j_* : H_3(\mathfrak{B}(d_i)) \rightarrow H_3(\mathfrak{B}(d_i), \mathfrak{B}_0(d_i)))$ is

d_i	d_5	d_6	d_7	d_8	d_9
$im(j_*)$	0	\mathbb{Z}^6	\mathbb{Z}^{20}	\mathbb{Z}^{12}	\mathbb{Z}^6

Proof As noted, the values for $d_9 > \delta_8$ follow immediately from Lemma 4.1.2. For $\delta_5 < d_i < \delta_8$, considering first the reduced spaces, the only non-trivial map is $\zeta_{Ri*} : H_3(\mathfrak{B}_{R0}(d_i)) \rightarrow H_3(\mathfrak{B}_R(d_i))$. From the exact sequences of the pairs $(\mathfrak{B}_R(d_i), \mathfrak{B}_R(d_9))$ we observe that $H_3(\mathfrak{B}_R(d_9)) \rightarrow H_3(\mathfrak{B}_R(d_i))$ is injective with torsion-free cokernel. This implies that $\zeta_{Ri*} : H_3(\mathfrak{B}_{R0}(d_i)) \rightarrow H_3(\mathfrak{B}_R(d_i))$ has rank 1 with torsion-free cokernel. The values for $H_*(\mathfrak{B}_R(d_i), \mathfrak{B}_{R0}(d_i))$ follow immediately.

Similarly, to compute $H_k(\mathfrak{B}(d_i), \mathfrak{B}_0(d_i))$ for $\delta_5 < d_i < \delta_8$, we need to compute $\zeta_{i*} : H_k(\mathfrak{B}_0(d_i)) \rightarrow H_k(\mathfrak{B}(d_i))$ for $k = 3, 4$. The same argument as above shows that $H_4(\mathfrak{B}_0(d_i)) \rightarrow H_4(\mathfrak{B}(d_i))$ has image \mathbb{Z} with torsion-free cokernel for all $\delta_5 < d_i < \delta_8$. For

$k = 3$, it suffices to show that ζ_{i*} has image $\mathbb{Z} \oplus \mathbb{Z}_2^5$ and torsion-free cokernel. The maps ζ_{i*} are sandwiched between ζ_{9*} and ζ_{5*}

$$\begin{array}{ccccc}
 & & H_3(\mathfrak{B}_0(d_i)) & & \\
 & \swarrow & \downarrow \zeta_{i*} & \searrow \zeta_{5*} & \\
 H_3(\mathfrak{B}(d_9)) & \xrightarrow{\gamma_{i9} \zeta_{9*}} & H_3(\mathfrak{B}_0(d_i)) & \xrightarrow{\gamma_{5i}} & H_3(\mathfrak{B}_0(d_5))
 \end{array}$$

with values

$$\begin{array}{ccccc}
 & & \mathbb{Z}^{12} & & \\
 & \swarrow & \downarrow \zeta_{i*} & \searrow \zeta_{5*} & \\
 \mathbb{Z}^7 \oplus \mathbb{Z}_2^5 & \xrightarrow{\gamma_{i9}} & \mathbb{Z}^{\alpha_i} \oplus \mathbb{Z}_2^5 & \xrightarrow{\gamma_{5i}} & \mathbb{Z}^7 \oplus \mathbb{Z}_2^5
 \end{array}$$

Both ζ_{9*} and ζ_{5*} have image $\mathbb{Z} \oplus \mathbb{Z}_2^5$ with torsion-free cokernel, and the maps γ_{ij} are seen by Lemma 4.3.1 to be torsion free, so it follows that for all i , ζ_{i*} has image $\mathbb{Z} \oplus \mathbb{Z}_2^5$ and torsion-free cokernel.

□

Data Availability Data sharing not applicable to this article as no data sets were generated or analyzed during the current study.

Declarations

Conflict of interest Not applicable

References

1. Albouy, A.: Integral manifold of the N-body problem. *Invent. Math.* **114**, 463–488 (1993)
2. Albouy, A.: Symétrie des configurations centrales de quatre corps. *C. R. Acad. Sci. Paris Sér. I Math.* **320**, 217–220 (1995)
3. Cabral, H.: On the integral manifolds of the N-body problem. *Invent. Math.* **20**, 59–72 (1973)
4. Cabral, H., McCord, C.: Topology of the integral manifolds of the N-body problem with positive energy. *J. Dyn. Differ. Eqs.* **14**, 259–293 (2002)
5. Havel, H., McCord, C.: Patterns in bifurcation levels of the integral manifolds of the N-body problem. *Eur. J. Phys* (To appear)
6. McCord, C., Meyer, K., Wang, Q.: The integral manifolds of thre three-body problem. *Mem. Amer. Math. Soc.* **628**, American Mathematical Society, Providence, RI (1998)
7. McCord, C.: Cross sections in the planar N-body problem, Hamiltonian systems and celestial mechanics (Pátzcuaro, 1998), 250–260, *World Sci. Monogr. Ser. Math.* **6** World Sci. Publishing, River Edge, NJ (2000)
8. McCord, C.: On the homology of the integral manifolds in the planar N-body problem. *Ergod. Theory Dyn. Syst.* **21**, 861–883 (2001)
9. McCord, C.: The Integral Manifolds of the N-Body Problem. *J. Dyn. Differ. Eqs.* **35**, 1–68 (2023)
10. McCord, C.: The integral manifolds of the 4-body problem with equal masses: bifurcations at infinity. *J. Dyn. Differ. Eqs.* (Accepted for publication)
11. McCord, C., Meyer, K.: Cross sections in the three-body problem. *J. Dyn. Differ. Eqs.* **12**, 247–271 (2000)
12. McCord, C., Meyer, K., Offin, D.: Are Hamiltonian flows geodesic flows? *Trans. Am. Math. Soc.* **355**, 1237–1250 (2003)
13. Moczurad, M., Zgliczyński, P.: Central configurations in planar n- body problem with equal masses for $n = 5, 6, 7$ *Cel. Mech. Dyn. Astro.* **131**, 46 (2019)

14. Moeckel, R.: Central Configurations, Periodic Orbits, and Hamiltonian Systems. Springer, Berlin (2015)
15. Smale, S.: Topology and mechanics. *Invent. Math.* **10**, 305–331 (1970)
16. Smale, S.: Topology and mechanics II. *Invent. Math.* **11**, 45–64 (1970)
17. Wang, Q.: The Hill's region of the four-body problem. *Celestial mechanics* (Evanston, IL, 1999), 239–266, *Contemp. Math.*, 292, Amer. Math. Soc., Providence, RI (2002)

Publisher's Note Springer Nature remains neutral with regard to jurisdictional claims in published maps and institutional affiliations.

Springer Nature or its licensor (e.g. a society or other partner) holds exclusive rights to this article under a publishing agreement with the author(s) or other rightsholder(s); author self-archiving of the accepted manuscript version of this article is solely governed by the terms of such publishing agreement and applicable law.